2017

Signaling complexes involving HCN channels

Fan, Jing

UNIVERSITY OF CALGARY

Signaling complexes involving HCN channels

by

Jing Fan

A THESIS

SUBMITTED TO THE FACULTY OF GRADUATE STUDIES

IN PARTIAL FULFILMENT OF THE REQUIREMENTS FOR THE

DEGREE OF DOCTOR OF PHILOSOPHY

GRADUATE PROGRAM IN NEUROSCIENCE

CALGARY, ALBERTA

November, 2017

Abstract

I_h is a hyperpolarization-activated current that is widely distributed in the brain and which contributes to various physiological processes. HCN channels that give rise to I_h are an important target of cellular signals that regulate neuronal responses to external stimuli. In this thesis, I characterize the HCN channel-associated signaling complex and its impact on hippocampal function at molecular and cellular levels.

Using whole cell-current recordings in hippocampal primary cultures prepared from wild-type (WT) and cellular prion protein (PrP^C) knockout (KO) mouse pups, I found that the absence of PrP^C profoundly affected the firing properties of cultured hippocampal neurons. These included an increased number of action potentials (APs) and a decreased spike threshold. By performing whole cell-voltage recordings, a reduced ionic current I_h was observed in KO neurons as indicated by a decreased voltage sag, a hyperpolarizing shift in activation gating and an enhanced input resistance. However, co-IP results did not reveal a molecular complex formed between HCN and PrP^C. These results indicate that HCN channels are functionally but not physically associated with PrP^C to regulate hippocampal neuronal excitability.

Further dissecting on HCN channel-associated signaling in tsA-201 cells revealed that HCN1 and Cav3.2 channels can be associated in a physical complex. The coexpression of HCN1 channels altered the functional properties of Cav3.2 currents, including a reduced Cav3.2 current density, altered channel kinetics and a depolarizing shift in activation gating. Mutual interaction regions in both channels were also determined.

Overall, these findings identify HCN channel-associated signaling at molecular and functional levels, including functional interactions between HCN channels and PrP^C, and physical interactions between HCN1 and Cav3.2 channels. This study provides a framework for understanding the HCN channel-associated interactions in the context of neuronal excitability.

Acknowledgements

There are many people who contributed to my study and I would like to express my thanks to all of these.

First of all, I am heartily thankful to my supervisor, Dr. Gerald Zamponi, whose enthusiasm, guidance and support from the initial to the final level enabled me to develop an understanding of the subject of this thesis.

I also wish to thank all my committee members, Drs. Ray Turner and Peter Stys for providing invaluable inputs to my research project.

I am thankful to all lab members for scientific and social interactions. My warm thanks are due to lab member, Drs. Norbert Weiss, Patrick Stemkowski who gave important guidance during my first steps into whole-cell patch-clamp technique. I wish to thank my colleague Dr. Maria Gandini, also my best friend, for helping me to get through the difficult time, and for all the support during the last moment of my thesis preparation. During this work, I have collaborated with many colleagues in the lab and I wish to extend my thanks to Drs. Ivana Souza, Fang-Xiong Zhang, and Lina Chen for their excellent technical assistance.

Finally, I wish to thank my wonderful family, Mark and little Hunter, and my parents for their love and support. Without their encouragement and understanding it would have been impossible for me to finish this work.

Table of Contents

List of Figures and Table

List of Abbreviations

ADP: afterdepolarizing potential

AHP: afterhyperpolorization

AMPA: α-amino-3-hydroxy-5-methyl-4-isoxazoleproprionate

AP: action potential

CA1: Cornu Ammonis 1

CaMKII: Ca^{2+}/calmodulin-dependent protein kinase II

cAMP: 3',5'-cyclic adenosine monophosphate

CNBD: cyclic nucleotide-binding domain

EPSPs: excitatory postsynaptic synaptic potentials

GABA: γ-Aminobutyric acid

GPI: glycosylphosphatidylinositol

HCN: hyperpolarization-activated cyclic nucleotide-gated channel

KO: knockout

LTP Long-term Potentiation

MAPKs: Mitogen-activated protein kinases

mEPSCs: miniature EPSCs

mGluR: metabotropic glutamate receptors

NMDA: N-methyl-D-aspartate

PKC: protein kinase C

PrP^{C}: cellular prion protein

PrP^{SC}: scrapie prion protein

ROS: reactive oxygen species

WT: wild-type

Chapter One: General Introduction

1.1. The hippocampus: from architecture to physiological and pathological function

The hippocampus has been among the most intensely studied brain regions throughout the modern neuroscientific era. It is easily recognized as a distinct structure in the brain and is long-known to be a key element in the brain's capacity to learn and to remember. Apart from the role of hippocampus in fundamentally important physiological processes, its pathological involvement in neuronal diseases like epilepsy is well established (Schwartzkroin, 1994, Bartsch, 2012). The initial insights into the role of the hippocampus stem from a patient named H.M. (Scoville and Milner). After his hippocampus was bilaterally removed in an operation due to intractable epilepsy, H.M was unable to build any new memories, and lived instead in a strange world where everything he experienced just faded away. Therefore, researchers have long been struggling to remove seizure prone hippocampal tissue while keeping memories reserved.

1.1.1. Hippocampal cells, layers and pathways

The unique role of hippocampus in brain function is governed by its distinct layered structure and circuit architecture. Pyramidal cells, the principal cells of the hippocampus, are clustered in a distinct layer that runs throughout the hippocampal formation: the stratum pyramidale (Anderson et al., 2007). In addition to these principal excitatory neurons, there are the dentate gyrus (DG) granule cells that send mossy fibers through the stratum lucidum in Cornu Ammonis 3 (CA3). In particular, many interneurons are contained in the stratum pyramidale, which greatly contributes to hippocampal network activity. Moreover, the hippocampal cells are clustered in different layers, named stratum alveus, oriens, pyramidale, radiatum and lacunosum moleculare. The fibers contained in these layers contribute to the intrahippocampal projection pathways (Schaffer, 1892, Swanson et al., 1978). Distinct intrahippocampal projection pathways link the three principal areas of the hippocampus, thereby forming a trisynaptic circuit going from the entorhinal cortex (EC) to DG, DG to CA3, then from CA3 to Cornu Ammonis 1 (CA1) (Figure 1-1). Aside from these principal pathways, the hippocampus is populated by diverse types of inhibitory neurons that are localized to distinct strata and exert distinct functions within the hippocampal trisynaptic circuit, such as feed-forward and feed-back interactions (Freund and Buzsaki, 1996)

1.1.2. A role for hippocampus in normal brain function and disease

The negative consequences of hippocampal damage on learning and memory are extensively studied and have established the view that the hippocampus system is critically involved in learning and memory processes (Jarrard, 1983; Morris *et al*., 1982; Olton and Papas, 1979). In the rabbit hippocampus, a Norwegian physiologist, Terje Lømo along with Tim Bliss first discovered long-term potentiation (LTP) in 1966 (Lømo, 1966), which is considered as molecular events of learning. In NMDAR-dependent LTP induction, the activation of NMDARs allows Ca^{2+} entry which subsequently activates CaMKII. This in turn induces crucial molecular events related to synaptic potentiation (Malenka and Bear, 2004). The basic observations on hippocampal mnemonic function are complemented by the landmark discovery that the firing rate of hippocampal neurons is correlated with the location of the animal in a test environment. Those neurons were named as "place cells" by John O'Keefe and his student, which established the foundation for an important role of hippocampal formation in spatial coding (O'Keefe and Dostrovsky, 1971).

Apart from these classical references, the hippocampus is considered to be a major brain structure that can be affected by seizures which are normally induced by an imbalance between excitation and inhibition (Schwartzkroin, 1994). A number of studies indicating how epilepsy alters behavior of hippocampal neurons have been published. At the level of individual neurons, epilepsy causes CA1 pyramidal cells to convert from regular firing to bust-firing mode (giving rise to the term "intrinsically bursting neurons") (Halliwell and Adams 1982; Staff *et al*., 2000). Additionally, posttraumatic human epilepsy eliminates a large number of hippocampal cells, particularly in the CA1 and CA3 areas (Swartz *et al*., 2006). The conclusion raised from these findings is that hippocampal neurons are selectively vulnerable to epileptic attack. Further progress has been made at the level of internal circuits where impairment of inhibitory circuits governed by hippocampal GABAergic interneurons (Magloczky and Freund, 2005) leads to a network imbalance and epileptogenesis. Particularly, a number of studies have documented that the morphological alterations in the hippocampus are commonly associated with memory defects in epileptic patients (Thompson, 1991). Therefore, at the level of synapses, it is not surprising to observe a limited generation of LTP in patients with epilepsy (Zhou *et al*., 2007). Hence, the epileptogenic network formed by seizures may interfere with physiological neuronal networks,

and therefore may impair normal brain function. Given that the abnormal firing within the individual neurons has the potential to propagate throughout the entire network, is important to understand how the activities of individual hippocampal neurons are regulated by various ion channels, and how this affects the integration of synaptic input and action potential output in epileptic processes.

Hyperpolarization-activated cyclic nucleotide-gated cation (HCN) channels are known to be activated by negative membrane potentials. They display unique biophysical properties that are essential for regulating neuronal excitability and electrical responsiveness of cells. In particular, there is abundant evidence for diverse effects of HCN channel activity on regulating hippocampal neuron firing. In the next section, I will focus on the specific aspects of HCN channels that endow them with a key role in regulating neuronal excitability and synaptic integration in the hippocampus.

1.2 The HCN channel family and basic biophysical properties of I_h

HCN channels form the subgroup of cyclic nucleotide-regulated cation channels and belong to the superfamily of voltage-gated pore loop channels with four pore-forming subunits (HCN1-4) encoded by the HCN1-4 gene family in mammals (Robinson and Siegelbaum, 2003). The underlying hyerpolarization-activated current, I_h, was first discovered in sino-atrial node tissue (Noma and Irisawa, 1976) and first characterized by Brown, Difrancesco and Noble (Brown et al., 1979, Brown and Difrancesco, 1980), and is now known to be widely distributed in the CNS. Unlike the majority of voltage-gated channels, HCN channels are activated upon membrane hyperpolarization, rather than depolarization, and do not exhibit voltage-dependent inactivation (Noma and Irisawa, 1976; Brown and Difrancesco, 1980; Maylie et al., 1981, Biel et al., 2009). HCN channel gating can be further modulated by cAMP and cGMP which can both facilitate the voltage-dependent activation of some types of HCN channels (Biel et al., 2009). Although their structure resembles that of the voltage-gated K^+ channels, HCN channels are mainly permeable to both K^+ and Na^+. Therefore, the reversal potential of HCN channels lies around -30mV in physiological saline, but this value may vary among different cell type. Since HCN channels are partially active at rest, I_h depolarizes and modulates the membrane potential, acting like a physiological "voltage clamp". In general, there are two distinct current components are processed when HCN channel is activated: one is the major voltage-dependent I_h current

which has slow developing phase of activation, the other is minor voltage-independent instantaneous current (I_{ins}) which is fully activated within a few milliseconds and can be pronounced by incomplete deactivation (Proenza et al. 2002; Proenza & Yellen, 2006, Mistrik et al. 2006).

Structurally, the HCN channels are tetramers of HCN1-HCN4 subunits. As shown in figure 1-2C, each subunit contains 6 transmembrane segments (S1-S6) connected by intracellular linkers and cytoplasmic N- and C-termini. Cloning and sequence analysis of HCN channels have revealed that the S4 segment is a positively charged voltage sensor that detects changes in transmembrane voltage and leads to opening of the channel pore. The ion selectivity filter is formed by a p-loop carrying a GYG motif between S5 and S6 (He et al, 2014). The C-terminus contains the C-linker and the cyclic nucleotide-binding domain (CNBD) that are important sites for the regulation of channel gating activity. More recently, the mechanism of cAMP modulation on HCN channels has been structurally analyzed based on the cryo-EM structure of the human HCN1 channel (Lee and Mackinnon, 2017). It was determined that binding of cAMP induces a local conformational change within the CNBD, which in turn propagates to the channel pore via C-linker (Figure 1-2D). Specifically, from an overlap structure of CNBD in the ligand-free and cAMP-bound states, cAMP binding appeared to rotate the C-linker and displaced the S6 helix towards the direction of pore vestibule, thus facilitating HCN channel opening (Lee and Mackinnon, 2017).

The HCN channel subunits exhibit diverse biophysical properties with regard to their respective activation kinetics, their steady-state voltage dependence, and their sensitivity to cAMP-dependent regulation. Among the HCN channel family, the activation of HCN1 is the fastest and is strongly voltage-dependent, while activation of HCN4 is the slowest, and HCN2, HCN3 display an intermediate activation time constant (He et al., 2014). Furthermore, HCN2 and HCN4 are strongly modulated by cAMP elevations, leading to shifts in the half activation potential by 10–25 mV (Biel et al., 2009). In contrast, cAMP exerts a weak regulation of HCN1 and HCN3. Last, the diversity of HCN subunits can be increased with heteromers formed between different HCN subunit isoforms. The biophysical properties of native I_h are thus determined by subunit composition.

HCN channels exhibit distinct expression patterns in the brain. HCN1 subunits are expressed in the hippocampus, neocortex, cerebellar cortex and brainstem (He et al., 2014, Biel et al., 2009). HCN2 subunits are distributed in the most brain areas with highest expression levels in the thalamus (He et al., 2014, Biel et al., 2009). HCN3 is preferentially expressed in the olfactory bulb and in some hypothalamic nuclei, but with generally low expression levels in the nervous system compared to other subunits (He et al., 2014, Biel et al., 2009). HCN4 is selectively located in various thalamic nuclei and basal ganglia (He et al., 2014, Biel et al., 2009). HCN channels are also present in peripheral neurons, such as dorsal root ganglia (He et al., 2014). Within a given neuron, HCN channels are not ubiquitously distributed. For example, in the hippocampus, HCN1 is preferentially expressed in the distal dendrites for a specific role on dendritic excitability and synaptic integration (Magee, 2000).

1.3 The behaviors and basic functions of HCN channels

The unique biophysical properties of I_h endow it to control neuronal activity and excitability at several levels, including regulation of membrane properties and shaping synaptic inputs. First, HCN channels are partially active at rest, therefore I_h contributes to establishing the resting membrane potential in many cells (Biel et al., 2009) (Figure 1-2B). Second, synaptic inhibition can be suppressed by HCN channels, because the hyperpolarizing conductance arising from inhibitory synaptic inputs triggers HCN channel activation, which then leads to depolarizing currents (Atherton et al., 2010). Conversely, partially opened HCN channels at rest reduce input resistance, and I_h thus can inhibit neuronal excitability by suppressing the effects of synaptic inputs on excitatory postsynaptic synaptic potentials (EPSPs) in a process termed "shunting inhibition". Therefore, I_h appears to stabilize membrane potential by counteracting both membrane depolarizations and hyperpolarizations.

HCN channels form heterotetramers or homotetramers, composed of HCN1-4 subunits, however, only HCN1 and HCN2 are highly expressed in hippocampus (Santoro et al., 2000, Figure 1-2A), indicating a location-correlated function. HCN1 and HCN2 channels are highly expressed in the central nervous system and are critically related to neuronal excitability at both single-cell and network levels, particularly in the hippocampus (Robinson and Siegelbaum, 2003). Moreover, HCN channels are involved in many physiological functions, which is particularly relevant to processes such as synaptic integration, oscillation, learning and memory

(He et al., 2014). Indeed, given the important roles of I_h in setting and regulating membrane properties, it is not surprising for HCN channels to have significant impact on synaptic integration. Numerous studies demonstrating the unique role of I_h in modulating neuronal integrative properties have been intensively performed in CA1 hippocampal (Magee et al., 1998, Magee et al., 1999), and neocortical layer 5 pyramidal neurons (Stuart and Spruston, 1998, Williams and Stuart, 2000, Berger et al., 2003). Specifically, the dendritic filtering phenomenon is not typically observed in these neurons due to a gradient distribution of I_h. The density of I_h in dendrites rises about six-fold with distance from the soma, though it is not the case for all types of neurons (Biel et al., 2009). Thus, the temporal summation is more inhibited in the distal dendrites, such that the amount of summation for distal inputs was twofold larger than for proximal input following bath application of the HCN channel blocker ZD7288 (Magee et al., 1999). The high density of HCN channels targeted in the dendrites allows I_h to significantly contribute to total membrane conductance of neurons. Therefore, it is expected that subtle changes in HCN channel activity would strongly influence neuronal intrinsic excitability.

Interestingly, the dysregulation of HCN channels is involved in several pathological conditions such as, pain and epilepsy (Biel et al., 2009; Noam et al., 2010). Given that HCN channels are key factors that control neuronal excitability, it is perhaps not surprising that dysfunction of HCN channels has been associated with epilepsy. For example, a rat model of childhood febrile seizures exhibits an increase in HCN2 and a decrease in HCN1 expression in hippocampal CA1 pyramidal neurons (Chen et al., 1999; Brewster et al., 2002). Recent studies showed that HCN2 KO mice display absence epilepsy (Ludwig et al., 2003), while HCN1 KO mice are more susceptible to chemical-induced seizures (Huang et al., 2009), indicating an isoform-specific effect. In addition to the redistribution of HCN channels in adult models of epilepsy, HCN expression and distribution appear to be developmentally regulated, as well as regulated by neuronal activity (Bender and Baram, 2008). Developmental dysregulation of HCN channel expression is considered to be potentially critical for epileptogenesis (Budde et al., 2005; Kuisle et al., 2006).

Taken together, the unique biophysical properties, distinct distribution pattern of HCN channels and various subunit compositions of HCN subunits have the propensity to contribute to

diversified neuron functions, and support different physiological roles of I_h throughout brain regions.

1.4 Regulation of HCN channels

A number of intracellular signaling pathways have been shown to converge on HCN channels to alter features such as their voltage dependence of activation, channel kinetics and trafficking (Figure 1-3). Signaling cascades acting on HCN channels include protein kinases (p38-MAPK, PKC, Ca^{2+}/CaMKII, etc), metabotropic receptors (Group1-mGluRs) and interacting proteins (TRIP 8b, etc). For example, activation of p38-MAPK strongly regulates HCN channel gating by a depolarizing shift of I_h activation in hippocampal pyramidal neurons (Poolos et al., 2006) where HCN1 and HCN2 are highly expressed. Importantly, the changes in I_h biophysical properties by the activation of p38-MAPK subsequently reduce input resistance and temporal summation, thus influencing neuronal excitability. Conversely, the activation of group I mGluR downregulates I_h followed by an activity-dependent increase in neuronal excitability, as has been described in hippocampal CA1 pyramidal neurons (Brager and Johnston, 2007). Further, TRIP8b, a well-recognized interacting protein of HCN channels, has been reported to regulate HCN channel gating, kinetics and trafficking by interacting with the CNBD of HCN channels (He et al., 2014). Finally, it has been reported that HCN1 subunits are distributed evenly instead of in a gradient pattern when Ca^{2+}/CaMKII blockers are applied (Shin and Chetkovich, 2007), suggesting that channel distribution is subject to second messenger regulation. Along these lines, membrane trafficking of HCN1 is blocked by glutamate-induced activation of NMDA/AMPA receptors (Noam et al., 2010). These results suggest that Ca^{2+} influx through activated NMDA/AMPA receptors may activate CaMKII, thus indirectly altering trafficking and surface expression of HCN1 channels.

Taken together, HCN channels are targets of various intracellular signaling pathways, which in turn can influence neuronal excitability. However, the detailed mechanisms underlying the actions of these protein kinases and interacting proteins, are still incompletely understood.

1.5 Cellular prion protein (PrP^C) in the hippocampus

There is growing evidence that the loss of PrP^C function interferes with neuronal activity, and therefore contributes to synchronized activities underlying neocortical and hippocampal

seizures (Walz *et al*., 2002). In this section, I will focus on the specific aspects of PrP^{C} that endow it with a key role in hippocampal function related to neuronal excitability, synaptic activity and neuroprotective effects.

PrP^{c} is a naturally occurring protein that is highly expressed in the CNS, especially in the hippocampus where it is mostly concentrated at synaptic site (Mironov et al., 2003, Zomosa-Signoret et al., 2008, Westergard et al., 2007). It contains 254 amino acids and has a mainly alpha-helical structure (Figure 1-4). The N-terminal domain contains a region that forms copper binding sites which may contribute to copper ion recycling within the cell. The C-terminal domain contains a sequence for a glycosylphosphatidylinositol (GPI) anchor, indicating a possible membrane associated function of this protein (Aguzzi and Heikenwalder, 2006). Most importantly, PrP^{C} can be converted into the pathological beta sheet-rich form PrP^{SC} whose accumulation is associated with many neurological disorders. Although the role of pathological PrP^{C} conformation in generating severe brain diseases has been established, the function of PrP^{C} in the normal brain remains less well established (Linden et al., 2008; Stys et al., 2012).

Given its high level of expression in hippocampal neurons, it is not surprising that PrP^{C} also plays an important functional role in these cells. Thus, in recent years, this issue was investigated by using knockout and transgenic mice. Indeed, several lines of evidence support the idea that PrP^{C} has neuroprotective functions and affects cell survival upon stress (Brown et al., 1997). For example, the PrP-null hippocampal cultures are susceptible to cell death induced by serum deprivation (Kuwahara et al., 1999), a process that appears to be linked to disruption of a function exerted normally by the N-terminal of PrP^{C} (Haigh et al., 2009). Moreover, PrP KO mice display an increased sensitivity to pharmacologically-induced seizures (Walz et al., 1999) and show a lower threshold for pain (Meotti et al., 2007; Gadotti and Zamponi, 2011). Interestingly, the enhanced pain responses in PrP KO mice can be ablated by the NMDAR antagonist MK801, indicating an involvement of glutamatergic pathways (Gadotti and Zamponi, 2011). This observation is in agreement with recent work from our lab. Indeed, mice lacking PrP^{C} show increased NMDAR activity in part due to an enhanced contribution of slowly deactivating GluN2D subunits (Khosravani et al., 2008). In addition to the essential role of neuroprotection, PrP^{C} is thought to be involved in regulating neuronal excitability and synaptic activity. Specifically, PrP-null mice display an enhanced basal excitability due to enhanced

NMDAR function (Khosravani et al., 2008). This study is in agreement with a previous study by Collinge (Collinge et al., 1994) showing altered synaptic transmission in PrP-null mice. Indeed, PrP-null neurons show increased amplitude and longer decay times of the NMDAR-mediated miniature excitatory postsynaptic currents (mEPSCs) (Khosravani et al., 2008). Notably, an increased susceptibility to glutamate toxicity can also be observed in those neurons with enhanced NMDAR function. Along these lines, PrP^C appears to play a neuroprotective role by suppressing the activity of NMDAR, which is further supported by evidence that PrP^C regulates the activity of other types of glutamate receptors including kainate (Rangel et al., 2007) and metabotropic glutamate receptors (Beraldo et al., 2011). More recent work has revealed that PrP^C regulates NMDAR function and glycine co-agonist activity by virtue of its copper binding properties (You et al., 2012). Altogether, NMDARs play a role in the PrP-mediated physiological functions, especially in the context of neuronal cell excitability within synapses and entire circuits.

A functional role of PrP^C in synapses is also suggested based on its high expression in both presynaptic and postsynaptic locations (Herms et al., 1999; Haeberle et al., 2000). More specifically, an impairment of LTP in PrP^C KO mice reveals an involvement of PrP^C in synaptic activity (Collinge et al., 1994; Manson et al., 1995). This result is highly consistent with evidence that PrP-null mice show deficits in spatial learning (Criado et al., 2005). In addition, a role for PrP^C in promoting synapse maturation was revealed (Kanaani et al., 2005). In this study, the authors found that incubation of cultured hippocampal neurons with recombinant PrP^C led to an increase in differentiation of axons and dendrites, and increased the number of synaptic contacts, highlighting a role in hippocampal development and the formation of functional synapses. Work in immature hippocampal slice has revealed a role of PrP^C in regulating synaptic plasticity and information processing in the developing hippocampus (Caiati et al., 2013).

Based on several lines of evidence, it has become increasingly clear that PrP^C is required for hippocampal development and the maintenance of physiological hippocampal function. Furthermore, interference with PrP^C function leads to epilepsy, neuropathic pain and impairment of learning and memory (Stys et al., 2012). Here, I focus on a new role of PrP^C in regulating HCN channels, and its consequence for neuronal excitability.

1.5.1 PrP^C, ion channels and neuronal excitability

PrP^C has been associated with a variety of ion channels whose functions are mostly correlated with the intrinsic physiology of neurons. Therefore, it may not be surprising to observe altered firing properties in hippocampal neurons from PrP KO animals. The hypothesis is supported with the discoveries of several electrophysiological and morphological abnormalities in hippocampal neurons from PrP KO mice (Collinge *et al*., 1994; Colling *et al*., 1996; Colling *et al*., 1997). First, an abnormal type A γ-Aminobutyric acid (GABA-A) inhibition has been reported in PrP-null mice (Colling *et al*., 1996) that may contribute to increased network excitability and, consequently, epileptiform activity. Second, PrP-null mice display aberrant sprouting of mossy fibres which is similar to sprouting induced by seizures (Colling *et al*., 1997), indicating that this reorganization of neuronal circuitry may contribute an "epileptic neuronal network". Third, a reduction in slow afterhyperpolorization currents (I_{AHP}), which is of fundamental importance for neuronal excitability, is evident in PrP-null mice (Colling *et al*., 1996; Herms *et al*., 2001; Mallucci *et al*., 2002; Fuhrmann *et al*., 2006). Although this reduction has long been reported, debates are on-going on the ionic mechanism that underlies enhanced neuronal cell excitability in the absence of PrP^C. In theory, the Ca^{2+} -activated potassium channel underlying the I_{AHP} mainly depends on calcium influx through L-type Ca^{2+} channels (VGCCs) (Sah and Clements, 1999; Bond *et al*., 2004; Pedarzani *et al*., 2005). Subsequently, Herms et al. found that the defect in slow AHP was indeed induced by an alteration in VGCC function in CA1 hippocampal neurons (Fuhrmann *et al*., 2006). However, this could not be observed in cerebellar granule neurons (Herms *et al*., 2000). A recent study by Powell and colleagues led to a new theory that neither K^+ channels nor voltage-gated Ca^{2+} channels are responsible for the disrupted I_{AHP} in PrP-null CA1 pyramidal neurons (Powell *et al*., 2008). Instead, increased intracellular Ca^{2+} buffering capacity and clearance of Ca^{2+} were reported as potential causes.

Taken together, it appears that there are multiple ways by which the absence of PrP^C can alter neuronal excitability at the single cell and entire network levels. However, the underlying ionic mechanism which drives increases in intrinsic excitability has not been extensively studied and remains controversial. Given its important role in the regulation of membrane excitability, HCN channels are an attractive candidate target for PrP^C.

1.5.2 PrP knock-out mice

There are several ways to study the physiological function of a protein. One of these is working with KO animals or cells derived from them. Therefore, a large number of studies have used PrP KO mice to explore the physiological function of PrP^{C}. Several lines of mice devoid of the PRNP gene which encodes PrP^{C} have been generated by homologous recombination in embryonic stem cells, including widely used Prnp0/0[Zürich] and $Prnp^{-/-}$[Edinburgh] (Büeler et al., 1992; Manson et al., 1994). Initial studies on those mouse lines revealed a mild pathology, such as a slight impairment of spatial learning as noted above (see section on PrP^{C} in the hippocampus), but, otherwise, a normal development (Büeler et al., 1992; Manson et al., 1994; Criado et al., 2005). Work has been extended with other lines of mice in an extensive ablation of the PRNP gene background ($Prnp^{-/-}$[Nagasaki], Rcm0, $Prnp^{-/-}$ [Zürich II]), in which not only reading frames, but their flanking regions are deleted. As a result, these mice present severe ataxia and Purkinje cell degeneration in later life (Sakaguchi et al., 1996; Moore et al., 1999; Silverman et al., 2000; Rossi et al., 2001; Weissmann and Flechsig, 2003). It was subsequently discovered that disruption of Dpl (a downstream gene of Prnp) is the cause of Purkinje cell loss in Nagasaki-type PrP KO mice (Weissmann and Flechsig, 2003). Apparently, the various phenotypes derived from those mouse lines are closely correlated with the approach taken for gene deletion. It is widely accepted that prion diseases result from accumulation of scrapie PrP^{SC} which is converted from normal PrP^{C} (Sailer et al., 1994). Due to a lack of substrate for generation of PrP^{SC}, PrP^{C} KO mice are resistant to prion infection. However, PrP KO mice appear to be vulnerable to various insults directed at the nervous system. As noted above, PrP^{C} KO mice display increased sensitivity and enhanced mortality in response to pharmacologically induced seizures (Walz et al., 1999). In addition, PrP^{C} KO (Zürich I) mice present aggressive and prolonged neuroinflammation upon experimental autoimmune encephalomyelitis (EAE) induced by immunization (Tsutsui et al., 2008). A further study documents that PrP KO (Zürich I) mice show reduced level of anxiety upon restraint or electric foot shock (Nico et al., 2005). In line with these results, more recent studies in our lab have reported that PrP KO (Zürich I) mice display depressive-like behavior (Gadotti et al., 2012), and show a decreased nociceptive threshold in models of inflammatory and neuropathic pain (Gadotti and Zamponi, 2011).

Taken together, these investigations support the conclusion that PrP^C is of critical importance for rodent physiology. Furthermore, PrP KO mice in Zürich I strains are well recognized to display a host of electrophysiological abnormalities. Therefore, the Zürich I strain will be used to explore how PrP^C regulates intrinsic physiology of hippocampal neurons in this study.

1.5.3 Signaling and interacting proteins

PrP^C is a GPI-anchored protein that mostly resides in lipid raft microdomains on the plasma membrane (Westergard et al., 2007) where a variety of signaling molecules are enriched (Kasahara and Sanai, 2000). However, its polypeptide chain is exposed to the extracellular milieu A large body of research has been carried out to search for PrP^C-associated extracellular proteins in order to support the idea that PrP^C acts as a signal transducer during functions such as neuroprotection (Chiarini et al., 2002; Zanata et al., 2002), neuronal excitability (Khosravani et al., 2008), cell adhesion, neurite outgrowth, neuronal toxicity, and neuronal survival (Linden et al., 2008; Biasini et al., 2012). Consistent with this concept, researchers first studied cyclic AMP (cAMP)/protein kinase A (PKA) signaling pathways by which PrP^C binding to stress-inducible protein 1 (STI1) produced neuroprotective effects in rat retinal explants (Chiarini et al., 2002; Zanata et al., 2002), and in the hippocampus (Lopes et al., 2005). Later on, a study by Vassallo et al (Vassallo et al., 2005) has identified PrP^C-copper binding-dependent recruitment of the phosphatidylinositol 3-kinase (PI3-kinase) cascade as important for cell survival. Moreover, the N-terminal region of PrP^C has been proposed to protect cells from reactive oxygen species (ROS) by binding to copper (Brown et al., 2001). In particular, recent work in the Zamponi lab, involving direct activation of NMDARs, has revealed that PrP^C physically interacts with NMDARs, and that this interaction mediates an allosteric, copper-dependent reduction in the affinity of the receptor for the co-agonist glycine (You et al., 2012; Stys et al., 2012). Based on several lines of evidence, the N-terminal domain of the copper binding sites on PrP^C appears to be a signal transducer that triggers intracellular signalling cascades that finally translate into regulation of several physiological functions. Therefore, the entire signalling pathway mediated by N-terminal domain must be tightly controlled to maintain normal physiological functions in the brain. The PrP^C-mediated molecular signaling pathway that regulates intrinsic neuronal excitability remains to be elucidated.

1.6 Association of HCN channels and T-type Ca^{2+} channels in the brain

1.6.1 T-type Ca^{2+} channel structure and biophysical properties

Calcium channels can be largely divided into two categories: high-voltage activated (HVA: L-type, P/Q-type, N-type, R-type) and low-voltage activated Ca^{2+} channels (LVA: T-type). Unlike HVA Ca^{2+} channels that usually require large membrane depolarizations to open, LVA T-type Ca^{2+} channels have low gating threshold and give rise to rapidly inactivating "transient" (T-type) currents (I_T) (Catterall et al., 2000, Catterall et al., 2005, Zamponi et al., 2015). T-type channels were first identified in nervous (Carbone and Lux, 1984) and cardiac tissues (Nilius et al., 1985), where the involvement of T-type channels in important cellular functions, such as cell excitability, oscillations, and cardiac pacemaking have been intensively studied (Catterall et al., 2005, Catterall, 2011, Zamponi et al., 2015).

At the molecular level, three different α1 subunits have been identified: α1G, α1H and α1I. These are now termed Cav3.1, Cav3.2 and Cav3.3 (Figure 1-5) (Catterall, 2000, Zamponi et al., 2015). Unlike HVA channels, T-type channels only consist of α1 pore-forming subunits and have no auxiliary subunits (Catterall et al., 2005, Zamponi et al., 2015). All of the Cavα1 subunits have the same membrane topology of four transmembrane domains (I-IV) (Figure 1-5), each of which contains six transmembrane segments (S1-S6) connected by intracellular linkers and cytoplasmic N- and C-termini. The C-terminus is very important for the regulation of channel gating activity (Staes et al., 2001). Cloning and sequence analysis of calcium channels have revealed that S4 segment of α1 subunit is positively charged due to the presence of the amino acids, arginine and lysine (Figure 1-5). This highly charged region, called the voltage sensor, detects changes in transmembrane voltage and allows the channel to open and close in response to membrane potential changes (Catterall, 2000, Iftinca and Zamponi, 2008).

It is well known that the classification of voltage gated Ca^{2+} channels is based on their voltage-dependent and pharmacological properties. LVA T-type channels are thus well distinguished from HVA-Ca^{2+} channels. First, T-type channels have a tiny single-channel conductance about 1 pS at physiological Ca^{2+} concentration (2 mM) (Huguenard, 1996) and, about 4~5 pS when using 10mM extracellular Ca^{2+} (Balke et al., 1992). Second, Cav3.1 and Cav3.2 display more rapid gating kinetics, whereas Cav3.3 displays a much larger time constant

of activation and inactivation (activation time constant at -10 mV, Cav3.3 (7 ms) > Cav3.2 (2 ms) > Cav3.1 (1 ms); inactivation time constant at -10 mV, Cav3.3 (69 ms) > Cav3.2 (16 ms) > Cav3.1 (11 ms)) (Catterall et al., 2005). Third, they have 'low' gating thresholds for both activation and inactivation (Perez-Reyes, 2003), allowing them to operate near the resting membrane potential. Fourth, a "window current" is induced and thus defined due to the overlap of activation and steady-state inactivation of T-type channel, which provides a mechanism for constant Ca^{2+} influx even at resing membrane potentials (Crunelli et al., 2005). Finally, T-type channels are insensitive to most blockers of HVA Ca^{2+} channels and non-selectively inhibited by Ni^{2+} (Perez-Reyes, 2003).

1.6.2 Functional roles of T-type channels

T-type channel isoforms are widely and differentially expressed throughout the brain and peripheral tissues (Table 1) (Catterall et al., 2005, Iftinca and Zamponi, 2008). As expected from their unique functional properties, T-type channels have been linked to a variety of physiological functions including gene transcription, cardiac pacemaking, neuronal excitability and secretion (Catterall, 2011, Zamponi et al., 2015).

First, their subcellular distribution of nervous tissue in a cell-specific fashion is often found in the cell body and dendrites where they partake in regulating neuronal excitability by contributing to the initiation of repetitive discharges (McKay et al., 2006, Todorovic and Jevtovic-Todorovic, 2006, Zamponi et al., 2009). Specifically, the unique biophysical properties attributed to T-type channels permits them to lower the AP threshold (Matthews and Dickenson, 2001), to promote bursting activity (Jahnsen and Llinas, 1984) and to generate subthreshold membrane oscillations (McCormick and Bal, 1997). For example, evidence that T-type channels play a critical role in bursting activity originally comes from studies in cells of the deep cerebellar nuclei where the 'rebound burst' was first identified (Gardette et al., 1985, Jahnsen, 1986). Subsequently, extensive in vitro studies have demonstrated that the cells in the 'bust mode' indeed through the interaction between subthreshold-operated I_h and I_T (Biel et al., 2009). Normally, a large portion of T-type channels is tonically inactivated at rest. Due to a low-threshold range of activation and inactivation for T-type channels, a brief membrane hyperpolarization by inhibitory inputs recovers T-type channels from inactivation, therefore

increasing the number of channels that are available for open upon subsequent membrane depolarization. Under physiological conditions, a small membrane depolarization by activated I_h is sufficient to induce a rebound low-threshold Ca^{2+} spike, therefore facilitating membrane depolarization and subsequently inducing a series of typical Na^+ spikes. The high depolarization during the spike deactivates I_h and inactivates $I_{T,}$ and therefore the low-threshold Ca^{2+} spike is terminated followed by a hyperpolarizing "overshoot". In turn, I_h is acitvated, the cycle resumes and a continuous rhythmic burst occurs (Biel et al., 2009). The single cell oscillations by the interplay of I_h and I_T are then synchronized in a large circuit (like the thalamocortical circuit) (McCormick and Bal, 1997), which in turn contributes to synaptic plasticity of cortical and thalamic neurons (Steriade et al., 2003) and sleep rhythms (Steriade et al., 1991, Steriade et al., 1993, Lee et al., 2004). In the heart, the rhythmic burst activity has been implicated in cardiac rhythmicity of the sinoatrial node where I_T and I_h interplay to induce "pacemaker" currents (Mangoni et al. 2006). This process appears to be modulated by the direct effects of cAMP on HCN channels (Biel et al., 2009). In addition to an interplay with I_h on neuronal excitability, T-type channels are thought to be physically and functionally associated with Ca^{2+}-dependent K^+ channels to regulate neuronal and synaptic activity (Turner and Zamponi, 2014). Moreover, it has been reported that all three T-type channel isoforms undergo extensive alternative splicing, which further enhances the functional complexity to the overall spectrum of T-type currents (Zamponi et al., 2015).

Altogether, the unique properties, pharmacological profile and distinct cellular and subcellular distribution endow voltage-activated T-type Calcium channels with a critical role in a wide range of physiological processes. Therefore, the dysregulation of T-type channels has been linked to several pathological diseases, such as epilepsy and pain (Iftinca and Zamponi, 2008). In particular, the low-voltage gating threshold for I_T and I_h allows a cross-talk between HCN and T-type channels which appears to be essential to some functional outputs.

1.6.3 Signal processing by T-type channel interactions

Although, T-type channels are primarily voltage operated, their activity is also regulated by second messengers (Iftinca and Zamponi, 2008). Several actions of cellular signal regulation on T-type channel activity were described. First, activation of different types of G-protein-coupled receptors triggering corresponding downstream second messenger pathways differentially

regulates T-type channel activity. Second, many phosphorylation sites for protein kinases, including PKA (Kim et al., 2006), PKC (Park et al., 2006), CaMKII (Welsby et al., 2003) and Rho kinase (Iftinca et al., 2007), etc. have been identified within T-type channels, supporting the regulatory role of these kinases on T-type channel activity (Chemin et al., 2006). Notably, the cross-talk among individual signaling pathways would likely trigger a complex series of signaling events in T-type channels.

In addition to the interaction with second messengers, Cav3 channels have been reported to be functionally and physically associated with other ion channels, including SK (KCa2.x) (Wolfart and Roeper, 2002), IK (KCa3.1), BK (KCa1.1) and Kv4 potassium channels (Kv4.1–4.3) (Turner and Zamponi, 2014). The relationships with these ion channels via direct or indirect interaction may further diversify the functional roles of Cav3 channels. For example, calcium influx through Cav3 channels had been identified to trigger the activation of calcium sensor, KChIP3 which, in turn, led to a hyperpolarizing shift in the voltage inactivation of Kv4 (A-type) current in cerebellum and, an altered firing behavior of cerebellar stellate cells (Anderson et al., 2010a; Anderson et al., 2010b). This study indicates that in addition to the established role in producing rebound burst activity, Cav3 channels prove capable of regulating neuronal excitability by forming a signaling complex with Kv4 channels. Furthermore, our lab recently reported a novel interplay between Cav3.2 and BK channels at both molecular and functional levels. In this study, it was found that Cav3.2 calcium influx altered current density and voltage-dependent gating of KCa1.1 channels in tsA-201 and medial vestibular neurons (MVN) (Rehak et al., 2013). Importantly, this Cav3.2-KCa1.1 complex was likely to be functionally significant, as the results observed were not only limited to altered biophysical properties of KCa1.1, but also the spike output in rat MVN cells appeared to be regulated. Furthermore, a recent study by Engbers and his colleagues revealed a novel nanodomain interaction between KCa3.1 and Cav3.2 channels (Engbers et al., 2012). In this study, the authors first confirmed cerebellar expression of KCa3.1 channel, which contrasts with previous findings that KCa3.1 channels were not believed to be expressed in central neurons. Furthermore, a physical complex of KCa3.1 channels with Cav3.2 from rat cerebellar lysate was demonstrated at the molecular level. In particular, this molecular complex appears to be the foundation by which KCa3.1 channels sense the intracellular Ca^{2+} changes associated with Cav3 influx at the level of a nanodomain. Importantly, the depolarizing effect of Cav3 channels was inverted when coupled with KCa3.1

leading to a suppression of termporal summation, which suggests a molecular and functional interplay between Cav3.2 and KCa3.1 channels.

Altogether, calcium influx through Cav3 channels appears to be a critical trigger to activate potassium channels which, in turn, regulate physiological process in neurons, although the underlying mechanism by which the host potassium channels sense calcium signal varies.

In addition to the identified molecular and functional complex formed with Kv4 or calcium-activated potassium channels, Cav3 channels have also been found to be functionally interact with HCN channels at synapses. Unlike the association with potassium channels, the interplay of Cav3 with HCN channels appears to be reciprocal. First, a cross-talk between T-type Ca^{2+} channels and HCN channels has been observed in both hippocampal and entorhinal cortical neurons and was shown to increase Cav3 inactivation, leading to alterations in presynaptic function (Tsay et al., 2007, Huang et al., 2011). Further, both I_h and I_T act within the subthreshold range, thus allowing for the regulation of neuronal processing in a subthreshold voltage range (Magee et al., 1995, Swensen et al., 2003, Engbers et al., 2011, Kole et al., 2006, Rehak et al., 2013). The best illustration for this is called "rebound bursting" in which I_h acts synergistically with I_T to generate precise burst output (Engbers et al., 2011, McCormick and Pape, 1990, Sangrey and Jaeger, 2010). Like calcium influx via Cav3 channels required for Cav3 channels to initiate the relationship with potassium channels, the regulation of HCN channel activity could also be calcium dependent. In 1998, Luthi and McCormick solved a long-lasting debate about whether hyperpolarization-activated cation currents are sensitive to alterations in intracellular calcium, and reported a calcium-dependent upregulation of I_h during the generation of rebound calcium spikes in thalamocortical cells. It was found that calcium entry during rebound calcium spikes enhanced the slow ADP, shifted the activation of I_h to more positive potentials, and increased the activation time constant of I_h (Luthi and McCormick, 1998). The dependence on calcium was also tested through 2–5 mM Ni^{2+} or internal perfusion of BAPTA or EGTA (Luthi and McCormick, 1998). Although the specificity of the calcium source is not verified, the activated T-type current during repetitive hyperpolarizing current injection is thought to be involved in this calcium-mediated upregulation of I_h. An indirect mechanism has also been proposed in this study and was experimentally tested later. Specifically, an increase in intracellular Ca^{2+} was only required for induction, but not for maintenance of I_h upregulation.

Instead, calcium-mediated activation of AC and cAMP release modified HCN channels and induced a persistent Ca^{2+}-independent activation of I_h in thalamocortical neurons (Luthi and McCormick, 1999).

Altogether, HCN channels appear to be an important target for cellular signaling processes. Although a bulk of data strongly support a dual directional relationship between HCN and T-type channels, a molecular association or a direct biophysical test on either channel, like that shown for Cav3 and BK channels has not been determined.

1.7 Hypotheses and Aims

Based on this collective evidence I *hypothesize* that:

(1) HCN channels associate with PrP^C and this mediates an alteration of intrinsic physiology of hippocampal neurons.

(2) HCN channels physically and functionally interact with Cav3.2 T-type calcium channels regulating Cav3.2 channel activity.

Aims in study (1):

(1) Determine how the firing patterns of hippocampal neurons are altered in the absence of PrP^C.

(2) Determine the ionic mechanism underlying altered intrinsic excitability of hippocampal neurons. More specifically, determine how HCN channels associate with PrP^C regulating neuronal intrinsic excitability.

(3) Determine the PrP^C-mediated signaling pathway by which HCN channel activity is regulated in hippocampus.

Aims in study (2):

(1) Determine the physical interaction between HCN1 and Cav3.2 channel in mouse brain and tsA-201 cells.

(2) Determine whether this molecular relationship has a functional implication.

(3) Determine the binding regions in both HCN1 and Cav3.2 channels.

Figure 1-1: Schematic circuitry within a hippocampal slice

Areas are labeled with capital letters, projection pathways with perforant path, mossy fiber and Schaffer collateral. Entorhinal Cortex (EC), Dentate Gyrus (DG), perforant path (pp), mossy fibers (mf), Schaffer collateral (sc), Cornu Ammonis 1 (CA1), Cornu Ammonis 3 (CA3).

Figure 1-1 indicates these pathways along with their site of origin and their site of projection. Thw main input to the hippocampus (perforant pathway) arises from the EC and passes through to the DG. From the granule cells of DG, connections are made to area CA3 of the hippocampus via the mossy fibers. CA3 sends connections to CA1 pyramidal cells via Schaffer collaterals, named after the Hungarian anatomist-neurologist Károly Schaffer. The major neurotransmitter in these three pathways is the excitatory amino-acid L-glutamate. CA1 neurons also receive inputs directly from the perforant path and send axons to the Subiculum. These neurons in turn send the main hippocampal output back to the EC, forming a loop. Additionally, afferents from extrahippocampal structures provide glutamatergic input. An important one is the association/commissural pathway within the CA3, arising from commissural projections from the contralateral CA3 area, to form recurrent connections within CA3 cells.

Adapted from Mikkonen *et al.,* (2002).

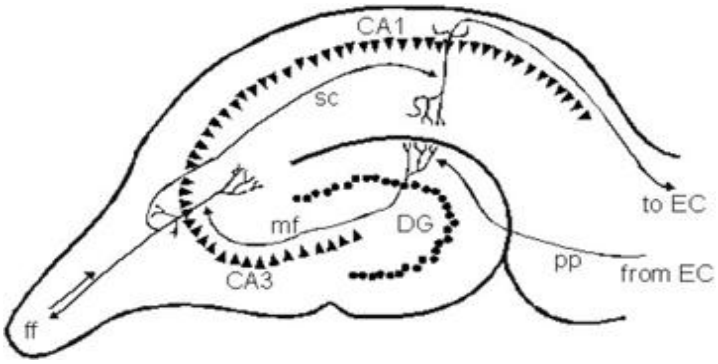
CA1
sc
to EC
mf
DG
pp
from EC
CA3
ff

Figure 1-2: An overview of HCN channel structure, expression and functional properties.

A, Left: The distribution of mRNA transcripts of HCN1 and HCN2 in hippocampus. Adapted from Santoro et al. (2000). Right: Representative immunoblots for HCN1 and HCN2 subunit proteins in membrane homogenates prepared from mouse hippocampi.

B, Left: The induction of I_h in response to a series of hyperpolarizing current injection. The voltage sag is subsequently induced by the inward I_h conductance and, characterized by an initial transient peak voltage response which settles to a less negative steady-state level within a few hundred milliseconds. Right: Steady-stage I_h activation is fitted with a single Boltzmann function in hippocampal CA1 pyramidal neurons, showing a half activation voltage of -90 mV for HCN channels, revealing partial opening at rest. Adapted from Chen et al. (2002).

C, Structure of HCN channel. The HCN subunit consists of an N-terminus, six transmembrane segments (S1-S6) and a C-terminus which is composed of the C-linker and the CNBD. The S4 helix is a voltage sensor carrying arginine of lysine residues. The ion conducting pore loop carries the GYG motif settling in between S5 and S6. Adapted from He et al. (2014).

D, Cartoon based on the cryo-electron microscopy structure of the human HCN1 channel, illustrating cAMP regulation in HCN1 channels. Adapted from Lee and Mackinnon, (2017).

A

mHCN1 mHCN2

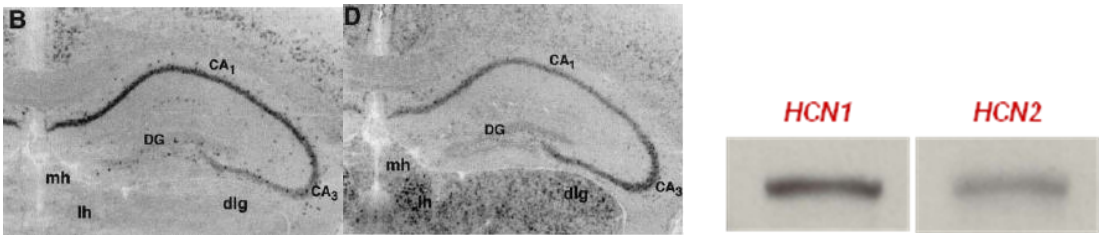

B

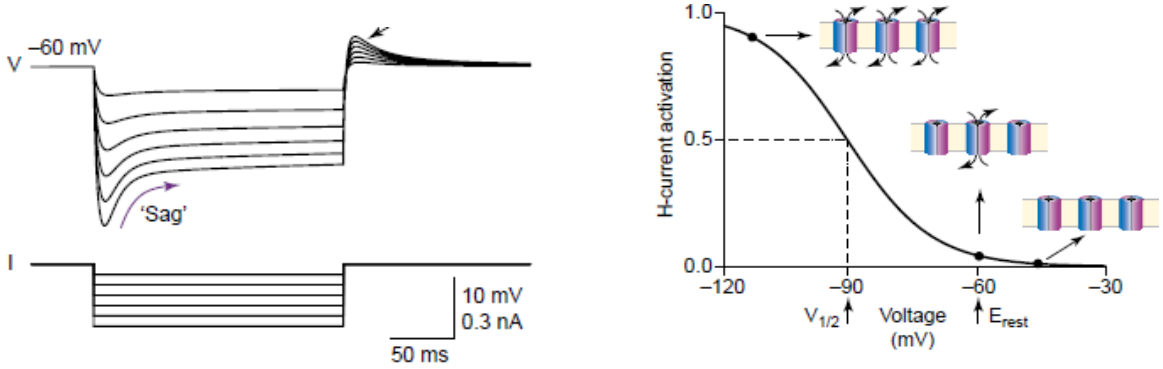

C

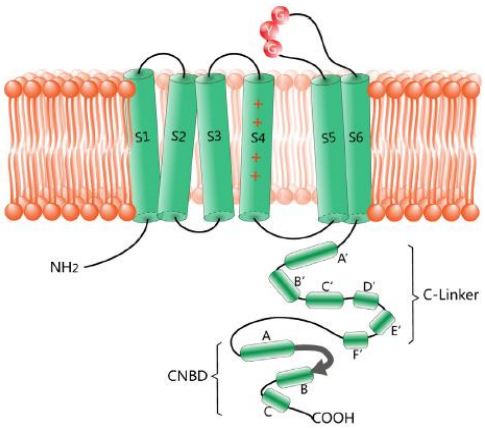

D

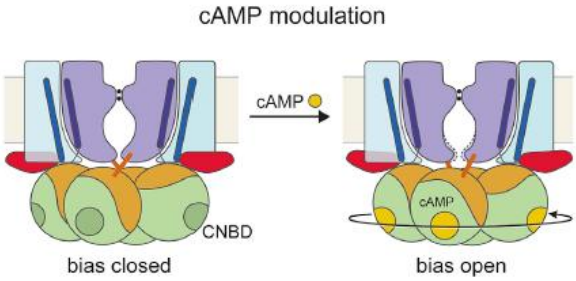

Figure 1-3: Summary of regulatory effects of various neurotransmitter and associated intracelullar signal pathways on HCN channels.

1) Glutamate (Glu) $\xrightarrow{(+)}$ NMDAR/AMPAR $\longrightarrow$ Ca^{2+} influx $\xrightarrow{(+)}$ CaMKII, activated CaMKII, in turn, either activates HCN channels through the interacting protein TRIP8b or inhibits HCN channels by Neuronal Restrictive Silencing Factor (NRSF) in pathological conditions.

2) PLC $\xrightarrow{(+)}$ PKC $\xrightarrow{(-)}$ HCN channels

3) p38MAPK $\xrightarrow{(+)}$ HCN channels

4) cAMP/cGMP $\xrightarrow{(+)}$ HCN channels

(+): Activate; (-): Inhibit.

Adapted from He et al, (2014).

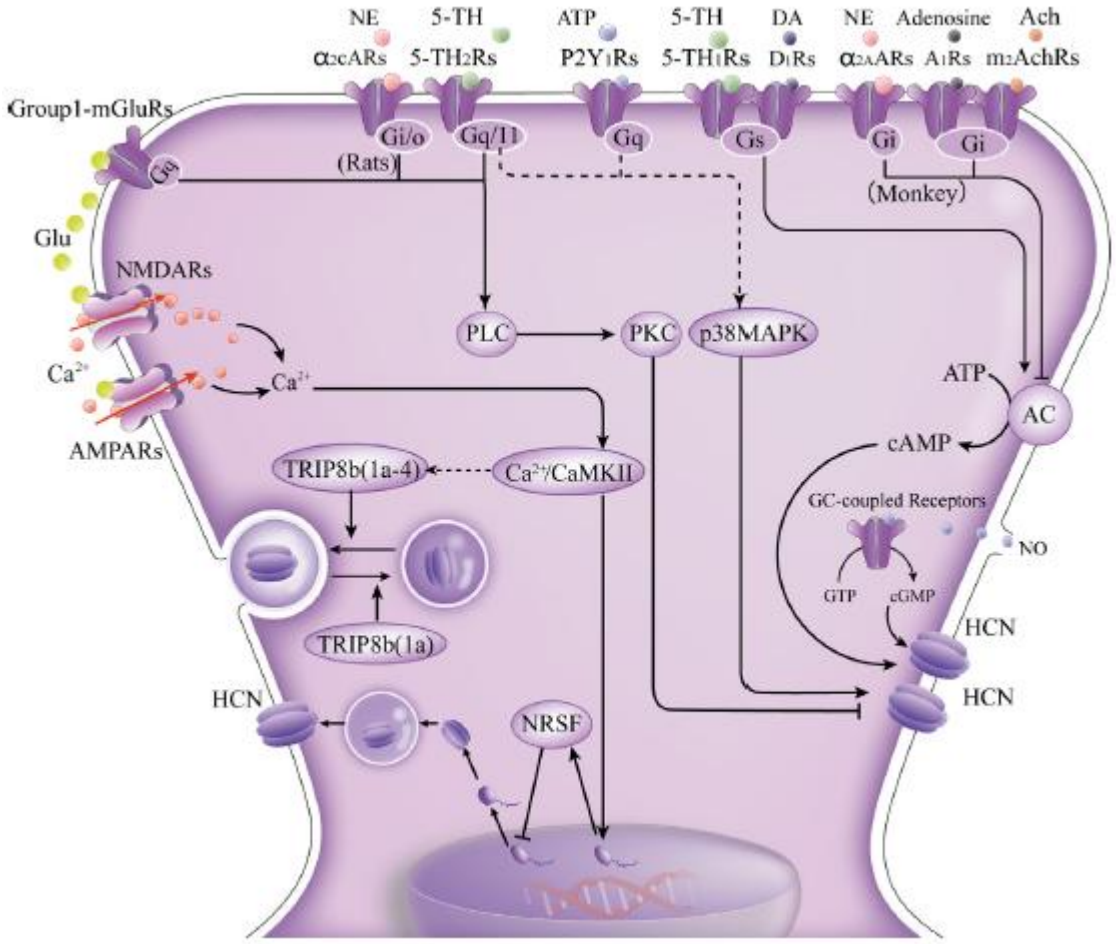
NE
5-TH
ATP
5-TH
DA
NE
Adenosine
Ach
α2cARs
5-TH2Rs
P2Y1Rs
5-TH1Rs
D1Rs
α2AARs
A1Rs
m2AchRs
Group1-mGluRs
Gi/o
Gq/11
Gq
Gs
Gi
Gi
(Rats)
(Monkey)
Glu
NMDARs
PLC
PKC
p38MAPK
ATP
AC
Ca2+
Ca2+
cAMP
AMPARs
TRIP8b(1a-4)
Ca2+/CaMKII
GC-coupled Receptors
NO
GTP
cGMP
HCN
TRIP8b(1a)
HCN
HCN
NRSF

Figure 1-4: Schematic representation of mouse cellular prion protein.

Cellular prion protein consists of a N-terminal part which includes a cleaved signal peptide (SP, residues 1-23), five histidine-containing octapeptide repeats (residues 51–90) which can bind Cu^{2+} and other bivalent metal ions, a central part, and a C-terminal part which includes three α-helices (α1: residues 143–152, α2: 171–191, and α3: 199–221), two β-sheets (β1: residues 127–129 and β2: 166–168), and a GPI-anchor signal (residues 230-253).

Adapted from Biasini et al. (2012).

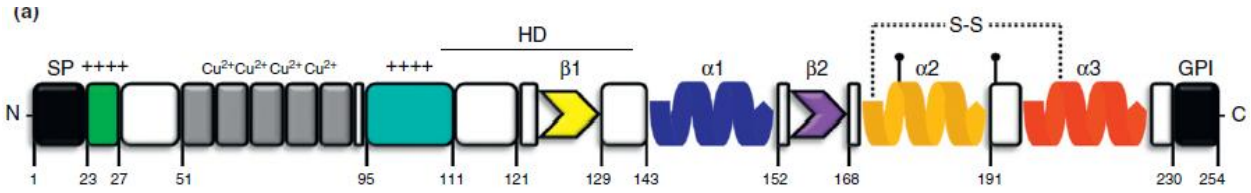
(a)
SP ++++
Cu2+Cu2+Cu2+Cu2+
++++
HD
β1
α1
β2
S-S
α2
α3
GPI
N
C
1
23
27
51
95
111
121
129
143
152
168
191
230
254

Figure 1-5. Transmembrane topology of T-type Ca^{2+} channels

Left, Membrane topology of a calcium channel α1 subunit (pore-forming) consisting of 4 domains (Domains I-IV) connected by cytoplasmic linkers. Each domain consists of 6 transmembrane helices and S5-helix-S6 pore loop. The positively charged fourth helix, S4, in each domain forms the voltage sensor. Right, Classification of voltage-gated T-type Ca^{2+} channels

Adapted from Iftinca and Zamponi, (2008).

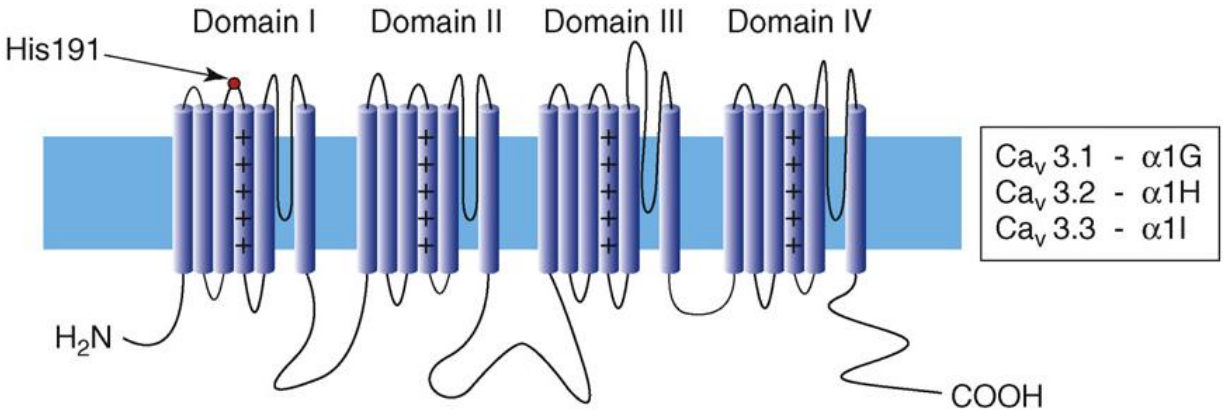
Domain I
Domain II
Domain III
Domain IV
His191
H_2N
COOH
Ca_v 3.1 - α1G
Ca_v 3.2 - α1H
Ca_v 3.3 - α1I

Table 1. Tissure distribution of T-type Ca^{2+} channel isoforms

Isoform	Distribution
Cav3.1	Brain, especially soma and dendrites of neurons in olfactory bulb, amygdala, cerebral cortex, hippocampus, thalamus, hypothalamus, cerebellum, brain stem ovary, placenta, heart.
Cav3.2	Kidney, rat smooth muscle, liver, adrenal cortex, brain (especially in olfactory bulb, striatum, cerebral cortex, hippocampus, reticular thalamic nucleus) and heart.
Cav3.3	Brain, especially olfactory bulb, striatum, cerebral cortex, hippocampus, reticular nucleus, lateral habenula, cerebellum.

References: Talley et al., (1999), Catterall et al., (2005), Mckay et al., (2006).

Chapter 2: Articles

2.1.1 Original article 1

Reduced Hyperpolarization-Activated Current Contributes to Enhanced Intrinsic Excitability in Cultured Hippocampal Neurons from $PrP^{(-/-)}$ Mice.

Fan J, Stemkowski PL, Gandini MA, Black SA, Zhang Z, Souza IA, Chen L, Zamponi GW

Front Cell Neurosci. Mar 24, 2016, 10:74

I contributed to this work by carrying out all the patch-clamp experiments in cultured hippocampal neurons and biochemical experiments, as well as performing corresponding data analysis. Moreover, together with my supervisor Dr. Gerald Zamponi, I designed this study and wrote the manuscript. P. L, Stemkowski was partially involved in designing the study and providing technical assistance, including teaching me to conduct whole-cell current clamp recordings. M. A. Gandini contributed to performing surface expression measurements (Figure 4A) and corresponding data analysis as requested by one of the referees. S.A, Black helped with doing some of primary cultures (WT and PrP-KO hippocampal neurons were used to test neuronal excitability as shown in Figure 1). Z, Zhang performed slice recordings as requested by referees. I. A, Souza and L, Chen provided technical assistance including instructions for western blotting and primary cultures, respectively.

Reduced hyperpolarization-activated current contributes to enhanced intrinsic excitability in cultured hippocampal neurons from $PrP^{-/-}$ mice

Fan, J., Stemkowski, P.L., Gandini, M.A, Black, S.A.G., Zhang, Z., Souza, I.A., Chen, L., and Zamponi, G.W.

Department of Physiology and Pharmacology, Hotchkiss Brain Institute, Cumming School of Medicine, University of Calgary, Calgary, Alberta T2N 4N1, Canada.

* Correspondence: Gerald W Zamponi, PhD; Cumming School of Medicine; University of Calgary
3330 Hospital Dr. NW; Calgary, T2N4N1; Canada
Email: zamponi@ucalgary.ca

Keywords: Cellular prion protein, HCN, excitability, I_h, hippocampus

Frontiers in Cellular Neuroscience | *www.frontiersin.org*

Published: 24 March 2016

doi: 10.3389/fncel.2016.00074

March 2016 | Volume 10 | Article 74

Abstract

Genetic ablation of cellular prion protein (PrP^C) has been linked to increased excitability and synaptic activity in the hippocampus. We have previously shown that synaptic activity in hippocampi of PrP-null mice is increased due to enhanced *N*-methyl-$_D$-aspartate receptor (NMDAR) function. Here, we focused on the effect of *PRNP* gene knock-out (KO) on intrinsic neuronal excitability, and in particular, the underlying ionic mechanism in hippocampal neurons cultured from P0 mouse pups. We found that the absence of PrP^C profoundly affected the firing properties of cultured hippocampal neurons in the presence of synaptic blockers. The membrane impedance was greater in PrP-null neurons, and this difference was abolished by the hyperpolarization-activated cyclic nucleotide-gated (HCN) channel blocker ZD7288 (100 μM). HCN channel activity appeared to be functionally regulated by PrP^C. The amplitude of voltage sag, a characteristic of activating HCN channel current (I_h), was decreased in null mice. Moreover, I_h peak current was reduced, along with a hyperpolarizing shift in activation gating and slower kinetics. However, neither HCN1 nor HCN2 formed a biochemical complex with PrP^C. These results suggest that the absence of PrP downregulates activity of HCN channels through activation of a cell signaling pathway rather than through direct interactions. This in turn increases membrane impedance to potentiate neuronal excitability in cultured hippocampus neurons.

Introduction

Cellular prion protein (PrP^C) is a naturally occurring protein, whose abnormal conformation can lead to a range of neurological disorders including Creutzfeldt-Jakob disease, Kuru and bovine spongiform encephalopathy (Knight and Will, 2004). This abnormal protein accumulates in the brain, forming polymeric aggregates that disrupt synapses, leading to loss of dendrites and finally neuronal death (Soto and Satani, 2011). Although this pathological role of misfolded PrP^C has been established and studied, the function of PrP^C in the normal brain remains largely unknown (Black et al., 2014; Linden et al., 2008; Stys et al., 2012; Zamponi and Stys, 2009). Initial studies with PrP-null mice revealed a mild pathology, such as a slight impairment of spatial learning (Collinge et al., 1994; Manson et al., 1995), but, otherwise, a normal development (Bueler et al., 1992; Criado et al., 2005; Manson et al., 1994). However, several lines of evidence show that PrP-null hippocampal neurons display enhanced susceptibility to cell death induced by serum deprivation (Haigh et al., 2009; Kuwahara et al., 1999), and to glutamate excitotoxicity (Khosravani et al., 2008), together indicating a central role of PrP^C in neuroprotection. Growing evidence supports the idea that the loss of PrP^C function interferes with normal neuronal activity, and therefore contributes to synchronized activities underlying neocortical and hippocampal seizures (Walz et al., 2002). More specifically, recordings from PrP-null neurons in vitro showed a variety of electrophysiological abnormalities, with reduced Ca^{2+}-dependent K^+ currents (Colling et al., 1996), abnormal GABA-A receptor inhibition (Collinge et al., 1994), as well as a significant reduction of afterhyperpolarization potentials (AHP) (Colling et al., 1996; Fuhrmann et al., 2006; Herms et al., 2001; Mallucci et al., 2002). However, the possibility of altered Ca^{2+} homeostasis, rather than electrical abnormalities, has been recently highlighted as a possible reason for the reduced slow AHP in PrP-null mice (Powell et al., 2008). Despite this progress, we do not yet fully understand how PrP^C regulates neuronal output.

In a previous study, we reported that PrP-null mice display enhanced synaptic activity that then gives rise to increased network excitability due to augmented *N*-methyl-$_D$-aspartate receptor (NMDAR) function (Khosravani et al., 2008). Here, we focused on the ability of PrP^C to regulate intrinsic neuronal firing properties. It is expected that differences in membrane excitability extend to the ionic mechanisms which drive neuronal cell electrical activity. Among various ion channels, the HCN1 and HCN2 channels are of particular interest. First, they are highly

expressed in the central nervous system and are critically related to neuronal excitability at both single-cell and network levels, particularly in the hippocampus (Robinson and Siegelbaum, 2003). Second, changes in HCN channels have been implicated for animal models of neurological disorders such as pain and epilepsy (Biel et al., 2009; Noam et al., 2011). We found that intrinsic excitability was enhanced in PrP-null hippocampal neurons, which is attributed to an increased input resistance and a related down-regulation in hyperpolarization-activated cyclic nucleotide-gated (HCN) channel activity in hippocampal cultures from P0 mice, but not in adult mouse hippocampal slices. These findings indicate that functional regulation of HCN channels by PrP^C might have an important role in maintaining normal electrical signals in the brain.

Materials and Methods

Primary hippocampal culture preparation

As previously described, mice used in these experiments were wild-type (WT) C57BL/6 mice and a PrP knock-out (KO) Zuerich 1 strain outbred to a pure C57 genetic background by Frank Jirik's laboratory (University of Calgary, Canada) (Khosravani et al., 2008; You et al., 2012). Primary hippocampal cells were obtained from P0-P1 pups as described by us previously (Khosravani et al., 2005; You et al., 2012). Cells were maintained in culture for 10-13 days (DIV 10-13) before experimentation.

Immunoblots and co-immunoprecipitations (co-IPs)

HCN1 and HCN2 protein levels were measured using a standard protocol as described by us previously (Khosravani et al., 2008). Two different protein loading amounts (100 and 150 μg) were used in each condition in order to verify a linear range of signal detection. Membranes were probed with mouse anti-HCN1 (1:500, Neuromab, 75-110) or mouse anti-HCN2 (1:500, Neuromab, 75-111). For co-IPs, mouse hippocampi were homogenized in cold lysis buffer with protease inhibitor and treated with 1 μM $CuSO_4$, and co-IPs between HCN1 or HCN2 and PrP^C were performed as described by us previously (Khosravani et al., 2008). Complexes were precipitated with the mouse anti-PrP 6H4 antibody (Prionics USA), and immunoblots were probed with mouse anti-HCN1 or mouse anti-HCN2 antibodies (1:500, Neuromab).

Electrophysiology

Whole-cell voltage and current clamp recordings from cultured neurons were performed in a bath solution containing (mM) 150 NaCl, 5 KCl, 2.5 $CaCl_2$, 1 $MgCl_2$, 10 HEPES and 10 D-glucose (adjusted to pH 7.4 with NaOH). The intracellular pipettes were pulled from borosilicate glass (with an impedance of 3-5 MΩ) and filled with an intracellular solution containing (mM) 130 KGluconate, 4 Mg-ATP, 0.3 Na-GTP, 10 EGTA, 2 $CaCl_2$ and 10 HEPES (adjusted to pH 7.2 with KOH; osmolarity 310-320 mOsm). Whole-cell recordings were made from hippocampal cultures at room temperature using an Axopatch 200B amplifier (Axon Instruments) with Clampex 9.2 software running on a computer to acquire data. Neurons were placed in bath solutions for 15-30 minutes prior to recordings. Electrical activity was assessed in current- and voltage-clamp configurations. Current-clamp recordings from neurons that had membrane potentials more negative than -50 mV were included in the analysis. The holding membrane potential was manually adjusted to -70 mV. During recordings, the command potential was monitored and compensated for the voltage drop across the electrode. The injecting currents for compensation were less than 100 pA. Series resistance in voltage-clamp recordings was compensated 50-70% and continually monitored through experiments. Recordings were terminated whenever significant increases (≥20%) in access resistance occurred. Voltage and current signals were filtered at 2 kHz and sampled at 5 kHz and 20 kHz (Digidata 1320A, Molecular Devices), respectively, in all experiments. Slice recordings from adult hippocampal slices were prepared as described by us previously (Khosravani et al., 2008) in the presence of synaptic blockers.

Current-clamp recordings

To investigate the firing patterns of neurons, 250 ms depolarizing current steps from -200 pA in increments of 50 pA were applied from a holding potential of -70 mV. The latency of each AP (cumulative latency) was measured in response to 0.7 nA, 500 ms depolarizing current ramps for the greatest number of both type of neurons to fire APs. APs were generated with 5-ms depolarizing current pulses. Electrical membrane properties, including resting membrane potential (E_m), $AP_{amplitude,}$ AP duration at 50% amplitude (AP half-width), maximum rate of depolarization (*dV/dtmax*), maximum rate of repolarization (*rV/rtmax*) were analyzed. The AP threshold was measured at rest by off-line differentiation of voltage traces, thereby determining

the first point on the rising phase of an AP where the rising rate exceeds 50 mV/ms (Stemkowski and Smith, 2012). In response to a -350 pA hyperpolarizing pulse with 800 ms duration, voltage sag amplitude was measured. Percentage sag was calculated using the equation: $Sag\ ratio = (\frac{Vpeak-Vss}{Vpeak}) \times 100\%$, where $Vpeak$ is the maximum voltage deflection and Vss is the steady state voltage at the end of the hyperpolarizing pulse (George et al., 2009).

Voltage-clamp recordings

Input resistance (Rin) was determined by a brief 20 mV hyperpolarizing pulse (from -70 mV to -90 mV, 40 ms duration) and reflected by a steady-state current. I_h was recorded in external and internal solutions that were the same as those used for AP recordings. I_h was evoked by a series of hyperpolarizing voltage steps from -50 mV to -150 mV in increments of 10 mV and also in decreasing durations from 4 s to 2 s. The amplitude of I_h was measured as the difference between the steady-state current at the end of each test potential and the instantaneous current immediately following each test potential. Under these recording conditions, the presence of I_h could be confirmed by susceptibility to the specific HCN channel blocker, ZD7288. The kinetics of I_h activation were best determined by fitting onset of the current with a single-exponential function: f (t) = Ae (-t/τ)+C. Additionally, to assess voltage-sensitivity of I_h, the half-maximal activation ($V_{0.5}$) was determined by fitting individual conductance-voltage (G-V) relationships to a Boltzmann function: G = Gmax/[1+exp(−(Vm−V0.5)/k)] , where $Gmax$ is the mean value of fit maximal conductance, $V0.5$ is the membrane potential for the half-activation and k is the slope factor. The conductance was calculated according to the equation: G =I_h/(Vm-Eh), where G is the conductance, I_h is the HCN tail current, Vm is the holding potential, and Eh is the reversal potential of I_h. The reversal potential of I_h was determined to be -46 ± 2 mV by linear extrapolation to the peak of the tail current from clamping at potentials between -40 and -80 mV.

Drugs and drug application

In all recordings, the ionotropic glutamate antagonists $_{D, L}$-APV (50 µM) and DNQX (20 µM) were added to the external solution. In voltage-clamp recordings, tetrodotoxin (TTX, 1 µM) and $BaCl_2$ (0.5 mM) were added to the external bath to improve isolation of I_h. Forskolin (20 µM)

was bath applied for pharmacological studies of HCN channels. ZD7288, DNQX, $_{D, L}$-APV and TTX were acquired from Tocris Bioscience. Other chemicals were from Sigma.

Data arrangement and statistical analysis

Statistical analyses were performed using Origin9 and Sigmaplot10.0. The cumulative latency analysis was conducted through the seventh current ramp step (0.7 nA) in order to reach the maximal numbers of spikes in both groups. Data are expressed as means ± SEM. Statistical analyses were done using two-tailed unpaired Student's *t*-tests. Significance was set at $p < 0.05$.

Results

Membrane properties and enhanced intrinsic excitability in cultured PrP-null neurons

Our previous studies demonstrated that mice lacking PrP^C display increased synaptic activity in part due to enhancement of NMDAR function (Khosravani et al., 2008). Here, we focused on intrinsic excitability of hippocampal neurons by examining the firing pattern and membrane properties of hippocampal neurons from PrP-null mice.

We used intracellular recordings from cultured hippocampal pyramidal neurons to characterize the effect of PrP^C on hippocampal neuron intrinsic excitability in the presence of synaptic blockers DNQX (20 µM) and $_{D, L}$-APV (50 µM). We found that the lack of PrP^C strongly affected firing properties of hippocampal neurons, increasing number of APs (Figure 1A and 1B) and decreasing the spike threshold (Figure 1C) in response to 250 ms depolarizing step current injections (369.2 ± 28.6 pA for WT (n=13) vs. 140.0 ± 14.5 pA for KO (n=10), $p < 0.001$). Further alterations in membrane excitability were determined through measurements of AP latency and the total number of APs generated in response to depolarizing current ramps (steps from 0.1 nA to 1.0 nA in increments of 0.1 nA). All analysis was conducted on ramps up to 0.7 nA, because responses saturated at higher stimulation intensities (Figure 1D, 1E and 1F). Significant reductions in cumulative AP latencies (Figure 1E), as well as a significant increase in total AP number were observed (5.5 ± 0.6 APs, n = 6 for WT vs. 10.1 ± 1.7 APs, n = 7 for KO, Figure 1F, $p < 0.05$). This is further suggestive of increased excitability in neurons lacking PrP^C, and is consistent with what was previously found in slice recordings (Colling et al., 1996). In

addition, a significant increase in input resistance was observed in PrP-null neurons (256 ± 35.6 MΩ for WT (n=8) vs. 361 ± 24.8 MΩ for KO (n=11), Table 1, $p < 0.05$). However, there was no significant difference in the resting membrane potential or in the AP characteristics between WT and null neurons (Table 1). Taken together, higher input resistance may partially account for the hyperexcitability found in PrP-null neurons.

We also carried out experiments in acute hippocampal slices from ~2 month wild type and PrP-null mice. Interestingly, under these conditions, we did not observe differences in input resistance (107.5 ± 5.8 MΩ for WT (n=6) vs. 96.0 ± 4.6 MΩ for KO (n=7), $p > 0.05$). There was no difference in the numbers of action potentials evoked over a wide range of current injections (from 150 pA to 650 pA), and there was no difference in spike threshold (210.l ± 43.0 pA for WT (n=5) versus 207.1 ± 17 pA for KO (n=7). Only cell with a leak smaller than 20 pA were included in this analysis. There was, however, a statistically significant decrease in voltage sag ratio (0.11 ± 0.01 for WT (n=10) vs. 0.07 ± 0.01 for KO (n=10), $p < 0.01$). While this latter observation generally fits with our observation in cultured neurons, this change does not appear to be sufficient to drive a statistically significant difference in the intrinsic excitability of the neurons in the slice preparation. Alternatively, it is possible that there are changes in other conductances that may compensate for the effects of the voltage sag in slices from these older animals compared to the culture neurons.

Reduced I_h and down-regulated HCN channel functional properties in hippocampal cultures from PrP-null mice

The HCN channel is a major determinant of input resistance (Yamada-Hanff and Bean, 2015). Given the role of these channels as a physiological voltage clamp, we determined whether the observed biophysical changes are related to alterations in HCN channel function.

I_h was induced by a series of hyperpolarizing voltage steps (Figure 2A). To improve stability in recordings, step increments decreased in duration from 4 s to 2 s. The maximal amplitude of peak current measured following the stimulation was decreased in PrP-null neurons (V_{cmd} = -150 mV: peak current 418.2 ± 41.7 pA for WT (n=24) vs. 242.6 ± 35.5 pA for KO (n=20), Figure 2B, $p < 0.01$). In addition, a voltage-independent component in the current trace that incorporated

HCN channels was activated instantaneously (I_{inst}) (Proenza et al., 2002; Proenza and Yellen, 2006). The amplitude of this instantaneous current in PrP-null neurons was also significantly downregulated (data not shown). To determine whether the decrease in I_h in PrP-null neurons resulted from alterations in the kinetics of I_h activation, we fitted the onset of the current with a single-exponential function. As shown in Figure 2C, the voltage-dependent time constant was decreased at more negative voltages in both WT and PrP-null neurons. However, time course became significantly slower in PrP-null neurons over the command voltage range ($p < 0.05$ at steps between -90 to -130 mV). A shift in the voltage dependence of I_h activation may also explain the reduction in I_h, and therefore the lack of PrP^C on steady-state activation was determined by fitting normalized conductance to a Boltzmann function. This revealed that the $V_{0.5}$ value was significantly shifted to a more hyperpolarized level in PrP-null neurons ($V_{0.5}$: -80.82 ± 2.16 mV for WT (n=22) vs. -89.86 ± 1.95 mV for KO (n=17), Figure 2D, $p < 0.05$). However the slope factor was indistinguishable (10.9 ± 0.7 mV for WT (n=22) vs. 11.6 ± 0.9 mV for KO (n=17), $p > 0.05$). Consistent with the changes observed for I_h, current-clamp recordings reveal that the amplitude of the voltage sag, a characteristic of I_h activation, was decreased in PrP-null neurons (sag ratio: 0.37 ± 0.03 for WT (n=8) vs. 0.25 ± 0.04 for KO (n=16), Figure 2E and 2F, $p < 0.05$). I_h and voltage sag recorded from WT and null neurons were completely blocked by the HCN blocker ZD7288 (100 μM) (see Figure 2G for sample recording from WT a neuron), indicating that the measured current including the instantaneous phase was indeed mediated by HCN channels. These results suggest that PrP^C functionally regulates the biophysical properties of HCN channels.

The difference in input resistance is eliminated by HCN blockers

As HCN channels are partially active at rest, activation of I_h depolarizes membrane potential and reduces membrane impedance (Wang et al., 2007). To explore whether the enhancement in input resistance in PrP-null neurons resulted from the decrease in I_h, we examined the effect of the HCN channel blockade (Figure 3A and 3B). In WT neurons, inhibition of I_h by ZD7288 resulted in an increase in input resistance ($p < 0.05$, compare panels B and C), which is consistent with a previous study (Aponte et al., 2006; Lupica et al., 2001). It is worth noting that the activation of I_h in PrP-null neurons was negligible at -70 mV (Figure 2D) where input resistance was measured. Therefore, the input resistance tested in PrP-null neurons before and after ZD7288

applied was similar ($p > 0.05$). Notably, the input resistance in WT and PrP-null neurons became indistinguishable in the presence of ZD7288 (Figure 3C, $p = 0.5$), providing evidence of a mechanistic link between PrP^C and HCN channel activity.

Exploration of HCN subunit composition and physical interaction with PrP^C

HCN subunit composition determines the functional properties of the channel, including cyclic adenosine monophosphate (cAMP) sensitivity, voltage-dependent activation and kinetics, as well as interactions with intracellular signaling pathways (He et al., 2014). We thus wished to explore whether the observed changes in HCN function were mediated by an HCN subunit switch. Antibodies against HCN1 or HCN2 subunits, the principal HCN subunits expressed in the hippocampus, were used in a standard immunoblotting procedure. To obtain sufficient material for these biochemical measurements, we used hippocampal homogenate from adult mice rather than cultured neurons. These experiments revealed that the expression of HCN1 and HCN2 subunits detected from hippocampal homogenates was similar in WT and null neurons (Figure 4A) (relative protein expression of HCN1: 1.24 ± 0.07 for WT (n=3) vs. 1.29 ± 0.06 for KO (n=3), $p > 0.05$; relative protein expression of HCN2: 1.47 ± 0.48 for WT (n=3) vs. 1.41 ± 0.07 for KO (n=3), $p > 0.05$). We also examined whether cell surface expression of HCN1 and HCN2 channels was altered in PrP null neurons, however, no statistically significant difference in plasma membrane protein level was observed (n=6, data not shown).

It is also possible that PrP^C mediated changes in HCN channel function arise from a direct association of PrP^C with the channel. To explore this possibility, we performed co-IPs from WT mouse hippocampal homogenate. However, neither HCN1 nor HCN2 could be co-immunoprecipitated with PrP^C (Figure 4B). Given that PrP^C function is copper-dependent (Black et al., 2014; Stys et al., 2012), the negative results from co-IP could potentially be due to the absence of copper ions in our solutions. Hence, the co-IP experiments were also repeated in the presence of a high concentration of 1 µM copper, which is near the resting copper concentration in the synaptic cleft (Millhauser, 2007; Stys et al., 2012). However, the results remained unchanged (data not shown). Taken together, these data indicate that the effect of PrP^C on HCN channel function is not due to alterations in HCN subunit expression, nor due to a direct physical effect of PrP^C as part of a molecular complex.

PrP^C-mediated cAMP-dependent pathway regulates HCN channel activity

One possible explanation for the reduction of I_h in PrP-null neurons is a PrP-mediated molecular signaling pathway that may downregulate HCN activity in the hippocampus. A prime candidate is the cAMP-dependent pathway, which is known to potently modulate HCN activity (Ingram and Williams, 1996; Wainger et al., 2001). This possibility was tested here by application of the adenylyl cyclase activator, forskolin (20 µM) on to PrP-null neurons (Figure 5A). Kinetics analysis showed that the slow activation kinetics could be reversed after a 10 min forskolin incubation in PrP-null neurons at voltages between -150 and -100 mV (Figure 5B). On the other hand, forskolin application did not modify Gmax or half-voltage activation of G-V curve (V0.5: -82.1 ± 3.0 mV for PrP-/- with DMSO (n=7) vs. -87.4 ± 2.5 mV for PrP-/- with Forskolin (n=15), $p > 0.05$) in PrP-null neurons. Therefore, a downregulation of basal cAMP-dependent signaling in PrP-null neurons accounts for the slow I_h kinetics observed in PrP-null neurons, whereas the effect of PrP^C on HCN current amplitude and voltage-dependence of activation may be cAMP-independent.

Discussion

The principal finding of this study is that intrinsic excitability in neonatal cultured hippocampal neurons is regulated by PrP^C via alterations of HCN channel activity.

Modulation of intrinsic excitability of hippocampal neurons by PrP^C

There is growing evidence that the loss of PrP^C function alters neuronal output, and therefore contributes to synchronized activities underlying neocortical and hippocampal seizures (Walz et al., 2002). Indeed, there are a number of electrophysiological and morphological abnormalities in hippocampal neurons from PrP-null mice (Colling et al., 1996; Colling et al., 1997; Collinge et al., 1994). First, an abnormal GABA-A receptor inhibition has been reported in PrP-null mice (Colling et al., 1996) that may contribute to increased network excitability and, consequently, epileptiform activity. Second, PrP-null mice display aberrant sprouting of mossy fibers which is similar to the sprouting induced by seizures (Colling et al., 1997), indicating that this reorganization of neuronal circuitry may contribute to an "epileptic neuronal network". Third, a reduction in slow afterhyperpolarization currents (I_{AHP}), which is of great importance for

neuronal excitability, is evident in PrP-null mice (Colling et al., 1996; Fuhrmann et al., 2006; Herms et al., 2001; Mallucci et al., 2002). A recent study led to a new theory that neither K^+ channels nor voltage-gated Ca^{2+} channels were responsible for this disrupted I_{AHP} in PrP-null CA1 pyramidal neurons (Powell et al., 2008). Instead, increased intracellular Ca^{2+} buffering capacity and clearance of Ca^{2+} were reported as potential causes. Finally, a previous study from our lab has established a functional link between PrP^C and NMDARs, suggesting that PrP-null mice display an enhanced basal excitability due to enhanced NMDAR function (Khosravani et al., 2008). It is however worth noting that many factors appear to affect what is observed in PrP-null mouse neurons, including the specific null mouse strain and age of the animals (Steele et al., 2007). Indeed, when we conducted experiments in hippocampal slices from adult mice, we did not observe differences in intrinsic excitability between WT and null mice, which might perhaps be due to age dependent changes in the regulation of HCN channels by PrP^C. Further work will be required to determine whether there are indeed age dependent effects, or whether the observed differences are due to the different preparations used. Indeed, it is important to acknowledge potential limitations of our culture work. First, neurons in culture are isolated from neonatal animals and grown in artificial culture medium supplemented with exogenous growth factors for approximately two weeks. These conditions may result in changes in ion channel and receptor expression that could be different from those during normal postnatal development *in vivo,* and it is unclear that what extent neurons grown in culture correspond to a specific age of neurons in an in vivo situation. Second, although we are confident that we were recording from pyramidal cells rather than interneurons, we cannot distinguish whether the cells were derived from the CA1 or CA3 regions and it is possible that cells from these two regions may express different levels of HCN channels. In contrast, in our slice recordings, we focused exclusively in CA1 pyramidal cells. Altogether, for future studies, it will be interesting to compare neuronal excitability in slices from younger (i.e., two week old) animals, and examine the properties of CA3 neurons in this preparation. Nonetheless, there appear to be multiple ways by which the absence of PrP^C can alter neuronal cell output that impacts network function, and at least in cultured neurons isolated from neonatal pups, PrP^C dependent regulation of HCN channels may be a contributing factor.

Modulation of HCN channel activity by PrP^C: a mechanistic link between PrP^C and HCN

HCN channels are highly expressed in the central nervous system and their function is critically related to neuronal excitability at both single-cell and network levels, particularly in the hippocampus (Robinson and Siegelbaum, 2003). HCN channels form heterotetramers or homotetramers, composed of HCN1-4 subunits; however, only HCN1 and HCN2 are highly expressed in hippocampus (Santoro et al., 2000), indicating a location-correlated function. They give rise to the I_h current, which we found to be downregulated in the absence of PrP^C. HCN channels have unique biophysical properties that allow them to be partially active at rest and to act like a physiological "voltage clamp". The decreased HCN current in cultured PrP-null mouse neurons can thus account for the observed increase in input resistance. Moreover, a corresponding decrease in I_{inst} may amplify input resistance, thereby further increasing neuronal excitability. Whether the reduced I_h may also contribute to the well-established alterations of the I_{AHP} in PrP-null neurons remains to be tested. It is interesting to note that the decrease in I_h was not correlated with any apparent change in total or cell surface HCN protein expression, nor did there appear to be an HCN channel subunit switch. Furthermore, we note that our biochemical measurements were performed from hippocampal homogenate from adult mice, whereas recordings were done in cultured neurons from P0 pups. Given that the functional regulation of HCN channels by PrP^C appeared to be absent in slices from 2 month old mice, the biochemical analysis presented in Figure 4 does not rule out the possibility that there could be PrP^C dependent changes in HCN channel expression in our cultures. Nonetheless, the observation that HCN kinetics were altered in PrP-null neurons suggests that PrP^C is certainly capable of regulating the functional properties of HCN channels in native cells.

Our co-IP results that PrP^C did not form a complex with HCN suggest that HCN channel activity is not directly modulated by PrP^C. It is well known that cAMP can directly bind to a cyclic-nucleotide domain in the C-terminal of the HCN channel (DiFrancesco and Tortora, 1991) and has been reported to shift the voltage dependence of HCN2 channel opening (Wainger et al., 2001); this in turn leads to an enhancement of I_h (Ingram and Williams, 1996). Although basal activities of cAMP have been observed to be enhanced in retinal tissue of PrP-null mice (Chiarini et al., 2002; Lopes et al., 2005; Zanata et al., 2002), the cAMP levels in hippocampal neurons of PrP-null mice remain unknown. Activation of cAMP affects numerous intracellular

signaling cascades, including the activation of p38 mitogen-activated protein kinase (p38 MAPK) via the MAPK pathway (Gerits et al., 2008). Importantly, these enzymes are well recognized players in the regulation of neuronal excitability. In addition, the inhibition of p38 MAPK has been shown to induce a hyperpolarizing shift in I_h voltage-dependent activation and an increased input resistance (Jung et al., 2010; Poolos et al., 2006). In particular, the level of p38 MAPK appears to be downregulated in PrP-null mice, which may explain a hyperpolarizing shift in I_h gating and an increased input resistance in PrP-null mice observed in our study. Bath applied forskolin in PrP-null neurons was only able to rescue the kinetics from the slow state, whereas other parameters were unaffected. This then suggests that other signalling pathways also contribute to the PrP^C-mediated regulation of HCN channels. Further experimentation will be required to delineate these signalling cascades.

In summary, our data suggest a regulatory role of PrP^C on HCN channel activity at both the cellular and molecular levels in cultured neurons, and suggests that PrP^C is coupled to signaling cascades that can converge on HCN channels.

Author contributions

J.F., P.L.S., and G.W.Z. designed the study. J.F. and G.W.Z. wrote the manuscript. J.F., S.A.G.B., I.A.S., M.A.G, Z.Z. and L.C. performed experiments. J.F. and M.A.G. did data analysis. G.W.Z. supervised the study.

Acknowledgments

J.F. is supported by a Dr. Chen Fong studentship. S.A.G.B. is the recipient of a Postdoctoral Fellowship from the Multiple Sclerosis Society of Canada. M.A.G. is supported by a Conacyt Fellowship. G.W.Z. holds a Canada Research Chair and is supported by an Operating Grant from the Canadian Institutes for Health Research.

Conflict of interest statement

The authors declare that the research was conducted in the absence of any commercial or financial relationships that could be construed as a potential conflict of interest.

References

Aponte, Y., et al., 2006. Hyperpolarization-activated cation channels in fast-spiking interneurons of rat hippocampus. J Physiol. 574, 229-43.

Biel, M., et al., 2009. Hyperpolarization-activated cation channels: from genes to function. Physiol Rev. 89, 847-85.

Black, S.A., et al., 2014. Cellular prion protein and NMDA receptor modulation: protecting against excitotoxicity. Front Cell Dev Biol. 2, 45.

Bonin, R.P., et al., 2013. Hyperpolarization-activated current (In) is reduced in hippocampal neurons from Gabra5-/- mice. PLoS One. 8, e58679.

Bueler, H., et al., 1992. Normal development and behaviour of mice lacking the neuronal cell-surface PrP protein. Nature. 356, 577-82.

Chiarini, L.B., et al., 2002. Cellular prion protein transduces neuroprotective signals. EMBO J. 21, 3317-26.

Colling, S.B., Collinge, J., Jefferys, J.G., 1996. Hippocampal slices from prion protein null mice: disrupted Ca(2+)-activated K+ currents. Neurosci Lett. 209, 49-52.

Colling, S.B., et al., 1997. Mossy fibre reorganization in the hippocampus of prion protein null mice. Brain Res. 755, 28-35.

Collinge, J., et al., 1994. Prion protein is necessary for normal synaptic function. Nature. 370, 295-7.

Criado, J.R., et al., 2005. Mice devoid of prion protein have cognitive deficits that are rescued by reconstitution of PrP in neurons. Neurobiol Dis. 19, 255-65.

DiFrancesco, D., Tortora, P., 1991. Direct activation of cardiac pacemaker channels by intracellular cyclic AMP. Nature. 351, 145-7.

Fuhrmann, M., et al., 2006. Loss of the cellular prion protein affects the Ca2+ homeostasis in hippocampal CA1 neurons. J Neurochem. 98, 1876-85.

George, M.S., Abbott, L.F., Siegelbaum, S.A., 2009. HCN hyperpolarization-activated cation channels inhibit EPSPs by interactions with M-type K(+) channels. Nat Neurosci. 12, 577-84.

Gerits, N., et al., 2008. Relations between the mitogen-activated protein kinase and the cAMP-dependent protein kinase pathways: comradeship and hostility. Cell Signal. 20, 1592-607.

Haigh, C.L., et al., 2009. Dominant roles of the polybasic proline motif and copper in the PrP23-89-mediated stress protection response. J Cell Sci. 122, 1518-28.

Han, Y., et al., 2011. Trafficking and gating of hyperpolarization-activated cyclic nucleotide-gated channels are regulated by interaction with tetratricopeptide repeat-containing Rab8b-interacting protein (TRIP8b) and cyclic AMP at distinct sites. J Biol Chem. 286, 20823-34.

He, C., et al., 2014. Neurophysiology of HCN channels: from cellular functions to multiple regulations. Prog Neurobiol. 112, 1-23.

Herms, J.W., et al., 2001. Prion protein affects Ca2+-activated K+ currents in cerebellar purkinje cells. Neurobiol Dis. 8, 324-30.

Ingram, S.L., Williams, J.T., 1996. Modulation of the hyperpolarization-activated current (Ih) by cyclic nucleotides in guinea-pig primary afferent neurons. J Physiol. 492 (Pt 1), 97-106.

Jung, S., et al., 2010. Downregulation of dendritic HCN channel gating in epilepsy is mediated by altered phosphorylation signaling. J Neurosci. 30, 6678-88.

Khosravani, H., et al., 2005. The Arg473Cys-neuroligin-1 mutation modulates NMDA mediated synaptic transmission and receptor distribution in hippocampal neurons. FEBS Lett. 579, 6587-94.

Khosravani, H., et al., 2008. Prion protein attenuates excitotoxicity by inhibiting NMDA receptors. J Cell Biol. 181, 551-65.

Knight, R.S., Will, R.G., 2004. Prion diseases. J Neurol Neurosurg Psychiatry. 75 Suppl 1, i36-42.

Kuwahara, C., et al., 1999. Prions prevent neuronal cell-line death. Nature. 400, 225-6.

Linden, R., et al., 2008. Physiology of the prion protein. Physiol Rev. 88, 673-728.

Lopes, M.H., et al., 2005. Interaction of cellular prion and stress-inducible protein 1 promotes neuritogenesis and neuroprotection by distinct signaling pathways. J Neurosci. 25, 11330-9.

Lupica, C.R., et al., 2001. Contribution of the hyperpolarization-activated current (I(h)) to membrane potential and GABA release in hippocampal interneurons. J Neurophysiol. 86, 261-8.

Mallucci, G.R., et al., 2002. Post-natal knockout of prion protein alters hippocampal CA1 properties, but does not result in neurodegeneration. EMBO J. 21, 202-10.

Manson, J.C., et al., 1994. 129/Ola mice carrying a null mutation in PrP that abolishes mRNA production are developmentally normal. Mol Neurobiol. 8, 121-7.

Manson, J.C., et al., 1995. PrP gene dosage and long term potentiation. Neurodegeneration. 4, 113-4.

Millhauser, G.L., 2007. Copper and the prion protein: methods, structures, function, and disease. Annu Rev Phys Chem. 58, 299-320.

Noam, Y., Bernard, C., Baram, T.Z., 2011. Towards an integrated view of HCN channel role in epilepsy. Curr Opin Neurobiol. 21, 873-9.

Poolos, N.P., Bullis, J.B., Roth, M.K., 2006. Modulation of h-channels in hippocampal pyramidal neurons by p38 mitogen-activated protein kinase. J Neurosci. 26, 7995-8003.

Powell, A.D., et al., 2008. Alterations in Ca2+-buffering in prion-null mice: association with reduced afterhyperpolarizations in CA1 hippocampal neurons. J Neurosci. 28, 3877-86.

Proenza, C., et al., 2002. Pacemaker channels produce an instantaneous current. J Biol Chem. 277, 5101-9.

Proenza, C., Yellen, G., 2006. Distinct populations of HCN pacemaker channels produce voltage-dependent and voltage-independent currents. J Gen Physiol. 127, 183-90.

Robinson, R.B., Siegelbaum, S.A., 2003. Hyperpolarization-activated cation currents: from molecules to physiological function. Annu Rev Physiol. 65, 453-80.

Santoro, B., et al., 2000. Molecular and functional heterogeneity of hyperpolarization-activated pacemaker channels in the mouse CNS. J Neurosci. 20, 5264-75.

Soto, C., Satani, N., 2011. The intricate mechanisms of neurodegeneration in prion diseases. Trends Mol Med. 17, 14-24.

Steele, A.D., Lindquist, S., Aguzzi, A., 2007. The prion protein knockout mouse: a phenotype under challenge. Prion. 1, 83-93.

Stemkowski, P.L., Smith, P.A., 2012. Long-term IL-1beta exposure causes subpopulation-dependent alterations in rat dorsal root ganglion neuron excitability. J Neurophysiol. 107, 1586-97.

Stys, P.K., You, H., Zamponi, G.W., 2012. Copper-dependent regulation of NMDA receptors by cellular prion protein: implications for neurodegenerative disorders. J Physiol. 590, 1357-68.

Wainger, B.J., et al., 2001. Molecular mechanism of cAMP modulation of HCN pacemaker channels. Nature. 411, 805-10.

Walz, R., et al., 2002. Cellular prion protein: implications in seizures and epilepsy. Cell Mol Neurobiol. 22, 249-57.

Wang, M., et al., 2007. Alpha2A-adrenoceptors strengthen working memory networks by inhibiting cAMP-HCN channel signaling in prefrontal cortex. Cell. 129, 397-410.

Yamada-Hanff, J., Bean, B.P., 2015. Activation of Ih and TTX-sensitive sodium current at subthreshold voltages during CA1 pyramidal neuron firing. J Neurophysiol. jn 00489 2015.

You, H., et al., 2012. Abeta neurotoxicity depends on interactions between copper ions, prion protein, and N-methyl-D-aspartate receptors. Proc Natl Acad Sci U S A. 109, 1737-42.

Zamponi, G.W., Stys, P.K., 2009. Role of prions in neuroprotection and neurodegeneration: a mechanism involving glutamate receptors? Prion. 3, 187-9.

Zanata, S.M., et al., 2002. Stress-inducible protein 1 is a cell surface ligand for cellular prion that triggers neuroprotection. EMBO J. 21, 3307-16.

Figure legends

Figure 1. Enhanced intrinsic excitability in cultured PrP-null neurons

A, Representative APs evoked by depolarizing pulses in a hippocampal neuron cultured from WT (black) and PrP-null mice (red). B, Average number of APs induced by increasing depolarizing currents in cultured neurons from WT (n = 13) and PrP-null mice (n = 10). C, Average spike threshold for wt and PrP-null neurons. D, Action potentials evoked by a 500 ms depolarizing current ramp for WT (black) and PrP-null (red) neuron. E, Cumulative AP latencies for WT and PrP-null neurons ($p < 0.001$ for the induced AP from the first to the seventh). F, Average number of APs during a current ramp application for WT (n = 6) and KO neurons (n = 7). *, $p < 0.05$, ***, $p < 0.001$.

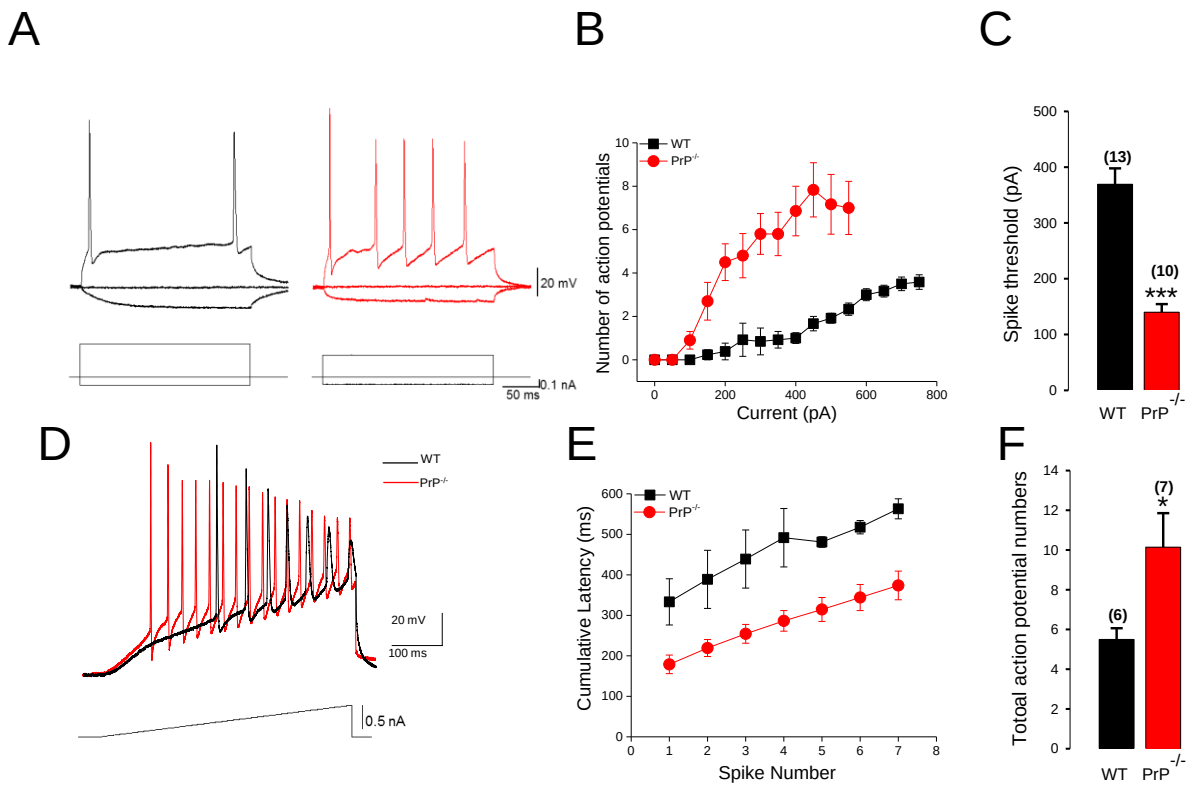
A
B
C
20 mV
0.1 nA
50 ms
WT
PrP-/-
Number of action potentials
Current (pA)
Spike threshold (pA)
(13)
(10)
***
WT
PrP-/-
D
E
F
WT
PrP-/-
20 mV
100 ms
0.5 nA
Cumulative Latency (ms)
Spike Number
Totoal action potential numbers
(6)
(7)
*
WT
PrP-/-

Figure 2. Characteristics of I_h in WT and PrP-null neurons

A, Evoked responses of WT and PrP-null neurons to hyperpolarizing voltage steps from -50 mV to -150 mV in increments of 10 mV and also in decreasing durations from 4 s to 2 s in the presence of Ba^{2+} (0.5 mM) and TTX (0.5 μM). B, C, Summary of I_h amplitude and activation time constant (τ). I_h amplitude was significantly smaller (n = 24 for WT, n = 20 for KO) and kinetics was slower in PrP-null neurons (n = 11 for WT, n = 9 for KO). D, Normalized HCN channel activation curves in PrP-null neurons showed a hyperpolarizing shift in half activation voltage (n = 22 for WT, n = 17 for KO). E, Sample recordings showing a voltage sag generated by I_h in response to the hyperpolarizing current step at -300 pA. PrP-null neurons displayed a decrease in the amplitude of the sag response. F. Summary of the voltage sag ratio between WT (n = 8) and PrP-null neurons (n = 16). G. Family of current records illustrating the effect of ZD7288 (100 μM) on I_h in WT neurons. The pulse protocol used for this experiment is depicted at the bottom.

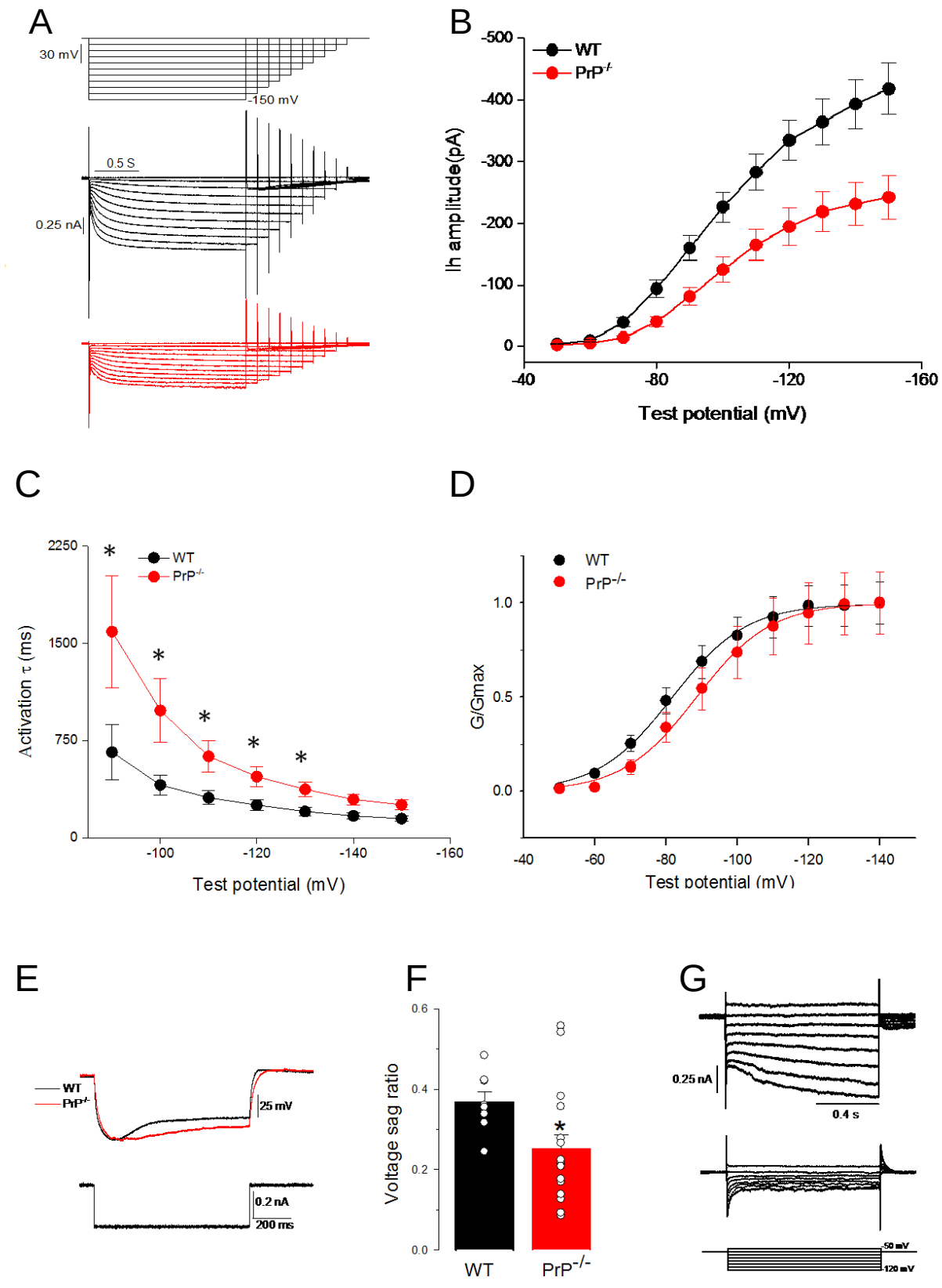
A
30 mV
-150 mV
0.5 S
0.25 nA
B
WT
PrP-/-
Ih amplitude(pA)
-500
-400
-300
-200
-100
0
-40
-80
-120
-160
Test potential (mV)
C
2250
1500
750
0
Activation τ (ms)
WT
PrP-/-
*
-100
-120
-140
-160
Test potential (mV)
D
WT
PrP-/-
1.0
0.5
0.0
G/Gmax
-40
-60
-80
-100
-120
-140
Test potential (mV)
E
WT
PrP-/-
25 mV
0.2 nA
200 ms
F
Voltage sag ratio
0.6
0.4
0.2
0.0
*
WT
PrP-/-
G
0.25 nA
0.4 s
-50 mV
-120 mV

Figure 3. Enhanced input resistance in cultured PrP-null neurons

A, Sample currents recorded from WT (black) and PrP-null neurons (red) in response to a short hyperpolarizing voltage step from -70 mV to -90 mV. B, Input resistance of PrP-null neurons (n = 11) was 29.2% higher than input resistance of WT (n = 8). C, there was no distinguishable difference in the input resistance of WT (n = 15) and PrP-null neurons (n = 13) in the presence of ZD7288. *, $p < 0.05$.

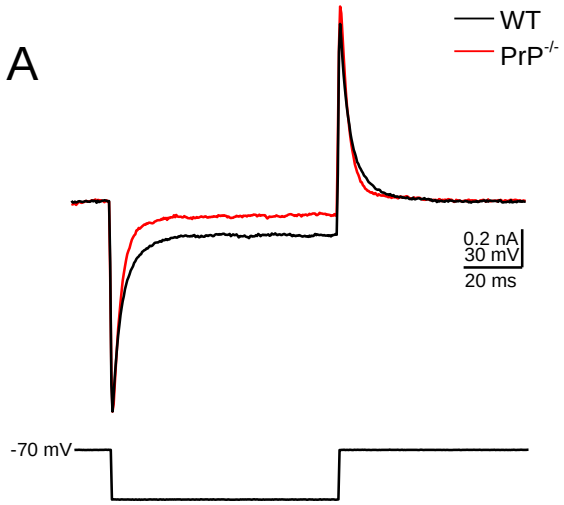
A
WT
PrP-/-
0.2 nA
30 mV
20 ms
-70 mV

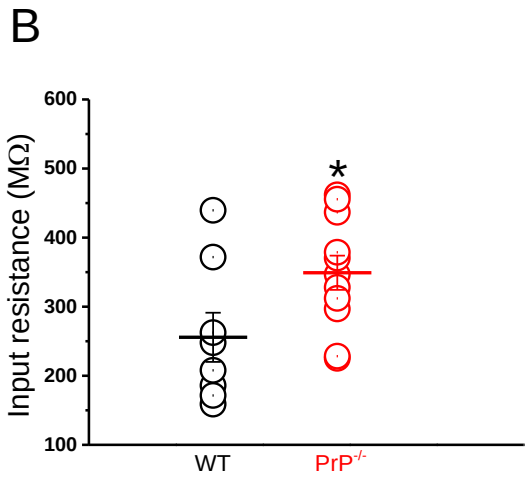
B
Input resistance (MΩ)
600
500
400
300
200
100
*
WT
PrP-/-

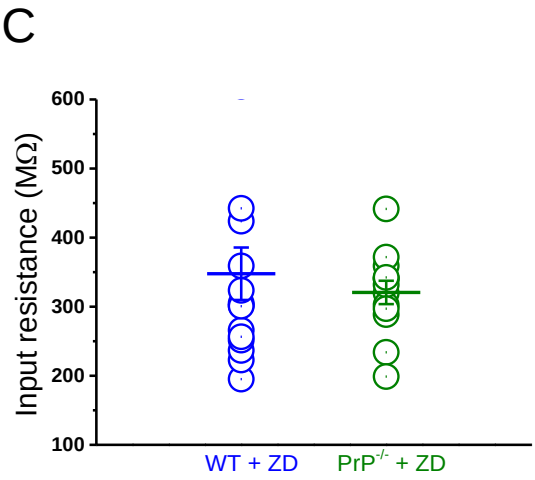
C
Input resistance (MΩ)
600
500
400
300
200
100
WT + ZD
PrP-/- + ZD

Figure 4. Analysis of HCN subunit expression

A, Representative immunoblots for HCN1 (left) and HCN2 subunit (right) proteins in membrane homogenates prepared from hippocampi of WT and PrP-null adult mice. α-tubulin was used as a loading control for each sample. This experiment is representative of three different repetitions (protein expression normalized to α-tubulin for HCN1: 1.24 ± 0.07 for WT vs. 1.29 ± 0.06 for KO, $p > 0.05$; for HCN2: 1.47 ± 0.48 for WT vs. 1.41 ± 0.07 for KO, $p > 0.05$). B, Co-IPs of PrP^C and HCN subunits using lysates from WT and PrP-null adult mice hippocampal tissue showing that neither HCN1 nor HCN2 associated with PrP^C. The lanes for a co-IP control (IP PrP^C) from PrP-null appeared to be blank which was as observed in the lanes for a bead-only control (data not shown). HCN1 and HCN2 protein could both be detected in hippocampal homogenates (input). This experiment was repeated three times with identical results.

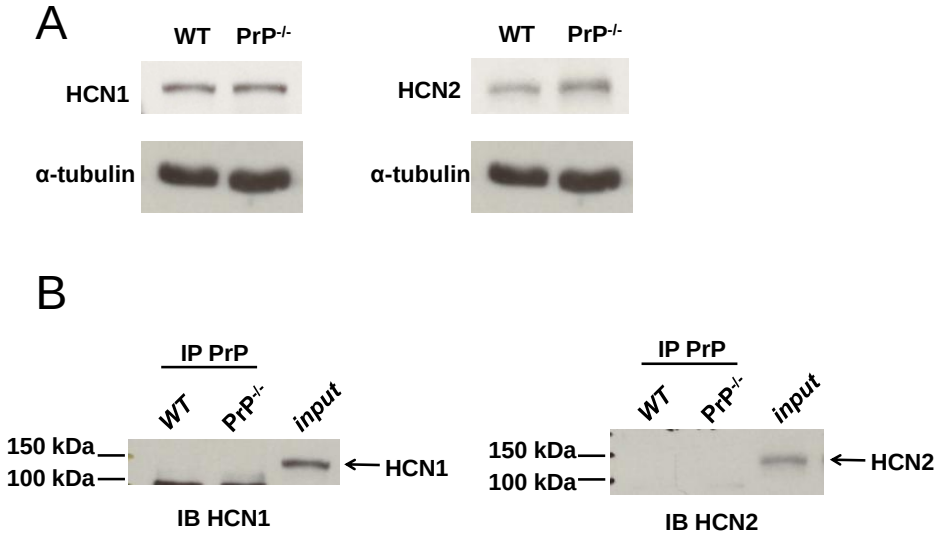
A
WT
PrP-/-
HCN1
α-tubulin
WT
PrP-/-
HCN2
α-tubulin
B
IP PrP
WT
PrP-/-
input
150 kDa
100 kDa
HCN1
IB HCN1
IP PrP
WT
PrP-/-
input
150 kDa
100 kDa
HCN2
IB HCN2

Figure 5. Effects of forskolin on I_h

A, Representative I_h current traces in the presence of forskolin or 0.1 % DMSO (vehicle control) in PrP-null neurons. B, Mean time constants of activation during hyperpolarizing steps from −150 to −100 mV after incubation with forskolin (n = 15) or vehicle (DMSO, n = 7) in PrP-null neurons. The slower kinetics in PrP-null neurons are reversed in the presence of forskolin.

A

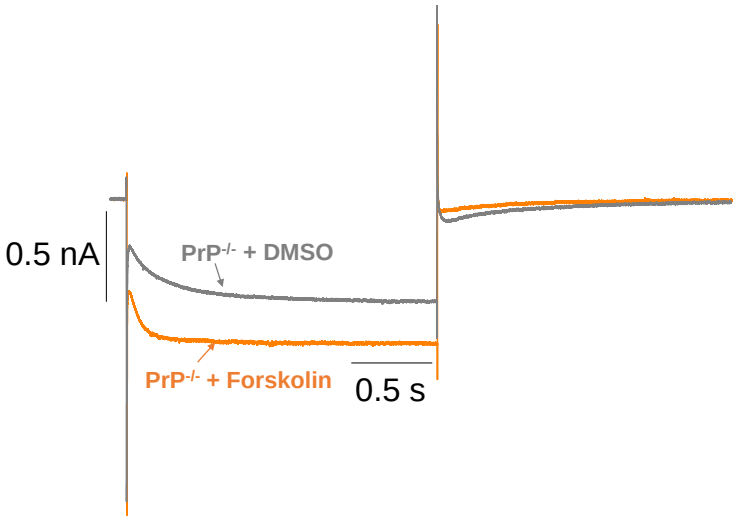
0.5 nA
PrP-/- + DMSO
PrP-/- + Forskolin
0.5 s

B

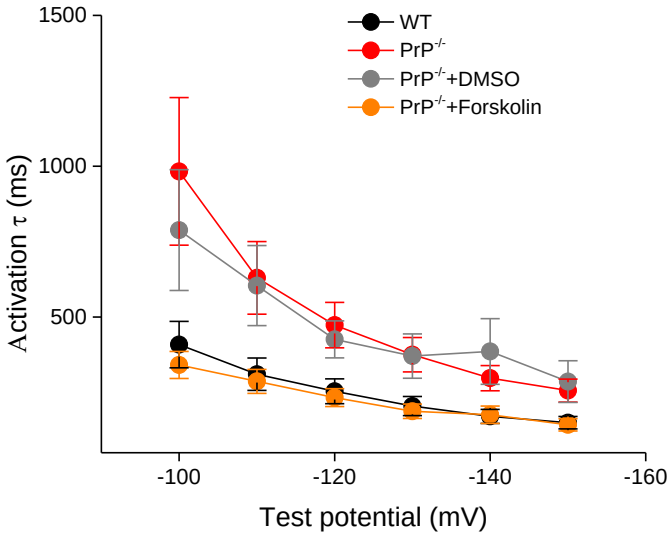
WT
PrP-/-
PrP-/-+DMSO
PrP-/-+Forskolin
Activation τ (ms)
1500
1000
500
-100
-120
-140
-160
Test potential (mV)

Table 1. Electrophysiological properties of hippocampal neurons in WT and PrP-null mice

Electrophysiological parameters were measured using whole-cell voltage clamp and current clamp recordings as described in *Materials and Methods*. Numbers of cells testes are shown in parentheses.

Group of cells	E_m (mV)	R_{in} (MΩ)	$AP_{amplitude}$ (mV)	AP_{50} (ms)	dV/dt_{max} (V/S)	rV/rtmax (V/S)	Threshold (mV)
WT (5)	-55 ± 1.4	256 ± 35.6*	107 ± 6.6	1.9 ± 0.2	132 ± 23.5	-67 ± 6.2	-42 ± 2.0
$PrP^{-/-}$ (9)	-54 ± 1.3	361 ± 24.8	116 ± 2.3	1.8 ± 0.1	136 ± 13.8	-76 ± 7.9	-39 ± 2.6

2.1.2. Article Summary

Prions have long been recognized to be critical for the pathogenesis of prion disease. Moreover, the underlying mechanism of prion pathology can be learned by inspecting its cellular isoform, PrP^C - a normal cell surface glycoprotein. It is widely accepted that the loss of PrP^C function is involved in epileptogenesis and modulation of seizure threshold. However, unmasking the neurobiological mechanisms underlying these deficits has remained a challenge.

Previous studies focused on the loss of function of PrP^C on neuronal excitability. These studies reported a variety of electrophysiological abnormalities in recordings from PrP-null neurons *in vitro*. However, the underlying ionic mechanism which is critically associated with normal electrical signals in the brain has yet to be determined.

In this study, I took advantage of PrP KO mice to examine the intrinsic firing pattern of cultured hippocampal neurons, and hypothesize that PrP^C associates with HCN channel regulating intrinsic physiology of hippocampal neurons. I found that the absence of PrP^C profoundly affected the firing properties of neurons, increasing the number of action potentials (APs) and decreasing the spike threshold by depolarizing current injections. The observations then raise the question as to what alterations in membrane properties underlie increases in cell excitability. By conducting voltage-clamp recordings, I found a significant increase in the input resistance of PrP^C-null neurons. This may, at least, partially explain differences in cell excitability, but it remains unclear if this alteration is induced by the modulation of HCN channels. To verify this, the functional investigation of HCN channel associated with cellular PrP^C in the hippocampal cultures was tested with the application of the HCN channel blocker, ZD7288 in voltage clamp experiments. The membrane impedance in WT and PrP-null neurons became indistinguishable in the presence of ZD7288, indicating a mechanistic link between PrP^C and HCN channel. Therefore, I lastly explored the relationship between HCN and PrP^C at both molecular and functional levels. It turns out that HCN appears to be functionally associated with PrP^C through an indirect interaction.

Taken together, with this study we have achieved three major steps in clarifying the loss of function of PrP^C on neuronal excitability:

(1) We have demonstrated that the lack of PrP^C enhances neuronal intrinsic excitability in hippocampus with an increased membrane impedance which can be reversed by HCN channel blockers.

(2) We have showed an altered biophysical properties of HCN channels when PrP^C is removed.

(3) We have established a novel interplay between HCN channel and PrP^C by which we are able to analyze the ionic mechanism underlying the fundamental role of PrP in hippocampal cell excitability.

The next important step will be to explore whether, and how, HCN channels interact with other critical regulator for neuronal excitability, such as voltage-gated T-type calcium channels.

2.2.1 Original article 2

Down-regulation of T-type Cav3.2 channels by hyperpolarizationactivated cyclic nucleotide-gated channel 1 (HCN1): evidence of a signaling complex

Jing Fan, Maria A. Gandini, Fang-Xiong Zhang, Lina Chen, Ivana A. Souza,

Gerald W. Zamponi

I contributed to this work by carrying out all the patch-clamp experiments and biochemical experiments, as well as performing corresponding data analysis. Moreover, together with my supervisor Dr. Gerald Zamponi, I designed this study and wrote the manuscript. M. A, Gandini contributed to repeat the co-IP result as shown in figure 1, and providing technical assistance including some help with data analysis methods. F, Zhang performed plasmid construction for mkate-tagged HCN1-N and HCN-C fragments. L, Chen helped with culturing tsA-201 cells and corresponding cDNA transfection. I. A, Souza provided technical assistance including co-IP experiment trouble shooting.

Down-regulation of T-type Cav3.2 channels by hyperpolarization-activated cyclic nucleotide-gated channel 1 (HCN1): evidence of a signaling complex

Jing Fan, Maria A. Gandini, Fang-Xiong Zhang, Lina Chen, Ivana A. Souza, Gerald W. Zamponi*

Department of Physiology and Pharmacology, Hotchkiss Brain Institute, Cumming School of Medicine, University of Calgary, Calgary, Alberta T2N 4N1, Canada.

* Correspondence: Gerald W Zamponi, PhD; Cumming School of Medicine; University of Calgary 3330 Hospital Dr. NW; Calgary, T2N4N1; Canada
Email: zamponi@ucalgary.ca

Key words: calcium channel, gating, trafficking, electrophysiology, channel activation

Channels (Austin). 2017 May 3:0. doi: 10.1080/19336950.2017.1326233.

ABSTRACT

Formation of complexes between ion channels is important for signal processing in the brain. Here we investigate the biochemical and biophysical interactions between HCN1 channels and Cav3.2 T-type channels. We found that HCN1 co-immunoprecipitated with Cav3.2 from lysates of either mouse brain or tsA-201 cells, with the HCN1 N-terminus associating with the Cav3.2 N-terminus. Cav3.2 channel activity appeared to be functionally regulated by HCN1. The expression of HCN1 induced a decrease in Cav3.2 Ba^{2+} influx ($I_{Ba}{}^{2+}$) along with altered channel kinetics and a depolarizing shift in activation gating. However, a reciprocal regulation of HCN1 by Cav3.2 was not observed. This study highlights a regulatory role of HCN1 on Cav3.2 voltage-dependent properties, which are expected to affect physiological functions such as synaptic transmission and cellular excitability.

INTRODUCTION

Low-voltage activation allows T-type Ca^{2+} channels to be critically involved in pacemaker activity as well as in regulating neuronal firing (Bourinet et al., 2014, Zamponi et al, 2015). A growing body of evidence supports the idea that dysregulation of Cav3 channel function interferes with normal neuronal firing, therefore contributing to a number of channelopathies, such as chronic pain and epilepsy (Zamponi et al, 2015). It has been reported that Cav3 channels are functionally coupled with HCN channels at synapses (Huang et al. 2011, Tsay et al., 2007). Such a cross-talk between T-type Ca^{2+} channels and HCN channels has been observed in both hippocampal and entorhinal cortical neurons and shown to increase Cav3 inactivation, leading to alterations in presynaptic function (Huang et al. 2011, Tsay et al., 2007). In addition, both I_h (the current mediated by HCN channels) and I_T (T-type calcium current) act within the subthreshold range, thus allowing for the regulation of neuronal processing in a subthreshold voltage range (Magee et al., 1995, Swensen and Bean, 2003, Engbers et al., 2011, Kole et al, 2006, Rehak et al., 2013). During the process of "rebound bursting", I_h acts synergistically with I_T to generate precise burst output (Engbers et al, 2011, McCormick and Pape, 1990, Sangrey and Jaeger, 2010). Although the functional interaction between HCN and T-type has been demonstrated in neurons, a detailed biophysical examination of a functional HCN-Cav3 interaction has not been reported, nor is it known whether there may be a physical interaction between these two channels.

Cav3.2 channels support a wide range of physiological processes (Kaku et al., 2003, Talavera and Nilius, 2006). In a previous study, we have reported that Cav3.2 is associated with BK potassium channels at both molecular and functional levels (Rehak et al., 2013). Here, we focused on the interaction between HCN1 and Cav3.2, specifically the regulation of HCN1 on the activity of Cav3.2. We found a signaling complex between HCN1 and Cav3.2 channels in both heterologous expression system and in mouse brain lysate. In addition, HCN1 channels functionally interact with Cav3.2 channels to alter Cav3.2 current density and its voltage-dependent properties. This in turn may modify physiological and pathological outputs that are mediated by these channels.

RESULTS

HCN channels physically interact with T-type channels

Among the HCN family, HCN1 and HCN2 subunits are highly expressed in the central nervous system and are critically involved in regulating neuronal excitability (Robinson and Siegelbaum, 2003). Previous studies from Huang *et al.*, (Huang et al. 2011) revealed a colocalization of HCN1 with Cav3.2, but not Cav3.1, at synapses of entorhinal cortical neurons. To examine whether this colocalization may be due to a physical association between Cav3 and HCN channels, we performed a series of co-IPs using mouse brain lysates. Co-IP experiments revealed that HCN1 channels immuno-precipitated with Cav3.2, but not Cav3.1 or Cav3.3 T-type channels (Figure 1A), in agreement with previous co-localization work (Huang et al. 2011). In contrast, HCN2 channels were not found to be associated with any of T-type subunits (Figure 1B). These data thus indicate a selective interaction between HCN1 and Cav3.2 channel subtypes.

Co-expression of HCN1 alters Cav3.2 T-type channel activity

It has been reported that the HCN channels regulate inactivation of T-type channels in hippocampal and entorhinal cortical neurons (Huang et al. 2011, Tsay et al., 2007). We thus tested whether the observed biochemical interactions are reflected in a change in Cav3.2 channel function. Whole-cell voltage clamp recordings were performed from tsA-201 cells transiently transfected with Cav3.2 cDNA in the presence or absence of HCN1 cDNA constructs. The current density-voltage relationship for Cav3.2 activation was then examined using whole cell patch clamp (Figure 2A, 2B), using ionic conditions in which HCN channels are functionally blocked (see Materials and methods). In the presence of HCN1, cells exhibited a decrease in Cav3.2 peak barium current across a wide range of voltages (between -45 to 30 mV; peak current density at -20 mV step, without HCN1: -91.3 ± 14.2 pA/pF, with HCN1: -44.8 ± 7.3 pA/pF, Figure 2B, $p < 0.005$). In addition, there was a reduction in maximal slope conductance in the presence of HCN1 (without HCN1: 1.7 ± 0.2 pS/pF, with HCN1: 0.9 ± 0.1 pS/pF, Figure 2G, $p < 0.005$). The kinetics of Cav3.2 channel activation and inactivation were determined by fitting the onset and decay of the current with mono-exponential functions. The time constant of inactivation was significantly slower in HCN1 co-expressing cells at a test potential of -20 mV

(without HCN1: 17.7 ± 0.4 ms, with HCN1: 27.8 ± 3.1 ms, Figure 2D, $p < 0.05$). However, the activation kinetics were not affected (Figure 2C, $p > 0.05$). In addition, HCN1 co-expression shifted the half-activation voltage of Cav3.2 to more depolarized potentials ($V_{0.5act}$ for the recordings without HCN1: -37.1 ± 1.7 mV, with HCN1: -32.1 ± 1.5 mV, Figure 2E and 2F, $p < 0.05$). The coexpression of HCN1 did not affect the steady state inactivation curves of Cav3.2 (Figure 2H, $p > 0.05$). These results suggest that HCN1 functionally interacts with Cav3.2 channels by altering Cav3.2 current density and Cav3.2 gating characteristics.

Examination of interaction sites between HCN1 and Cav3.2 channels

To examine the channel regions that are involved in the interaction between HCN1 and Cav3.2, we used GFP-tagged intracellular regions of Cav3.2 channels (Rzhepetskyy et al., 2016) which were co-transfected with full length HCN1 channels in tsA-201 cells. In this preparation, GFP-tagged Cav3.2 I-II linker, II-III linker, III-IV linker, N-terminus and C-terminus were tested. A series of co-IPs were performed to examine which intracellular region of Cav3.2 channels was associated with full length HCN1 channels. As a positive control we transfected full length Cav3.2. Consistent with the data in Figure 1, Cav3.2 channels interacted with HCN1 when expressed heterologously (Figure 3A). In addition, a strong interaction between the Cav3.2 N-terminus and HCN1 was observed (Figure 3B). However, none of the other tested Cav3.2 domain linkers nor the C-terminus were able to associate with HCN1 (Figure 3). To further refine the binding region in the Cav3.2 N-terminus, we took advantage of Cav3.2 N1-terminus (residues 1-50), N2-terminus (residues 51-100) and N3-terminus (residues 25-75) constructs that were described previously (Rzhepetskyy et al., 2016). We observed a strong band from the co-IP of HCN1 channels with the Cav3.2 N3-terminus compared with N1- or N2-termini (Figure 3C). To map the binding region in HCN1 channels, a similar approach was used. The cells were co-transfected with either mKate-tagged HCN1-N terminus or mKate-tagged HCN1-C terminus, and full length of Cav3.2 channels. As shown in Figure 3D, Cav3.2 interacted with HCN1 N-terminus (Figure 3D). These results provide strong evidence that the interaction between HCN1 and Cav3.2 involve the N-terminal regions of these channels.

There is no reciprocal regulation of HCN1 channel activity by Cav3.2

It has been reported that Ca^{2+} influx regulates HCN1 channel activity (Luthi and McCormick, 1998, Luthi and McCormick, 1999). We thus wished to explore whether there might be a reciprocal regulation of HCN1 channel properties by Cav3.2 channels. To determine the impact of Ca^{2+} influx through Cav3.2 channels on HCN1 channel activity, Ca^{2+} was removed from the intracellular solution, and cells were bathed in an external recording solution containing 2.5 mM Ca^{2+} to allow for T-type channel-mediated Ca^{2+} entry. When recording from T-type channels, cells are usually held at -100 mV to recover channels from voltage-dependent inactivation. However, this is also the voltage at which HCN1 channels are activated. Therefore, to minimize the leak I_h current, cells were held at -50 instead of -100 mV, followed by a hyperpolarizing pulse (P1) to -100 mV to remove inactivation of Cav3.2 and to measure I_h. Then a depolarizing step to -20 mV was applied to maximally activate Cav3.2 channels followed by a second hyperpolarizing pulse (P2) to again assess I_h (Figure 4A). As shown in Figure 4A, the activation of Cav3.2 current did not affect HCN1 current amplitude (HCN1: P2/P1 = 0.95 ± 0.05, n = 9; HCN1 + Cav3.2: P2/P1 = 0.93 ± 0.04, n = 11). Furthermore, there was also no effect of Cav3.2 coexpression on I_h current density (Figure 4B), suggesting that Cav3.2 channels do not augment HCN1 trafficking. In addition, the activation kinetics of HCN1 channels before and after Cav3.2 channel opening were examined by fitting the rising phase of I_h with a mono-exponential function. This kinetic analysis showed that the activation time constant of HCN1 remained unaltered (P1: 50 ± 3.8 ms, P2: 55 ± 5.8 ms, Figure 4C, $p > 0.05$). It is known that the HCN channel is potently modulated by cAMP (18, 19). To test whether there might be a synergistic role of Ca^{2+} and cAMP on I_h, 0.5 mM Dibutyryl-cAMP (Sigma, D0627), a cell-permeable cAMP analogue, was applied to the bath prior to testing the effects of Cav3.2 mediated Ca^{2+} influx. While delivery of cAMP increased HCN1 amplitude as expected (not shown), calcium influx via Cav3.2 did not further augment I_h amplitude (Figure 4D, $p > 0.05$).

Discussion

It is known that Cav3 and HCN conductances interact during the process of “rebound bursting” McCormick and Pape, 1990, Sangrey and Jaeger, 2010, Kaku et al., 2003). Several lines of evidence further showed that Cav3 channels may be functionally associated with HCN channels (Huang et al., 2011, Tsay et al., 2007), but the underlying molecular details had not been

explored. Here, we have identified a biochemical signaling complex between HCN1 and Cav3.2 channels in both native tissue and heterologous expression systems, showing that HCN1 channels robustly regulate Cav3.2 channel activity.

Our results revealed that the HCN1 channel forms a molecular complex with Cav3.2, but not with Cav3.1 and Cav3.3, in mouse brain tissue. This is consistent with what was previously found in cortical layer III pyramidal neurons where a colocalization of both channels was observed (Huang et al., 2011). We also found that coexpression of HCN1 decreased Cav3.2 current density, increased the inactivation time constant of Cav3.2, and shifted the half-activation voltage to slightly more depolarized potentials. It has been reported that HCN1 channels colocalize with and functionally regulate T-type channels in the entorhinal cortical layer III pre-synaptic terminals to regulate presynaptic release (Huang et al., 2011). A detailed analysis revealed that a reduction in HCN activity resulted in a gain of function in synaptic T-type channel currents (Huang et al., 2011). Similar effects of I_h on T-type channel activity have been demonstrated for dendrites of hippocampal CA1 pyramidal neurons in a recent study (Tsay et al., 2007). These findings support the notion of a functional interplay between I_h and T-type currents in the mammalian central nervous system. One key difference between these studies and our work is that we examined the effects of HCN1 on Cav3.2 channels functions under conditions in which HCN1 was blocked by cesium ions. We can thus not rule out the possibility that Cav3.2 channel activity might be further modulated in physiological saline where sodium is able to enter via HCN1. Notwithstanding this detail, our findings showing an effect of HCN1 coexpression on Cav3.2 current density and gating may help explain the reported crosstalk between these two channels in neurons.

A combination of mechanisms may underlie the various effects of HCN1 on Cav3.2 channel activity. Expression of HCN1 may induce a decrease in the membrane expression of Cav3.2 channels, thus reducing the current density of Cav3.2 channels. This could occur at either the transcriptional or translational levels, or as a result of altered channel trafficking. Alternatively, the effect of HCN1 may be due to a regulation of either single channel conductance or maximum open probability of Cav3.2. Further experiments, such as surface protein biotinylation and/or single channel recordings may shed further light on this issue. A direct effect on channel function is supported by the observation that the half-activation potential and the time course of

inactivation of Cav3.2 were altered. While the effect on activation gating is too small to account for the reduced whole cell current amplitude, it does suggest that the physical interaction between the channels impacts Cav3.2 activity beyond a possible effect on cell surface expression.

A number of interactions between Cav3 and other types of ion channels have been reported in the literature, including SK, IK, BK and Kv4 potassium channels (Rehak et al., 2013, Cueni et al, 2008, Engbers et al, 2012, Engbers et al., 2013, Anderson et al., 2010a, Anderson et al., 2010b) The channel structural determinants of these interactions have been delineated and shown to involve either the C-terminus region of Cav3 (Kv4) (Anderson et al., 2010a), or transmembrane regions (BK) (Rehak et al., 2013). Here, we report an interaction that involves the N-terminus region of Cav3.2. This region has, to our knowledge, not previously been implicated in Cav3 channel function or trafficking, and it remains unclear whether this region regulates channel function beyond serving as an anchor for HCN1. For Kv4 channels and calcium-activated potassium channels, the association with Cav3 was shown to confer a potent calcium regulation on potassium channel function (Rehak et al., 2013, Cueni et al, 2008, Engbers et al, 2012, Engbers et al., 2013, Anderson et al., 2010a, Anderson et al., 2010b). For HCN1, our data indicate that this does not appear the case, at least not in expression systems. Unlike Kv4 channels which interact with KChIPs (Anderson et al., 2010a) and calcium-activated potassium channels which either contain calcium sensors, or are conjugated to calmodulin (Faber and Sah, 2003), there appear to be no such processes in place for calcium regulation of HCN channels. Nonetheless, we note that our data are somewhat at odds with previous studies reporting a calcium-dependent upregulation of I_h current activity in neurons (Luthi and McCormick, 1998, Luthi and McCormick, 1999). In our experiments, it is possible that T-type calcium channel-mediated calcium entry evoked by a single membrane depolarization is simply insufficient to provide enough calcium to alter HCN channel activity, and that prolonged burst firing of neurons may result in a larger T-type channel mediated rise in intracellular calcium that then may be sufficient to modulate HCN channel function. Alternatively, there may be an indirect effect of a calcium-dependent signaling cascade that is present in neurons, but not expressed at sufficiently high levels in a heterologous system such as tsA-201 cells. Given the important role of HCN channels in regulating the neuronal excitability as well as dendritic integration, it is also possible that primary role of Cav3.2-HCN1 complexes is to modulate channel expression and trafficking

to specific subcellular loci such as dendrites, rather than providing a mechanism by which T-type channels may functionally alter I_h. In this context, it is worth noting that functional interactions between I_h and Cav3.2 calcium channels have been observed in thalamic neurons in Genetic Absence Epilepsy Rats from Strasbourg (GAERS) (Cain et al, 2015). These rats carry a gain-of-function mutation in Cav3.2 channels that appear to be accompanied by an upregulation of HCN1 and HCN3 channels (Cain et al, 2015), thus highlighting a possible crosstalk between Cav3.2 channel activity and HCN channel expression.

In summary, we demonstrate a physical interaction between HCN1 and Cav3.2 channels that alters Cav3.2 channel behavior. This in turn may result in altered firing and synaptic properties of neurons that coexpress these two channel types.

Materials and methods

Constructs

Mouse HCN1 cDNA was a gift from Dr. Eric Accili (University of British Columbia), and the human wild-type GFP-tagged Cav3.2 intracellular linker constructs were gifts from Dr. Nobert Weiss (Academy of Sciences of the Czech Republic) and were described previously (Rzhepetskyy et al., 2016). The mouse HCN1 N- (amino acid residues 1-135) and C- (amino acid residues 382-908) termini were amplified by PCR, followed by sequencing and subcloning into the pcDNA3.1 vector (Invitrogen, Carlsbad, CA); the mKate2 tag was amplified and inserted upstream of HCN1 fragments.

The primers used for HCN1 N-terminus were 5’ cgggatccATGGAAGGCGGCGGCAAACCC 3’ and 5’ccaccggtTCAATCCCAATAAAACCTGAAGTC3’, for HCN1 C-terminus were 5’cgggatccGCCACAGCTTTGATCCAGTCT3’ and 5’ ccaccggtTCATAAATTCGAAGCAAAACG3’. The primers used for amplifying mKate2 sequence were 5’ ggggtaccGCCACCATGGTGAGCGAGCT 3’ and 5’ cgggatccTCTGAGTCCGGAACCTCCTC 3’.

Transient transfection

TsA-201 cells were cultured and transiently transfected as described previously (Rehak et al., 2013). Briefly, cells were plated on 10 cm plates with or without glass coverslips and transfected using the calcium phosphate method using the following combination of cDNAs: for electrophysiology, 3 μg of Cav3.2 (or empty vector pcDNA3.1), 1 μg of HCN1 (or empty vector pcDNA3.1) and 0.5 μg of pEGFP were transfected. For the co-immunoprecipitation experiments to map the interaction site on HCN1: 1 μg of either full length HCN1, mKate-tagged HCN1 N-terminus or mKate- tagged HCN1 C-terminus and 3 μg of Cav3.2 were transfected. To map the interaction site on Cav3.2: 3 μg of either full length Cav3.2, GFP-tagged Cav3.2 N-terminus, GFP-tagged Cav3.2 C-terminus or GFP-tagged Cav3.2 intracellular linkers and 1 μg of full length HCN1 cDNAs were transfected. Cells were incubated for 72 hours after transfection and before experiments.

Co-Immunoprecipitation and western blotting

Mouse brain proteins were extracted in RIPA buffer (25 mM Tris-HCl, pH 7.6, 150 mM NaCl, 1% NP-40, 1% sodium deoxycholate, 0.1% SDS, 0.5 mM PMSF and protease inhibitor cocktail) and 1 mg of lysates was pre-cleared with 30 μl of Protein G Sepharose beads (GE Healthcare) for 2 hours at 4 ^{o}C. Samples were then centrifuged and supernatants were incubated with Protein G beads and 2 μg of one of the following antibodies: anti-Cav3.1 (Alomone, ACC-021), anti-Cav3.2 (Alomone, 025), anti-Cav3.3 (Alomone, ACC-0009) or an irrelevant antibody, overnight, at 4 ^{o}C, with rotation. Beads were washed three times with modified RIPA buffer (50 mM Tris-HCl, pH 8.0, 150 mM NaCl, 1 mM EDTA, 1% Triton X-100, 0.1 % SDS) and twice with PBS, and eluted with 2 X Laemmli sample buffer.

For the co-immunoprecipitation experiments using heterologous expression, cultured tsA-201 cells were transiently transfected as described above. Seventy-two hours after transfection, cells were lysed in modified RIPA buffer on ice, for 1 hour. Lysates were transferred to micro centrifuge tubes and centrifuged at 13,000 RPM for 20 min to clear debris. Supernatants were then incubated overnight at 4 ^{o}C with 2 μg of either anti-GFP (Santa Cruz, sc-8334) or anti-tRFP (against mKate-2, Evrogen, AB-233). After incubation with antibodies, Protein A Sepharose

beads were added to the samples and incubated at 4 ^{o}C for 1.5 hours. Beads were washed three times with modified RIPA buffer and proteins were eluted with 2 X Laemmli sample buffer.

Eluted samples were loaded on the appropriate percentage Tris-glycine gel and resolved using SDS-PAGE. Samples were transferred to a 0.2 μm nitrocellulose membrane (Bio-Rad) and western blot analysis was performed using one of the following antibodies: anti-HCN1 (1:300, Neuromab, 75-110), anti-HCN2 (1:300, Neuromab, 71-37), anti-Cav3.1 (1:200, Alomone, ACC-021), anti-Cav3.2 (1:200, Santa Cruz, sc-25691), and anti-Cav3.3 (1:200, Alomone, ACC-0009). Horseradish peroxidase-linked secondary anti-mouse and anti-rabbit antibodies were used at a 1:5,000 dilution and blots were developed using a C-DiGit blot scanner (LI-COR Biosciences).

Electrophysiology

Whole-cell voltage-clamp recordings were made from cultured tsA-201 cells at room temperature using an Axopatch 200B amplifier (Axon Instruments). The external solution for Cav3.2 recordings contained (mM): 125 CsCl, 10 $BaCl_2$, 1 $MgCl_2$, 10 D-glucose and 10 HEPES (adjusted to pH 7.4 with CsOH). The intracellular pipettes were pulled from borosilicate glass (with an impedance of 3-5 MΩ) and filled with an intracellular solution containing (mM) 140 CsCl, 2.5 $CaCl_2$, 1 $MgCl_2$, 5 EGTA, 2 Na-ATP, 0.3 Na-GTP, and 10 HEPES (adjusted to pH 7.3 with CsOH). The external solution for HCN recordings contained (mM): 150 NaCl, 5 KCl, 2.5 $CaCl_2$, 1 $MgCl_2$, 10 HEPES and 10 D-glucose (adjusted to pH 7.4 with NaOH). The internal contained (mM): 140 KGluconate, 4 Mg-ATP, 0.5 Na-GTP, 0.5 EGTA and 10 HEPES (adjusted to pH 7.2 with KOH).

I-V curves were fitted with the following Boltzmann equation: $I = \frac{Gmax*(Vm-Vr)}{\left\{1+\exp\left[\frac{(-Vm+Vo.sact)}{k}\right]\right\}}$ where *I* is the normalized current by the cell capacitance, *Gmax* is the value of maximal conductance, *Vm* is the membrane potential, *Vr* is the reversal potential, $V_{0.5act}$ is the membrane potential for the half-activation and κ is the slope factor. The conductance was calculated according to the equation: G =*I*/(*Vm*- *Vr*). The reversal potential of barium currents determined by the mean value of individual current fittings was 36.1 ± 0.9 mV (without HCN1) and 32.1 ± 1.5 mV (with HCN1). Steady-state inactivation curves were fitted with the modified Boltzmann equation:

$\frac{I}{Imax} = \frac{1}{\left\{1+\exp\left[-\frac{(Vp-Vo.sinact)}{k}\right]\right\}}$, where *I/Imax* is the normalized current, *Vp* is the conditioning prepulse, $V_{0.5inact}$ is the voltage for half-inactivation.

HCN currents were leak-subtracted using a p/4 subtraction protocol. Series resistance in voltage-clamp recordings was compensated 50-70% and continually monitored through experiments. Recordings were terminated whenever significant increases (≥20%) in access resistance occurred. Current signals were filtered at 2 kHz (Digidata 1320A, Molecular Devices), respectively, in all experiments. Clampex 9.2 software running on a computer was used to acquire data.

Statistical analysis

Statistical analyses were performed using Origin9 and Sigmaplot10.0. Data are expressed as means ± SEM. Statistical analyses were done using two-tailed unpaired Student's t-tests. Significance was set at $p < 0.05$.

Disclosure of potential conflicts of interest

No potential conflicts of interest were disclosed.

Funding

J.F. was supported by a Dr. Chen Fong studentship. M.A.G. is supported by an Alberta Innovates–Health Solutions Fellowship, I.A.S. and F.X.Z. were previously supported by this program. IAS is supported by a Fellowship from the Savoy Foundation. G.W.Z. holds a Canada Research Chair. This work was supported by a Discovery Grant from the Natural Sciences and Engineering Research Council.

Acknowledgements

We thank Dr. Nobert Weiss and Dr. Eric Accili for providing cDNA constructs.

Author contributions

J.F. and G.W.Z. designed the study and wrote the manuscript. J.F., M.A.G., F.X.Z., L.C., I.A.S. performed experiments. J.F. performed data analysis. G.W.Z. supervised the study.

References

Anderson D, Mehaffe WH, Iftinca M, Rehak R, Engbers JD, Hameed S, Zamponi GW, et al. (2010a) Regulation of neuronal activity by Cav3-Kv4 channel signaling complexes. Nat. Neurosci. 13:333–337.

Anderson D, Rehak R, Hameed S, Mehaffey WH, Zamponi GW, Turner RW. (2010b) Regulation of the K(V)4.2 complex by Ca(V)3.1 calcium channels. Channels (Austin). 4:163–167.

Bourinet E, Altier C, Hildebrand ME, Trang T, Salter MW, Zamponi GW. Calcium-permeable ion channels in pain signaling. Physiol. Rev. 2014;94(1):81–140.

Cueni L, Canepari M, Lujan R, Emmenegger Y, Watanabe M, Bond CT, Franken P, Adelman JP, Luthi A. T-type Ca^{2+} channels, SK2 channels and SERCAs gate sleep-related oscillations in thalamic dendrites. Nat Neurosci. 2008;11(6):683–692.

Cain SM, Tyson JR, Jones KL, Snutch TP. Thalamocortical neurons display suppressed burst-firing due to an enhanced I_h current in a genetic model of absence epilepsy. Pfluegers Arch 2015;467(6):1367-1382

Engbers JD, Anderson D, Tadayonnejad R, Mehaffey WH, Molineux ML, Turner RW. (2011) Distinct roles for I(T) and I(H) in controlling the frequency and timing of rebound spike responses. J.Physiol. 589:5391–5413.

Engbers JD, Anderson D, Asmara H, Rehak R, Mehaffe WH, Hameed S, Mckay BE, et al. (2012) Intermediate conductance calcium-activated potassium channels modulate summation of parallel fiber input in cerebellar Purkinje cells. Proc.Natl. Acad. Sci. U.S.A. 109:2601–2606.

Engbers JD, Zamponi GW, Turner RW. (2013) Modeling interactions between voltage-gated Ca^{2+}channels and KCa1.1 channels. Channels (Austin). 7:24–25.

Faber ES, Sah P. Calcium-activated potassium channels: multiple contributions to neuronal function. Neuroscientist. 2003;9(3):181-94.

Huang Z, Lujan R, Kadurin I, Uebele VN, Renger JJ, Dolphin AC, Shah MM. Presynaptic HCN1 channels regulate Cav3.2 activity and neurotransmission at select cortical synapses. Nat. Neurosci. 2011; 14(4):478–486.

Ingram SL, Williams JT. Modulation of the hyperpolarization-activated current (Ih) by cyclic nucleotides in guinea-pig primary afferent neurons. J Physiol. 1996;492(Pt1):97-106.

Kole MH, Hallermann S, Stuart GJ. Single I_h channels in pyramidal neurondendrites: properties, distribution, and impact on action potential output. J. Neurosci. 2006;26(6):1677–1687.

Kaku T, Lee TS, Arita M, Hadama T, Ono K. The gating and conductance properties of Cav3.2 low-voltage-activated T-type calcium channels. JJ. Physiol. 2003;53(3):165–172.

Luthi A, McCormick DA. Periodicity of thalamic synchronized oscillations: the role of Ca^{2+}-mediated upregulation of I_h. Neuron. 1998;20(3):553–563.

Luthi A, McCormick DA. $Ca^{(2+)}$-mediated up-regulation of I_h in the thalamus. How cell-intrinsic ionic currents may shape network activity. Ann. N.Y. Acad. Sci. 1999;868:765–769.

Magee JC, Christofi G, Miyakawa H, Christie B, Lasser-Ross N, Johnston D. Subthreshold synaptic activation of voltage-gated $Ca2^{+}$ channels mediates a localized Ca^{2+} influx into the dendrites of hippocampal pyramidal neurons. J. Neurophysiol. 1995;74(3):1335–1342.

McCormick DA, Pape H C. Properties of a hyperpolarizationactivated cation current and its role in rhythmic oscillation in thalamic relay neurones. J. Physiol. 1990;431:291–318.

Rehak R, Bartoletti TM, Engbers JD, Berecki G, Turner RW, Zamponi GW. (2013) Low voltage activation of KCa1.1 current by Cav3-KCa1.1 complexes. PLoS ONE. 8:e61844.

Robinson RB, Siegelbaum SA. Hyperpolarization-activated cation currents: from molecules to physiological function. Annu. Rev. Physiol. 2003;65:453–480.

Rzhepetskyy Y, Lazniewska J, Proft J, Campiglio M, Flucher BE, Weiss N. A Cav3.2/Stac1 molecular complex controls T-type channel expression at the plasma membrane. Channels (Austin.) 2016;10(5):346–354.

Sangrey T, Jaeger D. Analysis of distinct short and prolonged components in rebound spiking of deep cerebellar nucleus neurons. Eur. J. Neurosci. 2010;32(10):1646–1657.

Swensen AM, Bean BP. Ionic mechanisms of burst firing in dissociated Purkinje neurons. J. Neurosci. 2003;23(29):9650–9663.

Tsay D, Dudman JT, and Siegelbaum SA. (2007) HCN1 channels constrain synaptically evoked Ca^{2+} spikes in distal dendrites of CA1 pyramidal neurons. Neuron. 56:1076–1089.

Talavera K, Nilius B. Biophysics and structure-function relationship of T-type Ca^{2+} channels. Cell Calcium 2006;40(2):97–114.

Wainger BJ, DeGennaro M, Santoro B, Siegelbaum SA, Tibbs GR. Molecular mechanism of cAMP modulation of HCN pacemaker channels. Nature. 2001;411(6839):805-10.

Zamponi GW, Striessnig J, Koschak A, Dolphin AC. (2015) The Physiology, Pathology, and Pharmacology of Voltage-Gated Calcium Channels and Their Future Therapeutic Potential. Pharmacol. Rev. 67:821–870.

Figure 1. HCN1 channels interact with Cav3.2 channels in mouse brain. A, Co-immunoprecipitation of HCN1 and T-type Ca^{2+} channel subunits using lysates from adult mouse brain showed that HCN1 channels associate with Cav3.2 T-type channels (lane 4). The samples were blotted with anti-HCN1 antibody. B, western blot showing that HCN2 channels did not co-immunoprecipitate with any of the T-type channel subunits. HCN1 and HCN2 protein could both be detected in mouse brain homogenates (input). The Nuclear receptor related 1 protein (NURR1) was used here as an irrelevant antibody for the purpode of a negative control. The samples were blotted with anti-HCN2 antibody. These experiments were repeated four times (with tissue obtained from four different mice) with identical results.

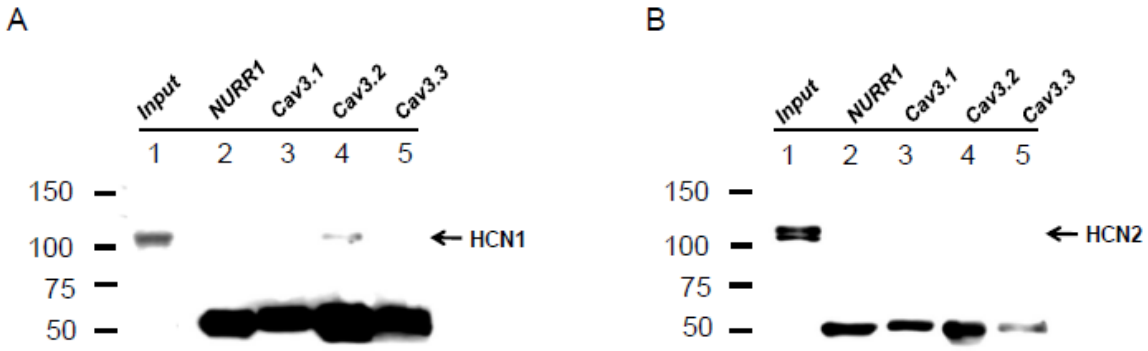
A
Input
NURR1
Cav3.1
Cav3.2
Cav3.3
1 2 3 4 5
150
100
75
50
HCN1
B
Input
NURR1
Cav3.1
Cav3.2
Cav3.3
1 2 3 4 5
150
100
75
50
HCN2

Figure 2. HCN1 channels alter Cav3.2 channel activity. Data shown are from whole-cell voltage clamp recordings from tsA-201 cells transiently transfected with Cav3.2 cDNA with or without HCN1 construct. A, Representative Ba^{2+} current traces recorded from Cav3.2-expressing cells with or without coexpression of HCN1 channels in response to 250 ms depolarizing steps varied from −80 to +40 mV from a holding potential of −100 mV. B, Corresponding current-voltage relationship for Cav3.2-expressing cells with or without coexpression of HCN1 channels (without HCN1, n = 14; with HCN1, n = 21). C, Corresponding mean activation time constants of Cav3.2 currents recorded at a command potential -20 mV (without HCN1, n = 14; with HCN1, n = 21). D, Corresponding mean inactivation time constants of Cav3.2 currents recorded at -20 mV (without HCN1, n = 14; with HCN1, n = 21). E, Normalized Cav3.2 channel activation curves from Cav3.2-expressing cells with coexpression of HCN1 channels showed a depolarizing shift in half activation voltage (without HCN1, n = 14; with HCN1, n = 21). F, G, Summary of half activation voltage and maximal conductance (without HCN1, n = 14; with HCN1, n = 21). H, Inactivation curves were determined in response to a pulse at -20 mV after 5 s-lasting depolarizing prepulses to different potentials from a holding potential of −110 mV (without HCN1, n = 16; with HCN1, n = 16). *, $p < 0.05$, **, $p < 0.005$ *.

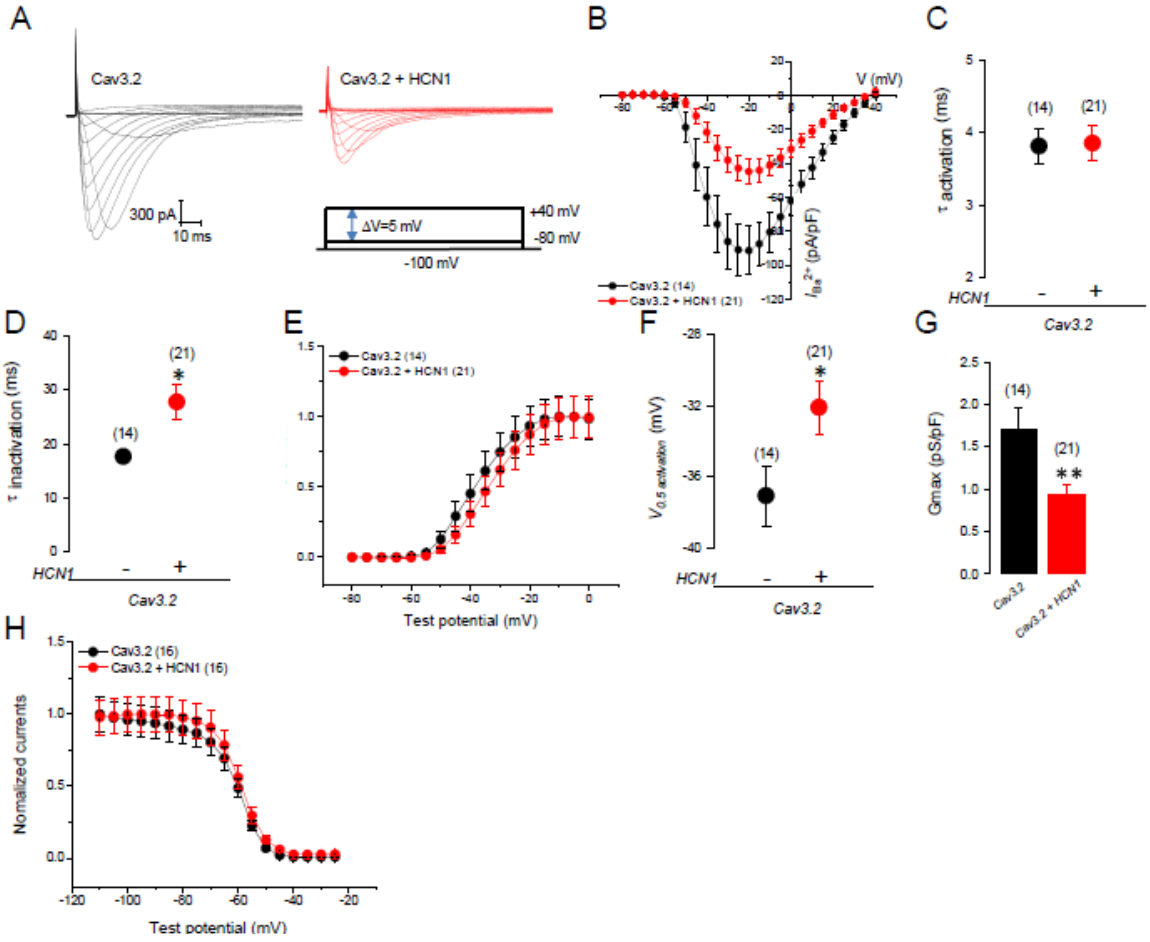
A
Cav3.2
Cav3.2 + HCN1
300 pA
10 ms
ΔV=5 mV
+40 mV
-80 mV
-100 mV
B
V (mV)
Cav3.2 (14)
Cav3.2 + HCN1 (21)
C
τ activation (ms)
(14)
(21)
HCN1
Cav3.2
D
τ inactivation (ms)
(14)
(21)
HCN1
Cav3.2
E
Cav3.2 (14)
Cav3.2 + HCN1 (21)
Test potential (mV)
F
(14)
(21)
HCN1
Cav3.2
G
(14)
(21)
Cav3.2
Cav3.2 + HCN1
H
Cav3.2 (16)
Cav3.2 + HCN1 (16)
Normalized currents
Test potential (mV)

Figure 3. HCN1 channels interact with the N terminus region of Cav3.2 channels. A, Left column, western blot of transfected tsA-201 cell lysates showed the expression of HCN1 (input) in every condition. Right column, western blot showed co-immunoprecipitation between HCN1 and full length Cav3.2 (lane 2), but not between HCN1 and Cav3.2 I-II linker, II-III linker, and GFP-tag only (lanes 3, 4 and 5 respectively). Lane 1 showed mock transfection. Lane 6 showed IgG control. B, Left column, western blot of transfected tsA-201 cell lysates showed the expression of HCN1 (input) in every condition. Right column, western blot showing co-immunoprecipitation between HCN1 and Cav3.2 full length (lane 2) and Cav3.2 N terminus (lane 4), but not between HCN1 and Cav3.2 III-IV linker, C terminus and GFP-tag only (lanes 3, 5 and 6 respectively). Lane 1 reflects mock transfection and lane 7 depicts IgG control. C, Left column, western blot showing expression of HCN1 (input) in every condition. Right column, western blot showing co-immunoprecipitation between HCN1 and full length Cav3.2, N terminus and N3 terminus (amino acids 25-75) (lanes 2, 3 and 6). Lanes 4, 5 and 7 demonstrate that HCN1 did not co-immunoprecipitate with N1 (1-50) and N2 (51-100) terminus and with a GFP-tag alone. Lane 1 reflects mock transfection and lane 8 is an IgG control. D, Left column, western blot showing Cav3.2 expression in every condition. Right column, western blot showing co-immunoprecipitation between full length Cav3.2 and HCN1 N terminus (lane 5), but not between Cav3.2 and HCN1 C terminus and mKate tag alone. Lane 1 reflects transfection and lane 3 indicates IgG control. For experiments represented in panels A, B and C, immunoprecipitations were done using an anti-GFP antibody and membranes were blotted with an anti-HCN1 antibody. For experiments represented in panel D, immunoprecipitation was performed with anti-tRFP (against mKate tag) and blots were done with anti-Cav3.2 antibody. These experiments were repeated three times with identical results.

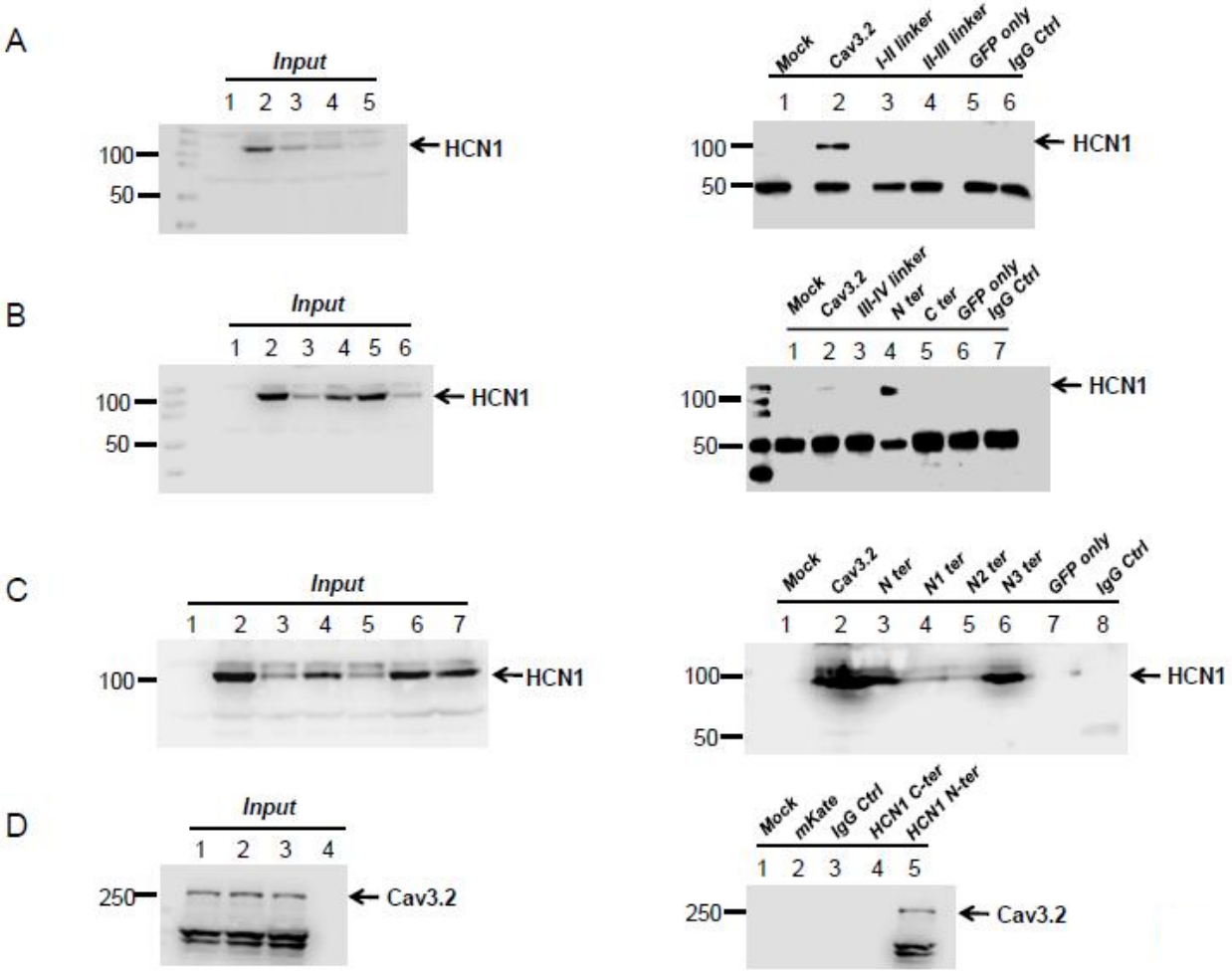
A
Input
1 2 3 4 5
100
50
HCN1
Mock
Cav3.2
I-II linker
II-III linker
GFP only
IgG Ctrl
1 2 3 4 5 6
100
50
HCN1
B
Input
1 2 3 4 5 6
100
50
HCN1
Mock
Cav3.2
III-IV linker
N ter
C ter
GFP only
IgG Ctrl
1 2 3 4 5 6 7
100
50
HCN1
C
Input
1 2 3 4 5 6 7
100
HCN1
Mock
Cav3.2
N ter
N1 ter
N2 ter
N3 ter
GFP only
IgG Ctrl
1 2 3 4 5 6 7 8
100
50
HCN1
D
Input
1 2 3 4
250
Cav3.2
Mock
mKate
IgG Ctrl
HCN1 C-ter
HCN1 N-ter
1 2 3 4 5
250
Cav3.2

Figure 4. Cav3.2 co-expression does not alter current density or kinetics of HCN1 channels. A, Sample I_h currents recorded from tsA-201 cells without (black) or with co-expression of Cav3.2 channels (red) in response to a hyperpolarizing voltage step from -50 mV to -100 mV. The currents were leak subtracted using a P/4 protocol. To obtain stable recordings, the cells were held at -50 mV to minimize leakage currents from the opening of HCN1 channels at rest. To maximally recover Cav3.2 channels from inactivation and to measure I_h, a 500 ms hyperpolarizing pulse to -100 mV was first applied. Then, a 200 ms pulse to -20 mV was applied to activate maximum calcium influx via Cav3.2. Finally, I_h was activated by 1 s hyperpolarizing pulse to -100 mV (10 ms return to the holding at -50 mV before test pulse applied). The extracellular solution contained 2.5 mM Ca^{2+}. B, Effect of Cav3.2 coexpression on the mean peak current density of HCN1 channels (without Cav3.2, n = 9; with Cav3.2, n = 11). C, Corresponding mean activation time constants of I_h recorded at a command potential -100 mV (before Cav3.2 activation, n = 9; after Cav3.2 activation, n = 11). D, Normalized I_h peak current recorded form cells co-expressing Cav3.2 and HCN1 (expressed as the current ratio obtained after and before application of a Cav3.2 activating pulse) before and after the bath application of dibutyryl-cAMP (n = 11).

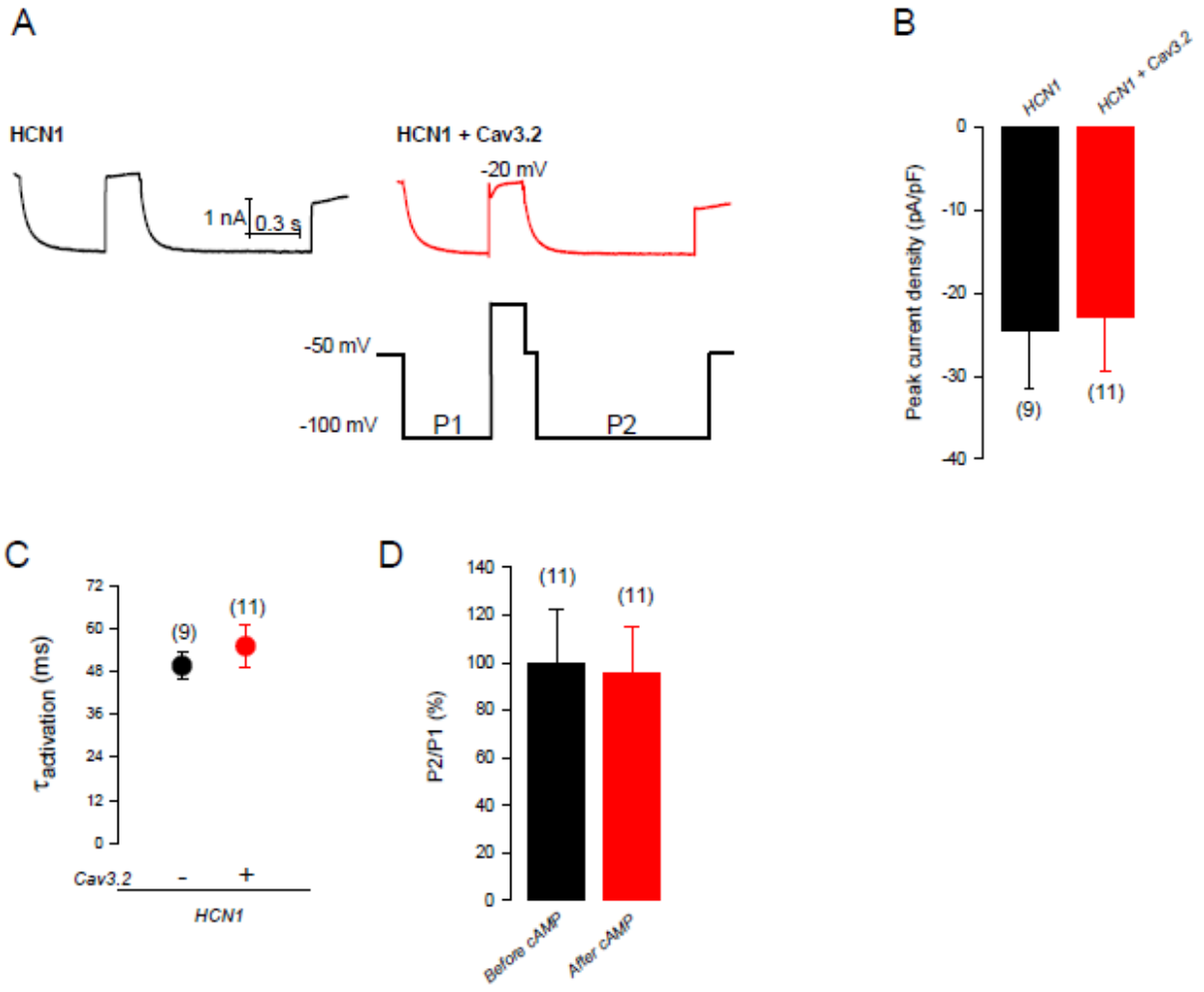
A
HCN1
HCN1 + Cav3.2
-20 mV
1 nA
0.3 s
-50 mV
-100 mV
P1
P2
B
HCN1
HCN1 + Cav3.2
Peak current density (pA/pF)
0
-10
-20
-30
-40
(9)
(11)
C
τactivation (ms)
72
60
48
36
24
12
0
(9)
(11)
Cav3.2
-
+
HCN1
D
P2/P1 (%)
140
120
100
80
60
40
20
0
(11)
(11)
Before cAMP
After cAMP

2.2.2. Article Summary

Signal processing in brain relys on both activity of individual channels and complex interactions between ion channels. Converging evidence shows HCN channels are functionally associated with Cav3 channels. In particular, there are different outcomes from the regulation of Cav3 channels when HCN channels interact with conductance, expression or activity of Cav3 channel on the membrane, which resulting in various impacts on the neuronal function, such as neuronal excitability and synaptic transmission. However, direct biophysical tests for a Cav3-HCN interaction that would support a direct effect on channel function have not been reported, and whether a molecular interaction involved in this signaling complex has not been determined.

In this study, we set out to investigate the specificity of the interaction between Cav3 and HCN channels. First, to determine whether HCN channels and Cav3 channels can be associated as a physical complex, co-IP experiments of all three T-types with both HCN1 and HCN2 by using whole brain homogenates were performed. As a result, only Cav3.2 formed a complex with HCN1, which is in agreement with previous immunostaining results. Subsequently, by performing a direct biophysical test, I found that coexpression of HCN1 channel in tsA-201 cells, altered the functional properties of Cav3.2 currents. Conversely, there appear to be no reciprocal alterations to HCN1 functional properties by Cav3.2 coexpression. To further detect the binding regions that would support the physical complex formed between Cav3.2 and HCN1 channels, a series of physical mapping co-IP experiments were carried out with tsA-201 cells. As a result, the N-terminal region of Cav3.2 was observed to physically interact with the N-terminal region of HCN1.

This study has established a new regulatory role of HCN channels on Cav3 channel activity.

In particular,

(a) We identified a specific interaction between HCN1 and Cav3.2 channels.

(b) We described that not only HCN1 and Cav3.2 formed a molecular complex, but HCN1 channels functionally interacted with Cav3.2 channels changing its current density and voltage-dependent properties.

We view this study as an important step towards a potential link between Cav3.2-HCN1 signaling and their impact on relevant neuronal outputs. Furthermore, the identified binding regions in this biochemical complex may open new possibilities to better explore neuronal behavior where Cav3.2 interplay with HCN1channels.

Chapter3: Final Conclusions

Unlike most other voltage-gated ion channels, HCN channels are dually regulated by interdependent voltage and ligand binding (Kusch et al., 2010, Wu et al., 2011). Additional notable characteristics of the HCN channels become evident when comparing their properties to other voltage-gated ion channels, i.e., their hyperpolarized and subthreshold voltage for activation (induced depolarizing currents), and the ability to remain partially open at rest. Due to its unique properties, HCN channel activity in the plasma membrane appears to be a "voltage clamp" (Nolan et al., 2007), to counteract both excitatory and inhibitory inputs to stabilize the membrane potential. Moreover, HCN channels appear to be a key target for cell signaling pathways involved in regulating various neuronal activities in response to external stimuli. In particular, HCN channel activity is regulated via various mechanisms, including transcriptional regulation, trafficking and channel modification, etc (He et al., 2014). As introduced in the "General Introduction" above, the surface expression and functional activities of HCN channels are dramatically regulated by a wide range of cellular signals. It is however worth noting that an altered expression or function of HCN channels might result in pathological conditions in the nervous system (Lewis and Chetkovich, 2011), which importantly links HCN channel dysregulation with disease. Therefore, exploring the potential cellular signals associated with HCN channels if of great importance.

The principal result of this thesis is that I have established that HCN channels engage in molecular and functional interactions with diverse partners. I consider these results of importance for future approaches towards understanding biochemical and biophysical mechanisms underlying HCN channel-associated signaling complex. In that respect, I would like to emphasize the following key observations. First, I established a novel functional interaction between HCN channels and PrP^C, and provided a mechanistic link between this interaction and a relevant functional output (Paper 1). Second, I identified a new regulatory mechanism by which HCN channels specifically interact with T-type Cav3.2 channels (Paper 2). The two identified interactions, between HCN and PrP^C and, HCN and Cav3.2 channels give rise to two very different forms of HCN channel regulation. In the following discussion and conclusion, I therefore expand and integrate those topics that I consider as the most relevant.

In Paper 1:

From the recordings on PrP-KO hippocampal neurons, I found that those neurons behaved hyperexcitably. Unexpectedly, I observed a reduction in HCN channel function in PrP-KO hippocampal neurons as indicated by the decreased I_h, decreased voltage sag and enhanced input resistance. Notably, voltage-dependent activation and kinetics of HCN channels were also found to be altered in KO neurons. However, the evidence we obtained from co-IP and surface expression tests does not support either mechanism of subunit composition switch or direct physical interaction responsible for the altered HCN channel activity. Nonetheless, based on our observations, we suggest that the modified HCN channel activities by the loss of PrP^C appear to contribute to the enhanced intrinsic excitability in cultured hippocampal neurons. Importantly, the regulation of HCN channel activity by PrP^C might be mediated by a second messenger pathway, and further work is needed to identify these pathways. Moreover, a number of additional experimental steps could be taken to definitely exclude the possible influence of other variables:

(a) Although an altered HCN channel activity appears to contribute to the observed effects in PrP null neurons, we can not exclude the possibility that other ionic conductances might have been involved in altering neuronal hyperexcitability. To rule out the possible impact of other ion channels, it would be thus interesting to perform pharmacological studies by bath application of HCN channel blockers during assessment of firing patterns from PrP-KO neurons. If I_h was the only ionic conductance involved, then the difference in neuronalexcitability between WT and PrP-KO should be ablated with the blockage of HCN channel activity.

(b) A reduction in both medium and slow afterhyperpolarization currents (I_{AHP}), which is of great importance for neuronal excitability and is a key determinant of spike frequency adaptation in hippocampal neurons (Lancaster and Nicoll, 1987), is evident in PrP-null mice (Colling et al., 1996, Herms et al., 2001, Mallucci et al., 2002, Fuhrmann et al., 2006, Powell et al., 2008). Given the significant involvement of I_h in generation of somatic medium AHP in hippocampal pyramidal neurons (Gu et al., 2005), it would be important to further explore the functional impact of I_h on PrP-KO neuronal hyperexcitability by investigating the effect of ZD7288 on the AHP in both WT and KO neurons.

(c) The dysregulation of HCN channels, in particular, HCN1 and HCN2 subunits, is involved in pathological conditions, such as epilepsy (Poolos, 2012, He et al., 2014). For example, a loss of function of HCN1 and HCN2 subunits has been indicated in epilepsy in hippocampus in animal models of epilepsy (Jung et al., 2007, Jung et al., 2010). Similarly, PrP-KO mice have shown an enhanced sensitivity to seizures (Walz *et al*., 1999, Walz *et al*., 2002). Thus, it is possible that reduced I_h may contribute to the enhanced sensitivity to seizures of PrP-KO neurons. It will be of future interest to determine whether alterations in I_h contribute to the known behavioural phenotype of PrP-KO mice.

(d) Our study has shown that activation of cAMP only reverses slow activation kinetics, but Gmax and half-activation voltage remained unaltered in PrP-KO neurons, suggesting that cAMP is not the only modulator for the reduced I_h. Indeed, a shift in I_h voltage-dependent activation is thought to be associated with altered protein kinase levels (Yu et al., 2004, Zong et al., 2005, Poolos et al., 2006, Jung et al., 2010). Recently, it was determined that inhibition of p38-MAPK induced a ~25 mV hyperpolarizing shift in I_h voltage-dependent activation along with an increased input resistance in hippocampal pyramidal neurons (Poolos et al., 2006, Jung et al., 2010). The functional consequence of p38-MAPK inhibition for I_h is similar with what was observed in PrP-KO neurons. Therefore, additional evidence, such as the regulation of p38-MAPK needs to be investigated to provide a cellular basis for the altered voltage-dependent activation of I_h in PrP-KO neurons.

Together, these approaches would supply further proof that HCN channels functionally associated with PrP^C regulate neuronal excitability and provide a mechanism to better explain the robust relationship between HCN and PrP^C, and subsequent effect on neuronal activity.

In Paper 2:

In addition to the identified relationship with PrP^C, several recent studies have been reported on the functional association of HCN channels with voltage-gated ion channels, such as T-type Ca^{2+} channels (Huang et al. 2011, Tsay et al., 2007), further indicating a diversified HCN-associated signaling. Such a cross-talk between T-type Ca^{2+} channels and HCN channels has been observed in both hippocampal and entorhinal cortical neurons and shown to increase Cav3 inactivation, leading to alterations in presynaptic function (Huang et al. 2011, Tsay et al.,

2007), but a direct interaction had not been determined. Our co-IP experiments revealed for the time that HCN1 channels immuno-precipitated with Cav3.2 channels from mouse brain lysates with defined binding regions. This association appears to be specific to the Cav3.2 isoform with no co-IP observed between HCN protein and Cav3.1 or Cav3.3 isoforms. In contrast, HCN2 channels were not found to be associated with any of the three T-type isoforms. These data indicate that HCN1 and Cac3.2 channels are selectively associated as a physical complex. However, we do not know if the HCN1-Cav3.2 complex has any functional implications. We therefore, conducted a direct biophysical test to investigate the functional effect of HCN channels on Cav3.2 channel activity. We found that coexpression of HCN1 protein altered Cav3.2 channel behavior by decreasing Cav3.2 current density, increasing the inactivation time constant of Cav3.2, and shifting the half-activation voltage to slightly more depolarized potentials. Conversely, Cav3.2 channel activity remained unaltered with HCN2 protein coexpression, suggesting that HCN2 channels fail to co-IP with Cav3.2 isoform to regulate Cav3.2 channel activity.

Additional questions and implications arising from the current study are as follows: First, what is the mechanism that underlies the various effects of HCN1 on Cav3.2 current density and voltage-dependent properties? As indicated in the paper, expression of HCN1 may induce a decrease in the membrane expression of Cav3.2 channels, thus reducing Cav3.2 current density. This could occur at either the transcriptional or translational levels, or as a result of altered channel trafficking. Alternatively, the effect of HCN1 may be due to a regulation of either single channel conductance or maximum open probability of Cav3.2. Further experiments, such as surface protein biotinylation and/or single channel recordings may shed further light on this issue. Second, it will be important to test at which level the formation of the signaling complex takes place, whether this association is established at the level of the Golgi complex or if the channel-complex is translocated to the membrane for the subsequent functional output. Although HCN and T-type channels are primarily voltage operated, both of them, in particular, HCN channels, are highly regulated by intracellular signals in terms of activity-dependent trafficking and membrane expression (He et al., 2014, Iftinca and Zamponi, 2009). Therefore, further investigation into where and how the HCN1-Cav3.2 interaction formed is required. Third, although a T-type channel-dependent regulation of HCN channels in thalamocortical cells on the generation of rebound calcium spikes has long been recognized (Luthi and McCormick, 1998),

we did not observe such a process in our experimental configuration. Given the tiny single channel conductance and lower open probability of T-type channels, it is possible that in our experiments, the voltage steps used for activating Cav3.2 channels may not be sufficient to provide enough Ca^{2+} influx to regulate HCN channels. It has been determined that there is a nanodomain interaction between Cav3 channels and KCa3.1 channels (Fakler and Adelman, 2008). If this was the case in the interplay between Cav3 and HCN channels, it would be necessary and sufficient to have intracellular Ca^{2+} precisely regulated in order to see the effect, which might not be evident from the current preparation. Last, Both HCN and T-type channels are widely expressed in the CNS and their activities are critically correlate to the physiological functions, such as neuronal excitability and synaptic transmission (Zamponi et al., 2015, He et al., 2014). It thus, would be an advantage to analyze the contribution of HCN1-Cav3.2 complex on the functional output by blocking the physical interaction with cell permeable peptides corresponding to the determined binding regions in the complex.

Broader view: A role of neuronal hyperexcitability in diverse neurodegenerative diseases

The identification of HCN channel mediated interactions, as well as the correspondingly altered neuronal activity, suggests that my observations may have relevance to neurodegenerative diseases where neuronal excitability is dysregulated. As stated above, this may involve the molecular (through HCN-Cav3.2 interactions) and ionic mechanisms (through HCN-PrP^C interactions) that are likely important in the generation of neuronal hyperexcitability.

Neurodegenerative diseases such as Alzheimer's Disease (AD), Amyotrophic Lateral Sclerosis (ALS), Multiple Sclerosis, Parkinson's Disease (PD) and Prion Disease, etc, have been characterized as a progressive dysfunction of the nervous system, which results in escalating damage or death of neurons in brain. Tremendous efforts have been made to understand neurodegenerative pathogenesis and pathology. One major challenge is to know why certain classes of neurons preferentially die in different neurodegenerative diseases. It has been suggested that network hyperactivity and hyperexcitability contribute to this selective loss leading to cognitive impairment in AD, the most common neurodegenerative disorder (Morcom et al., 2007, Putcha et al., 2011). Moreover, spontaneous epileptic seizures have been observed in AD patients as well as in transgenic AD mouse models (Rao et al., 2009, Noebels, 2011), which

occur as a result of increased network hyperexcitability (Hazra et al., 2013). In particular, the hippocampus has been found to be one of the first areas in the brain affected during AD, with a shrinkage of volume. This in turn contributes to an impairment of memory as well as development of dementia. In addition, hippocampal hyperactivation is associated with seizures in AD patients (Jin et al., 2004, Noebels, 2011, Hazra et al., 2013).

Given that the dysregulation of HCN channels is implicated in various epilepsies (Brewster et al., 2002, Budde et al., 2005, Chen et al., 1999, Kuisle et al., 2006), the HCN-associated complex discovered here may hold clues towards seizure activity in AD.

Cellular PrP may serve as a chaperone for the assembly of signaling modules at the cell surface (Linden et al., 2008). Although PrP^C does not appear to be part of a physical complex with HCN channels, PrP^C might perhaps indirectly (perhaps even via cAMP signaling) contribute to the assembly of HCN channels and Cav3.2 channels in hippocampal neurons where HCN channels regulate Cav3.2 channel current density and activity (Figure 3-1). Indeed, as suggested by a number of studies, PrP^C has a tightly molecular and functional association with ion channels (Bond et al., 2004, Collinge et al., 1996, Herms et al., 2001, Pedarzani et al., 2005). Alternatively, PrP^C-mediated regulation of HCN channels may indirectly regulate the activity/cell surface expression of Cav3.2. Importantly, loss of PrP function has been reported to increase neuronal excitability (Khosravani et al., 2008) and synaptic plasticity (Lauren et al., 2009), which may contribute to synchronized activities underlying epileptic seizures in hippocampus (Walz et al., 1999). For example, previous work in Pr-null mice reported that PrP^C not only interacts with GluN2D NMDA receptors, but upregulates its function in hippocampal neurons (Khosravani et al., 2008). In addition, an increased susceptibility to glutamate toxicity can be also observed in those neurons along with the enhanced NMDA receptor function (Khosravani et al., 2008). Apart from these, the loss of PrP function was also tested by Lauren in $Prnp^{-/-}$ hippocampal slices (Lauren et al., 2009). They reported that PrP^C is a high-affinity receptor for amyloid beta (Aß) oligomers. Importantly, this ligand-receptor pair has a therapeutic implication in AD such that Aß-induced synaptic toxicity is dependent on this interaction and is mediated by PrP^C. It would be very interesting to test whether Cav3.2 T-type channel activity might be dysregulated in PrP-KO mice, which would further contribute to alterations in neuronal hyperexcitability. This could fit the observation that PrP-null mice show increased sensitivity to

pharmacologically induced seizures (Walz et al., 1999). As noted in the INTRODUCTION, PrP-null neurons thus, usually present a hyperexcitable stage that could be due to the dysregulated ionic conductances as discovered in my studies.

Normal PrP^{C} is converted into scrapie PrP, PrP^{SC} during prion disease (Sailer et al., 1994), rasing the possibility that this misfolded form of PrP could lead to alterations in HCN channel activity during prion disease, therefore subsequently leading to electrophyiological and synatic alterations. Indeed, recent studies on neurodegenrative diseases including AD, PD, ALS and prion disease indicate that early neurodegeneration is probably not caused by the accumulation of misfolded proteins in the brain, but perhaps instead by subtle neuronal dysfunction (Soto, 2007). Therefore, understanding the cause of these alterations may help slow disease progression during early stages. This underscors the potential impact of our work. In conclusion, by combining multiple experimental approaches, this study establishes a framework for understanding the HCN channel-associated signaling in neuronal function. Taken together, the data demonstrate the HCN-associated complex is in a diversified fashion. Our observations that HCN1-Cav3.2 and HCN-PrP^{C} can form molecular and functional associations point out a likely mechanism underlying neuronal function and hippocampus-related behavior.

Figure 3-1. Schematic illustration of PrP loss-of-function hypothesis for the final conclusion

Left: In WT neurons, cellular PrP may regulate HCN1 and Cav3.2 channel assembly either directly or through an indirect signaling cascade mediated by cAMP. HCN1 channels then modulate Cav3.2 channel activity. Right: Therefore, the connection of HCN-associated complex might be broken in PrP-null neurons. As a result, on one hand, the activity of HCN channels might be reduced subsequently leading to an increased neuronal excitability. On the other hand, the dysregulation of HCN channels would probably alter Cav3.2 channel level, thus further contributing to neuronal hyperexcitability.

WT

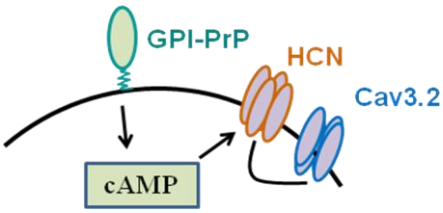

PrP-null

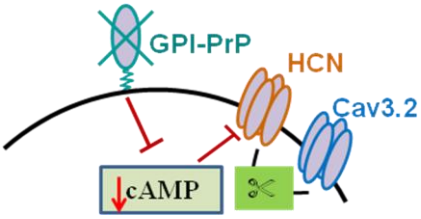

References

Aguzzi A, Heikenwalder M (2006). Pathogenesis of prion diseases: current status and future outlook. Nat Rev Microbiol. 4, 765–775.

Anderson P, Morris R, Amaral D, Bliss T, O'Keefe J. (2007). "The hippocampal formation". The hippocampus book (first ed.). New York: Oxford University Press.

Atherton JF, et al. (2010) Selective participation of somatodendritic HCN channels in inhibitory but not excitatory synaptic integration in neurons of the subthalamic nucleus. J Neurosci. 30:16025–16040.

Balke CW, Rose WC, Marban E, Wier WG. (1992) Macroscopic and unitary properties of physiological ion flux through T-type Ca^{2+} channels in guinea-pig heart cells, J. Physiol. 456, 247–265.

Bartsch T. (2012) The hippocampus in neurological disease. Chapter in the clinical neurobiology of the hippocampus: Oxford Scholarship Online Press.

Bender RA, Baram TZ. (2008) HCN channels in developing neuronal networks. Progress in Neurobiology 86:129–140.

Beraldo FH, Arantes CP, Santos TG, Machado CF, Roffe M, Hajj GN, Lee KS et al. (2011) Metabotropic glutamate receptors transduce signals for neurite outgrowth after binding of the prion protein to laminin gamma1 chain. FASEB J 25:265–279.

Berger T, Senn W, Luscher HR. (2003) Hyperpolarization-activated current Ih disconnects somatic and dendritic spike initiation zones in layer V pyramidal neurons. J Neurophysiol 90: 2428–2437.

Biasini E, Turnbaugh JA, Unterberger U, Harris DA. (2012) Prion protein at the crossroads of physiology and disease. Trends Neurosci 35:92–103.

Biel M, Wahl-Schott C, Michalakis S, Zong X. (2009) Hyperpolarization-activated cation channels: from genes to function. Physiol. Rev. 89, 847–885.

Brager DH, Johnston D. (2007) Plasticity of intrinsic excitability during long-term depression is mediated through mGluR-dependent changes in I (h) in hippocampal CA1 pyramidal neurons, J Neurosci 27:13926-37.

Brewster AL, Bender RA, Chen Y, Dubé C, Eghbal-Ahmadi M, Baram TZ. (2002) Developmental febrile seizures modulate hippocampal gene expression of hyperpolarization-activated channels in an isoform and cell-specific manner. J Neurosci 22:4591–4599.

Brown DR, Schulz-Schaeffer WJ, Schmidt B, Kretzschmar HA. (1997). Prion protein-deficient cells show altered response to oxidative stress due to decreased SOD-1 activity. Exp Neurol 146, 104-112.

Brown DR, Clive C, Haswell SJ. (2001) Antioxidant activity related to copper binding of native prion protein. J Neurochem 76:69–76.

Brown DR, Schulz-Schaeffer WJ, Schmidt B, Kretzschmar HA (1997) Prion protein-deficient cells show altered response to oxidative stress due to decreased SOD-1 activity. Exp. Neurol. 146:104–112.

Brown HF, Difrancesco D (1980) Voltage-clamp investigations of membrane currents underlying pace-maker activity in rabbit sino-atrial node. Journal of Physiology, 308, 331– 351.

Brown HF, DiFrancesco D, Noble SJ (1979). How does adrenaline accelerate the heart? Nature, 280, 235-236.

Budde T, Caputi L, Kanyshkova T, Staak R, Abrahamczik C, Munsch T, Pape HC. (2005) Impaired regulation of thalamic pacemaker channels through an imbalance of subunit expression in absence epilepsy. J Neurosci 25:9871–9882.

Büeler H, Fischer M, Lang Y, Bluethmann H, Lipp HP, DeArmond SJ, Prusiner SB, et al. (1992) Normal development and behaviour of mice lacking theneuronal cell-surface PrP protein. Nature 356:577–82.

Caiati MD, Safiulina VF, Fattorini G, Sivakumaran S, Legname G, Cherubini E. (2013) PrP^{C} controls via protein kinase A the direction of synaptic plasticity in the immature hippocampus. J Neurosci 33:2973–2983.

Carbone E, Lux HD. (1984) A low voltage-activated, fully inactivating Ca^{2+} channel in vertebrate sensory neurones. Nature. 310, 501–502.

Catterall WA. (2000) Structure and regulation of voltage-gated Ca^{2+}. Annual Review of Cell and Developmental Biology. 16:521-555.

Catterall WA. (2011) Voltage-Gated Calcium Channels. Cold Spring Harb Perspect Biol. 3:a003947.

Catterall WA, Perez-Reyes E, Snutch TP, Striessnig J. (2005) International Union of Pharmacology. XLVIII. Nomenclature and structure-function relationships of voltage-gated calcium channels. Pharmacol Rev. 57: 411-425.

Chen K, Aradi I, Santhakumar V, Soltesz I. (2002) H-channels in epilepsy: new targets for seizure control? Trends Pharmacol Sci, 23:552-557.

Chen K, Aradi I, Thon N, Eghbal-Ahmadi M, Baram TZ, Soltesz I. (2001) Persistently modified h-channels after complex febrile seizures convert the seizure-induced enhancement ofvinhibition to hyperexcitability. Nat. Med. 7, 331–337.

Chen K, Baram TZ, Soltesz I. (1999) Febrile seizures in the developing brain result in persistent modification of neuronal excitability in limbic circuits. Nat Med. 5:888–894.

Chemin J, Traboulsie A, Lory P. (2006) Molecular pathways underlying the modulation of T-type calcium channels by neurotransmitters and hormones. Cell Calcium 40, 121–134.

Chiarini LB, Freitas AR, Zanata SM, Brentani RR, Martins VR, Linden R. (2002) Cellular prior protein transduces neuroprotective signal. EMBO J 21:3317–3326.

Collinge J Whittington MA, Sidle KC, Smith CJ, Palmer MS, Clarke AR, Jefferys JG. (1994) Prion protein is necessary for normal synaptic function. Nature 370:295–297.

Colling SB, Collinge J, Jefferys JG. (1996) Hippocampal slices from prion protein null mice: Disrupted $Ca^{(2+)}$- activated K^{+} currents. Neurosci. Lett 209:49–52.

Colling SB, Khana M, Collinge J, Jefferys JG. (1997) Mossy fibre reorganization in the hippocampus of prion protein null mice. Brain Res 755:28–35.

Criado JR, Sánchez-Alavez M, Conti B, Giacchino JL, Wills DN, Henriksen SJ, Race R, et al. (2005) Mice devoid of prion protein have cognitive dei cits that are rescued by reconstitution of PrP in neurons. Neurobiol. Dis 19:255 – 265.

Crunelli V, Tóth TI, Cope DW, Blethyn K, Hughes SW. (2005) The 'window' T-type calcium current in brain dynamics of different behavioural states. J. Physiol. 562, 121–129.

Droogmans G, Nilius B. (1989) Kinetic properties of the cardiac T-type calcium channel in the guinea-pig, J. Physiol. 419, 627–650.

Engbers JD, Anderson D, Tadayonnejad R, Mehaffey WH, Molineux ML, Turner RW. (2011) Distinct roles for I(T) and I(H) in controlling the frequency and timing of rebound spike responses. J.Physiol. 589:5391–5413.

Engbers JD, Anderson D, Asmara H, Rehak R, Mehaffe WH, Hameed S, Mckay BE, et al. (2012) Intermediate conductance calcium-activated potassium channels modulate summation of parallel fiber input in cerebellar Purkinje cells. Proc.Natl. Acad. Sci. U.S.A. 109:2601–2606.

Engbers JD, Zamponi GW, Turner RW. (2013) Modeling interactions between voltage-gated Ca^{2+}channels and KCa1.1 channels. Channels (Austin). 7:24–25.

Fakler B, Adelman JP. (2008) Control of K(Ca) channels by calcium nano/microdomains. Neuron. 59:873–881.

Freund TF, Buzsaki G. (1996) Interneurons of the hippocampus. Hippocampus 6:347-470.

Fuhrmann M, Bittner T, Mitteregger G, Haider N, Moosmang S, Kretzschmar H, Herms J. (2006) Loss of the cellular prion protein affects the Ca^{2+} homeostasis in hippocampal CA1 neurons. J Neurochem 98:1876 –1885.

Gadotti VM and Zamponi GW. (2011) Cellular prion protein protects from inflammatory and neurochiarinipathic pain. Mol Pain 7:59.

Gadotti VM, Bonfield SP and Zamponi GW. (2012) Depressive-like behaviour of mice lacking cellular prion protein. Behav Brain Res 227:319–323.

Gardette R, Debono M, Dupont JL, CREPEL F. (1985) Electrophysiological studies on the postnatal development of intracerebellar nuclei neurons in rat cerebellar slices maintained in vitro. I. Postsynaptic potentials. Brain Res. 351: 47–55.

Gu N, Vervaeke K, Hu H, Storm JF. (2005) Kv7/KCNQ/M and HCN/h, but not KCa2/SK channels, contribute to the somatic medium after-hyperpolarization and excitability control in CA1 hippocampal pyramidal cells. J Physiol. 566:689-715.

Haeberle AM, Ribaut-Barassin C, Bombarde G, Mariani J, Hunsmann G, Grassi J, Bailly Y. (2000) Synaptic prion protein immunoreactivity in the rodent cerebellum. Microsc Res Tech. 50:66–75.

Haigh CL, Drew SC, Boland MP, Masters CL, Barnham KJ, Lawson VA, Collins SJ. (2009) Dominant roles of the polybasic proline motif and copper in the PrP23-89-mediated stress protection response. J.Cell Sci 122:1518–1528.

Halliwell JV and Adams PR. (1982) Voltage-clamp analysis of muscarinic excitation in hippocampal neurons. Brain Res 250:71-92.

Hazra A, Gu F, Aulakh A, Berridge C, Eriksen JL, Ziburkus J. (2013) Inhibitory neuron and hippocampal circuit dysfunction in an aged mouse model of Alzheimer's disease. PLoS One. 8:e64318.

He C, Chen F, Li B, Hu Z. (2014) Neurophysiology of HCN channels: from cellular functions to multiple regulations. Prog. Neurobiol 112:1–23.

Herms J, Tings T, Gall S, Madlung A, Giese A, Siebert H, Schürmann P, et al. (1999) Evidence ofpresynaptic location and function of the prion protein. J Neurosci 19: 8866–8875

Herms JW, Korte S, Gall S, Schneider I, Dunker S, Kretzschmar HA. (2000) Altered intracellular calcium homeostasis in cerebellar granule cells of prion protein-deficient mice. J Neurochem 75:1487–1492.

Herms JW, Tings T, Dunker S, Kretzschmar HA. (2001) Prion protein affects Ca^{2+}-activated K^{+} currents in cerebellar Purkinje cells. Neurobiol Dis 8:324 –330.

Huang Z, Walker MC, Shah MM. (2009) Loss of dendritic HCN1 subunits enhances aeba excitability and epileptogenesis. J Neurosci . 29:10979–10988.

Huang Z, Lujan R, Kadurin I, Uebele VN, Renger JJ, Dolphin AC, Shah MM (2011) Presynaptic HCN1 channels regulate Cav3.2 activity and neurotransmission at select cortical synapses. Nat. Neurosci. 14:478–486.

Huguenard JR. (1996) Low-threshold calcium currents in central nervous system neurons. Annu. Rev. Physiol. 58, 329–348.

Iftinca MC, Hamid J, Chen L, Varela D, Tadayonnejad R, Altier C, Turner RW, et al. (2007) Regulation of Cav3.1 T-type calcium channels by Rho-associated kinase. Nat. Neurosci. 10, 854–860.

Iftinca MC, Zamponi GW. (2008) Regulation of neuronal T-type calcium channels. Trends Pharmacol Sci. 30:32-40.

Jahnsen H. (1986) Electrophysiological characteristics of neurones in the guinea-pig deep cerebellar nuclei in vitro. J Physiol. 372:129–147.

Jahnsen H, Llinas R. (1984) Voltage-dependent burst-to-tonic switching of thalamic cell activity: an in vitro study. Arch. Ital. Biol. 122:73-82.

Jarrard LE. (1983) Selective hippocampal lesions and behavior: effects of kainic acid lesions on performance of place and cue tasks. Behav Neurosci 97:873-889.

Jin K, Peel AL, Mao XO, Xie L, Cottrell BA, Henshall DC, Greenberg DA. (2004) Increased hippocampal neurogenesis in Alzheimer's disease. Proc Natl Acad Sci U S A. 101:343-7.

Jung S, Bullis JB, Lau IH, Jones TD, Warner LN, Poolos NP. (2010) Downregulation of dendritic HCN channel gating in epilepsy is mediated by altered phosphorylation signaling. J. Neurosci. 30, 6678–6688.

Jung S, Jones TD, Lugo JN Jr, Sheerin AH, Miller JW, D'Ambrosio R, Anderson AE, (2007) Progressive dendritic HCN channelopathy during epileptogenesis in the rat pilocarpine model of epilepsy. J. Neurosci. 27, 13012–13021.

Kanaani J, Prusiner SB, Diacovo J, Baekkeskov S, Legname G. (2005) Recombinant prion protein induces rapid polarization and development of synapses in embryonic rat hippocampal neurons in vitro. J Neurochem. 95:1373-86.

Kasahara K and Sanai Y. (2000) Functional roles of glycosphingolipids in signal transduction via lipid rafts. Glycoconj. J 17:153–162.

Khosravani H, Zhang Y, Tsutsui S, Hameed S, Altier C, Hamid J, Chen L, et al. (2008) Prion protein attenuates excitotoxicity by inhibiting NMDA receptors. J. Cell Biol. 181:551–565.

Kim JA, Park JY, Kang HW, Huh SU, Jeong SW, Lee JH. (2006) Augmentation of Cav3.2 T-type calcium channel activity by cAMP-dependent protein kinase A. J. Pharmacol. Exp. Ther. 318, 230–237.

Kole MH, Hallermann S, Stuart GJ. (2006) Single I_h channels in pyramidal neurondendrites: properties, distribution, and impact on action potential output. J. Neurosci. 26:1677–1687.

Kuisle M, Wanaverbecq N, Brewster AL, Frere SG, Pinault D, Baram TZ, et al. (2006) Functional stabilization of weakened thalamic pacemaker channel regulation in rat absence epilepsy. J Physiol 575:83–100.

Kusch J, Biskup C, Thon S, Schulz E, Nache V, Zimmer T, Schwede F, et al. (2010) Interdependence of receptor activation and ligand binding in HCN2 pacemaker channels. Neuron. 67, 75–85.

Kuwahara C, Takeuchi AM, Nishimura T, Haraguchi K, Kubosaki A, Matsumoto Y, Saeki K, et al. (1999) Prions prevent neuronal cell-line death. Nature. 400:225–226.Lancaster B, Nicoll RA. (1987) Properties of two calcium-activated hyperpolarizations in rat hippocampal neurones. J Physiol. 389:187–203.

Laurén J, Gimbel DA, Nygaard HB, Gilbert JW, Strittmatter SM. (2009) Cellular prion protein mediates impairment of synaptic plasticity by amyloid-beta oligomers. Nature. 457:1128-32.

Lee MG, Manns ID, Alonso A, Jones BE. (2004) Sleep-wakerelateddischarge properties of basal forebrain neurons recorded with micropipettes in head-fixed rats. J Neurophysiol 92:1182–1198.

Lee CH, MacKinnon R. (2017) Structures of the human HCN1 hyperpolarization-activated channel. Cell. 168:111-120.

Lewis AS, Chetkovich DM. (2011) HCN channels in behavior and neurological disease: too hyper or not active enough? Mol. Cell. Neurosci. 46, 357–367.

Linden R, Martins VR, Prado MA, Cammarota M, Izquierdo I, Brentani RR (2008) Physiology of the prion protein. Physiol. Rev. 88:673–728.

Lopes MH, Hajj GN, Muras AG, Mancini GL, Castro RM, Ribeiro KC, Brentani RR, et al. (2005) Interaction of cellular prion and stress-inducible protein 1 promotes neuritogenesis and neuroprotection by distinct signaling pathways. J Neurosci. 25:11330–11339.

Ludwig A, Budde T, Stieber J, Moosmang S, Wahl C, Holthoff K, Langebartels A, et al. (2003) Absence epilepsy and dysrhythmia in mice lacking the pacemaker channel HCN2. EMBO J 22:216–224.

Luthi A, McCormick DA. (1998) Periodicity of thalamic synchronized oscillations: the role of Ca^{2+}-mediated upregulation of I_h. Neuron 20:553–563.

Luthi A, McCormick DA. (1999) $Ca^{(2+)}$-mediated up-regulation of I_h in the thalamus. How cell-intrinsic ionic currents may shape network activity. Ann. N.Y. Acad. Sci. 868:765–769.

Lømo T. (1966) Frequency potentiation of excitatory synaptic activity in the dentate area of the hippocampal formation. Acta Physiol. Scand. 68(Suppl. 277), 128.

Magee JC. (1998) Dendritic hyperpolarization-activated currents modify the integrative properties of hippocampal CA1 pyramidal neurons. J. Neurosci. 18:7613– 24.

Magee JC. (1999) Dendritic Ih normalizes temporal summation in hippocampal CA1 neurons Nat. Neurosci. 2:508–514.

Magee JC. (2000) Dendritic integration of excitatory synaptic input. Nat Rev Neurosci. 1:181–190.

Magee JC, Christofi G, Miyakawa H, Christie B, Lasser-Ross N, Johnston D. (1995) Subthreshold synaptic activation of voltage-gated Ca^{2+} channels mediates a localized Ca^{2+} influx into the dendrites of hippocampal pyramidal neurons. J. Neurophysiol. 74:1335–1342.

Magloczky Z, Freund TF. (2005) Impaired and repaired inhibitory circuits in the epileptic human hippocampus. Trends Neurosci. 28:334–340.

Malenka R, Bear M. (2004) "LTP and LTD: an embarrassment of riches". Neuron. 44: 5–21.

Mallucci GR, Ratté S, Asante EA, Linehan J, Gowland I, Jefferys JG, Collinge J. (2002) Post-natal knockout of prion protein alters hippocampal CA1 properties, but does not result in neurodegeneration. EMBO J 21:202–210.

Mangoni ME, Traboulsie A, Leoni AL, Couette B, Marger L, Le Quang K, Kupfer E, et al. (2006) Bradycardia and slowing of the atrioventricular conduction in mice lacking CaV3.1/a1G T-type calcium channels. Circ Res. 98:1422-30.

Manson JC, Clarke AR, Hooper ML, Aitchison L, McConnell I, Hope J. (1994) 129/Ola mice carrying a null mutation in PrP that abolishes mRNA production are developmentally normal. Mol Neurobiol 8:121–7.

Manson JC, Hope J, Clarke AR, Johnston A, Black C, MacLeod N. (1995) PrP gene dosage and long term potentiation. Neurodegeneration 4:113–114.

Matthews EA, Dickenson AH. (2001) Effects of ethosuximide, a T-type $Ca^{(2+)}$ channel blocker, on dorsal horn neuronal responses in rats. Eur. J. Pharmacol. 415, 141–149.

Maylie J. Morad M, and Weiss J. (1981) A study of pace-maker potential in rabbit sino-atrial node: measurement of potassium activity under voltage-clamp conditions. J Physiol 311:161–178.

McCormick DA, Bal T. (1997) Sleep and arousal. Thalamocortical mechanisms. Annu Rev Neurosci 20:185-215.

McCormick DA, Pape HC. (1990) Properties of a hyperpolarizationactivated cation current and its role in rhythmic oscillation in thalamic relay neurones. J. Physiol. 431:291–318.

McKay BE, McRory JE, Molineux ML, Hamid J, Snutch TP, Zamponi GW, Turner RW. (2006) Ca(V)3 T-type calcium channel isoforms differentially distribute to somatic and dendritic compartments in rat central neurons. Eur J Neurosci. 24:2581-94.

Meotti FC, Carqueja CL, Gadotti Vde M, Tasca CI, Walz R, Santos AR. (2007) Involvement of cellular prion protein in the nociceptive response in mice. Brain Res 1151:84-90.

Mikkonen JE, Grönfors T, Chrobak JJ, Penttonen M. (2002) Hippocampus Retains the Periodicity of Gamma Stimulation In Vivo. J Neurophysiol. 88:2349-54.

Mironov A Jr, Latawiec D, Wille H, Bouzamondo-Bernstein E, Legname G, Williamson RA, Burton D, et al. (2003) Cytosolic Prion Protein in Neurons. Journal of Neuroscience. 23: 7183-7193.

Mistrik P, Pfeifer A, Biel M. (2006) The enhancement of HCN channel instantaneous current facilitated by slow deactivation is regulated by intracellular chloride concentration. Pflugers Arch 452, 718–727.

Moore RC, Lee IY, Silverman GL, Harrison PM, Strome R, Heinrich C, Karunaratne A, et al. (1999) Ataxia in prion protein (PrP)-deficient mice is associated with upregulation of the novel PrP-like protein doppel. J. Mol. Biol., 292, 797–817.

Morcom AM, Li J, Rugg MD. (2007) Age effects on the neural correlates of episodic retrieval: increased cortical recruitment with matched performance. Cereb Cortex 17:2491-506.

Morris RG, Garrud P, Rawlins JN, O'Keefe J. (1982) Place navigation impaired in rats with hippocampal lesions. Nature 297:681-683.

Nagano F, Kawabe H, Nakanishi H, Shinohara M, Deguchi-Tawarada M, Takeuchi M, et al. (2002) Rabconnectin-3, a novel protein that binds both GDP/GTP exchange protein and GTPase-activating protein for Rab3 small G protein family. J Biol Chem. 277:9629-9632.

Nico PB, de-Paris F, Vinade ER, Amaral OB, Rockenbach I, Soares BL, Guarnieri R, et al. (2005) Altered behavioural response to acute stress in mice lacking cellular prion protein. Behav. Brain Res. 162, 173–181.

Nilius B, Hess P, Lansman JB, Tsien RW. (1985) A novel type of cardiac calcium channel in ventricular cells. Nature. 316:443–446.

Nolan MF, Dudman JT, Dodson PD, Santoro B. (2007) HCN1 channels control resting and active integrative properties of stellate cells from layer II of the entorhinal cortex. J Neurosci. 27: 12440–12451.

Noam Y, Zha Q, Phan L, Wu RL, Chetkovich DM, Wadman WJ, Baram TZ. (2010) Trafficking and surface expression of hyperpolarization-activated cyclic nucleotide-gated channels in hippocampal neurons. J. Biol. Chem. 285, 14724–14736.

Noebels J. (2011) A perfect storm: Converging paths of epilepsy and Alzheimer's dementia intersect in the hippocampal formation. Epilepsia. 52 Suppl 1:39-46.

Noma A and Irisawa H, (1976) “Membrane currents in the rabbit sinoatrial node cell as studied by the double microelectrode method,” Pfl¨ugers Archiv 364, 45–52,

O'Keefe J and Dostrovsky J. (1971) The hippocampus as a spatial map. Preliminary evidence from unit activity in the freely-moving rat. Brain Res 34:171-175.

Olton DS and Papas BC. (1979) Spatial memory and hippocampal function. Neuropsychologia 17:669-682.

Park JY, Kang HW, Moon HJ, Huh SU, Jeong SW, Soldatov NM, Lee JH. (2006) Activation of protein kinase C augments T-type Ca^{2+} channel activity without changing channel surface density. J. Physiol. 577, 513–523.

Pedarzani P, McCutcheon JE, Rogge G, Jensen BS, Christophersen P, Hougaard C, Strøbaek D, et al. (2005) Specific enhancement of SK channel activity selectively potentiates the afterhyperpolarizing current IAHP and modulates the firing properties of hippocampal pyramidal neurons. J Biol Chem. 280:41404–41411.

Perez-Reyes E. (2003) Molecular physiology of low-voltage-activated T-type calcium channels. Physiol. Rev. 83, 117–161.

Poolos NP. (2012) Hyperpolarization-Activated Cyclic Nucleotide-Gated (HCN) Ion Channelopathy in Epilepsy. Jasper's Basic Mechanisms of the Epilepsies [Internet]. 4th edition.

Poolos NP, Bullis JB, Roth MK. (2006) Modulation of h-channels in hippocampal pyramidal neurons by p38 mitogen-activated protein kinase. J Neurosci 26: 7995– 8003.

Powell AD, Toescu EC, Collinge J, Jefferys JG. (2008) Alterations in Ca2+-buffering in prion-null mice: association with reduced afterhyperpolarizations in CA1 hippocampal neurons. J Neurosci. 28:3877–3886.

Proenza C, Angoli D, Agranovich E, Macri V, Accili EA. (2002) Pacemaker channels produce an instantaneous current. J Biol Chem 277, 5101–5109.

Proenza C, Yellen G. (2006) Distinct populations of HCN pacemaker channels produce voltage-dependent and voltage-independent currents. J Gen Physiol 127, 183–190.

Putcha D, Brickhouse M, O'Keefe K, Sullivan C, Rentz D, Marshall G, Dickerson B, et al. (2011) Hippocampal hyperactivation associated with cortical thinning in Alzheimer's disease signature regions in non-demented elderly adults. J Neurosci. 31:17680-8.

Rangel A, Burgaya F, Gavín R, Soriano E, Aguzzi A, Del Río JA. (2007) Enhanced susceptibility of Prnp-deficient mice to kainate-induced seizures, neuronal apoptosis, and death: role of AMPA/kainate receptors. J. Neurosci. Res 85:2741–2755.

Rao SC, Dove G, Cascino GD, Petersen RC. (2009) Recurrent seizures in patients with dementia: frequency, seizure types, and treatment outcome. Epilepsy Behav. 14:118-20.

Rehak R, et al. (2013) Low voltage activation of KCa1.1 current by Cav3-KCa1.1 complexes. PLoS ONE. 8:e61844.

Robinson RB and Siegelbaum SA. (2003) Hyperpolarization-activated cation currents: from molecules to physiological function. Annu. Rev. Physiol 65:453–480.

Rossi D, Cozzio A, Flechsig E, Klein MA, Rülicke T, Aguzzi A, Weissmann C. (2001) Onset of ataxia and Purkinje cell loss in PrP null mice inversely correlated with Dpl level in brain. EMBO J 20:694–702.

Sah P, Clements JD. (1999) Photolytic manipulation of [Ca^{2+}]i reveals slow kinetics of potassium channels underlying the afterhyperpolarization in hippocampal pyramidal neurons. J Neurosci 19:3657–3664.

Sailer A, Büeler H, Fischer M, Aguzzi A, Weissmann C. (1994) No propagation of prions in mice devoid of PrP. Cell 77:967–8.

Sakaguchi S, Katamine S, Nishida N, Moriuchi R, Shigematsu K, Sugimoto T, Nakatani A, et al. (1996) Loss of cerebellar Purkinje cells in aged mice homozygous for a disrupted PrP gene.

Santoro B, Chen S, Luthi A, Pavlidis P, Shumyatsky GP, Tibbs GR, Siegelbaum SA. (2000) Molecular and functional heterogeneity of hyperpolarization-activated pacemaker channels in the mouse CNS. J. Neurosci. 20:5264–75.

Sangrey T, Jaeger D. (2010) Analysis of distinct short and prolonged components in rebound spiking of deep cerebellar nucleus neurons. Eur. J. Neurosci. 32:1646–1657.

Schaffer K. (1892) Beitrag zur Histologie der Ammonshorn-formation. Arch. Mikr. Anat. 39: 611-632.

Schwartzkroin PA. (1994) Role of the Hippocampus in Epilepsy. Hippocampus. 4:239-242.

Scoville, WB and Milner B. (1957) Loss of recent memory after bilateral hippocampal lesions. J Neuropsychiatry Clin Neurosci 12:103-113.

Shin M, Chetkovich DM. (2007) Activity-dependent regulation of h channel distribution in hippocampal CA1 pyramidal neurons. J. Biol. Chem. 282, 33168–33180.

Silverman GL, Qin K, Moore RC, Yang Y, Mastrangelo P, Tremblay P, Prusiner SB, et al. (2000) Doppel is an N-glycosylated, glycosylphosphatidylinositol-anchored protein. Expression in testis and ectopic production in the brains of Prnp (0/0) mice predisposed to Purkinje cell loss. J Biol Chem 275:26834–41.

Soto C. (2007) Reversibility of prion-induced neurodegeneration. Lancet Neurol. 6:294-5.

Staff NP, et al. (2000) Resting and active properties of pyramidal neurons in subiculum and CA1 of rat hippocampus. J Neurophysiol 84:2398-2408.

States M, Talavera K, Klugbauer N, Prenen J, Lacinova L, Droogmans G, Hofmann F. (2001) The amino side of the C-terminus determines fast inactivation of the T-type calcium channel α1G. J Physiol. 530:35-45.

Steriade M, Dossi RC, Nunez A. (1991) Network modulation of a slow intrinsic oscillation of cat thalamocortical neurons implicated in sleep delta waves: cortically induced synchronization and brainstem cholinergic suppression. J Neurosci. 11:3200–3217.

Steriade M, McCormick DA, Sejnowski TJ. (1993) Thalamocortical oscillations in the sleeping and aroused brain. Science. 262: 679– 685.

Steriade M, Timofeev I. (2003) Neuronal plasticity in thalamocortical networks during sleep and waking oscillations. Neuron. 37: 563– 576.

Stuart G, Spruston N. (1998) Determinants of voltage attenuation in neocortical pyramidal neuron dendrites. J. Neurosci. 18:3501–3510.

Stys PK, You H, Zamponi GW. (2012) Copper-dependent regulation of NMDA receptors by cellular prion protein: implications for neurodegenerative disorders. J Physiol 590:1357–1368.

Swanson LW, Wyss JM, Cowan WM (1978) An autoradiographic study of the organization of intrahippocampal association pathways in the rat. J Comp Neurol 787: 681-716.

Swartz BE, et al. (2006) Hippocampal cell loss in posttraumatic human epilepsy. Epilepsia 47:1373–1382.

Swensen AM, Bean BP. (2003) Ionic mechanisms of burst firing in dissociated Purkinje neurons. J. Neurosci. 23:9650–9663.

Talley EM, Cribbs LL, Lee JH, Daud A, Perez-Reyes E, Bayliss DA. (1999) Differential distribution of three members of a gene family encoding low voltage-activated (T-type) calcium channels. J Neurosci 19:1895–1911.

Thompson PJ. (1991) Memory function in patients with epilepsy. Adv. Neurol 55: 369–384.

Todorovic SM, Jevtovic-Todorovic V. (2006) The role of T-type calcium channels in peripheral and central pain processing. CNS Neurol. Disord. Drug Targets. 5, 639–653.Tsay D, Dudman JT, Siegelbaum SA. (2007) HCN1 channels constrain synaptically evoked Ca^{2+} spikes in distal dendrites of CA1 pyramidal neurons. Neuron. 56:1076–1089.

Tsutsui S, Hahn JN, Johnson TA, Ali Z, Jirik FR. (2008) Absence of the cellular prion protein exacerbates and prolongs neuroinflammation in experimental autoimmune encephalomyelitis. Am J Pathol 173:1029–1041.

Turner RW, Zamponi GW. (2014) T-type channels buddy up. Channels. Circ Res 98:1422–1430.

Vassallo N, et al. (2005) Activation of phosphatidylinositol 3-kinase by cellular prion protein and its role in cell survival, Biochem. Biophys. Res. Commun 332:75–82.

Walz R, Amaral OB, Rockenbach IC, Roesler R, Izquierdo I, Cavalheiro EA, Martins VM, et al. (1999) Increased sensitivity to seizures in mice lacking cellular prion protein. Epilepsia 40:1679–1682.

Walz R, Castro RM, Velasco TR, Carlotti CG Jr, Sakamoto AC, Brentani RR, Martins VR. (2002) Cellular prion protein: implications in seizures and epilepsy. Cell Mol Neurobiol 22:249–257.

Weissmann C and Flechsig E. (2003) PrP knock-out and PrP transgenic mice in prion research. Br Med Bull 66:43–60.

Welsby PJ, Wang H, Wolfe JT, Colbran RJ, Johnson ML, Barrett PQ. (2003) A mechanism for the direct regulation of T-type calcium channels by Ca^{2+}/calmodulin-dependent kinase II. J. Neurosci. 23, 10116–10121.

Westergard L, Christensen HM, Harris DA. (2007) The cellular prion protein (PrP(C)): its physiological function and role in disease. Biochim Biophys Acta, 1772:629-644.

Williams SR, Stuart GJ. (2000) Site independence of EPSP time course is mediated by dendritic I(h) in neocortical pyramidal neurons. J Neurophysiol 83: 3177–3182.

Wolfart J and Roeper J. (2002) Selective coupling of T-type calcium channels to SK potassium channels prevents intrinsic bursting in dopaminergic midbrain neurons. J. Neurosci. 22, 3404-3413.

Wu S, Vysotskaya ZV, Xu X, Xie C, Liu Q, Zhou L. (2011) State-dependent cAMP binding to functioning HCN channels studied by patch-clamp fluorometry. Biophys. J. 100, 1226–1232.

You H, Tsutsui S, Hameed S, Kannanayakal TJ, Chen L, Xia P, Engbers JD, et al. (2012) Aβ neurotoxicity depends on interactions between copper ions, prion protein and N-methyl-D-aspartate receptors. Proc. Natl. Acad. Sci. USA 109: 1737–1742.

Yu HG, Lu Z, Pan Z, Cohen IS. (2004) Tyrosine kinase inhibition differentially regulates heterologously expressed HCN channels. Pflu¨gers Arch. 447:392– 400.

Zamponi GW, Lewis RJ, Todorovic SM, Arneric SP, Snutch TP. (2009) Role of voltage-gated calcium channels in ascending pathway. Brain Res Rev. 60:84-9.

Zamponi GW, Striessnig J, Koschak A, Dolphin AC. (2015) The Physiology, Pathology, and Pharmacology of Voltage-Gated Calcium Channels and Their Future Therapeutic Potential. Pharmacol Rev. 67:821-70.

Zanata SM, Lopes MH, Mercadante AF, Hajj GN, Chiarini LB, Nomizo R, Freitas AR, et al. (2002) Stress-inducible protein 1 is a cell surface ligand for cellular prion that triggers neuroprotection. EMBO J. 21:3307–3316.

Zhou JL, Shatskikh TN, Liu X, Holmes GL. (2007) Impaired single cell firing and long-term potentiation parallels memory impairment following recurrent seizures. Eur J Neurosci 25:3667–3677.

Zomosa-Signoret V, Arnaud JD, Fontes P, Alvarez-Martinez MT, Liautard JP. (2008) Physiological role of the cellular prion protein. Vet Res. 39 (4):9.

Zong X, Gerstner A, Much B, Baumann L, Michalakis S, Zeng R, Chen Z, et al. (2005) A novel mechanism of modulation of hyperpolarizationactivated cyclic nucleotide-gated channels by SRC kinase. J Biol Chem. 280:34224 –34232.

Appendix

Appendix I: Unpublished data related to my project

Supplementary Figure 1: Supplementary data related to my thesis work (Paper 1) showing electrophysiological recordings performed in acute hippocampal slices from ~2 month WT and PrP-null mice to examine neuronal excitability and HCN channel activity.

A, There was no difference in spike threshold (210.1 ± 43.0 pA for WT (n = 5) vs. (207.1 ± 17 pA for KO (n = 7), $p > 0.05$).

B, There was no difference in the numbers of action potentials evoked over a wide range of current injections (from 150 pA to 650 pA).

C, Under these conditions, we did not observe differences in input resistance (107.5 ± 5.8 MΩ for WT (n = 6) vs. 96.0 ± 4.6 MΩ for KO (n = 7), $p > 0.05$). Only cells with a leak smaller than 20 pA were included in this analysis.

D, There was, however, a statistically significant decrease in voltage sag ratio (0.11 ± 0.01 for WT (n = 10) vs. 0.07 ± 0.01 for KO (n = 10), $p < 0.01$).

A

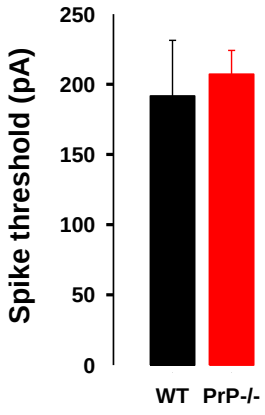
Spike threshold (pA)
250
200
150
100
50
0
WT
PrP-/-

B

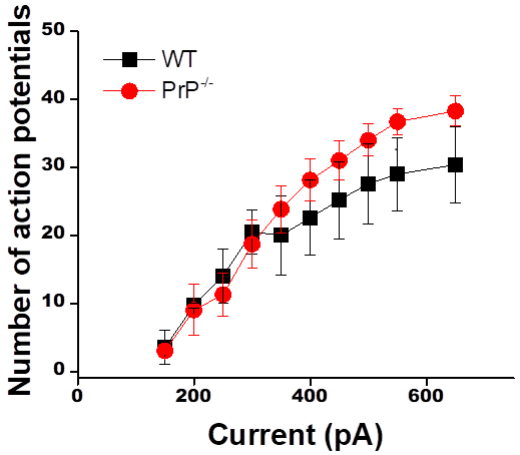
Number of action potentials
50
40
30
20
10
0
WT
PrP-/-
0
200
400
600
Current (pA)

C

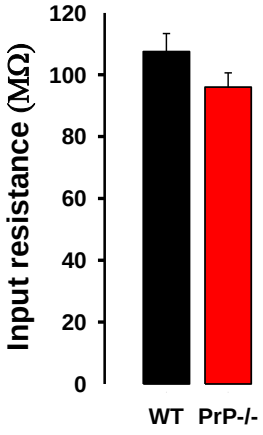
Input resistance (MΩ)
120
100
80
60
40
20
0
WT
PrP-/-

D

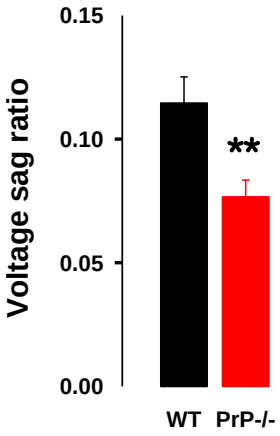
Voltage sag ratio
0.15
0.10
0.05
0.00
**
WT
PrP-/-

Supplementary Figure 2: Supplementary data related to my thesis work (Paper 1) showing electrophysiological recordings performed in cultured hippocampal neurons to examine the amplitude of the instantaneous current (I_{ins}) of HCN channels. The mean current amplitude of I_{ins} in WT (Vm = -120 mV, 359.2 ± 30.0 pA, n = 15), and PrP-null hippocampal neurons (270.1 ± 31.2 pA, n = 15, $P < 0.05$) using voltage steps from -70 to -120 mV.

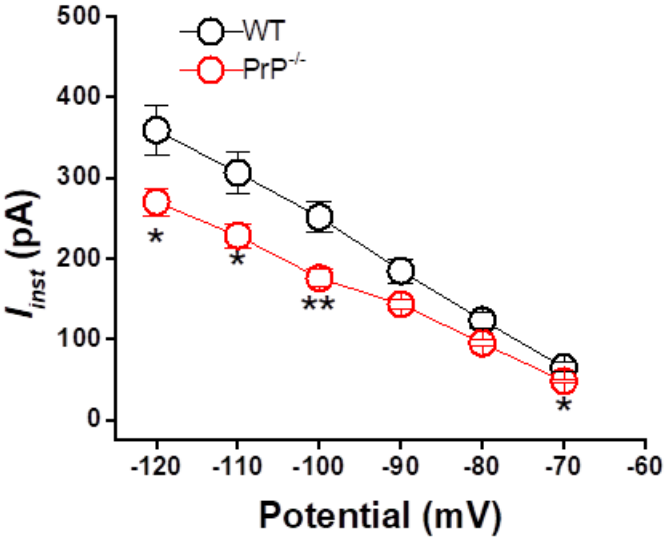
WT
PrP-/-
500
400
300
200
100
0
I_{inst} (pA)
*
*
**
*
-120
-110
-100
-90
-80
-70
-60
Potential (mV)

Supplementary Figure 3: Supplementary data related to my thesis work (Paper 1) showing analysis of HCN1 and HCN2 subunit distribution.

A, Western blot analysis of HCN1 and HCN2 protein membrane expression in hippocampal tissue obtained from WT and PrP-null mouse. Na^+/K^+-ATPase expression was used as a loading control.

B, C, Corresponding mean HCN1 (B) and HCN2 (C) surface expression of WT and PrP-null was presented as percent of WT, respectiviely (n=6, $P > 0.05$).

D, E, Coimmunoprecipitation of PrP^C and HCN1 or HCN2 showing that PrP^C does not form a complex with HCN1 (D) or HCN2 (E). The blot was probed with a PrP antibody, and in the bottom panel, membrane was detected with HCN1 or HCN2 antibody. The experiment is a representative example of three different repetitions for both WT and PrP-null adult mouse hippocampal tissue.

A

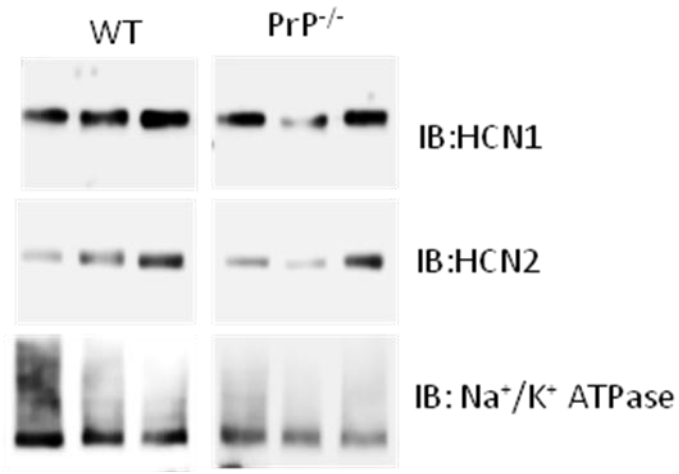
WT
PrP-/-
IB:HCN1
IB:HCN2
IB: Na+/K+ ATPase

B

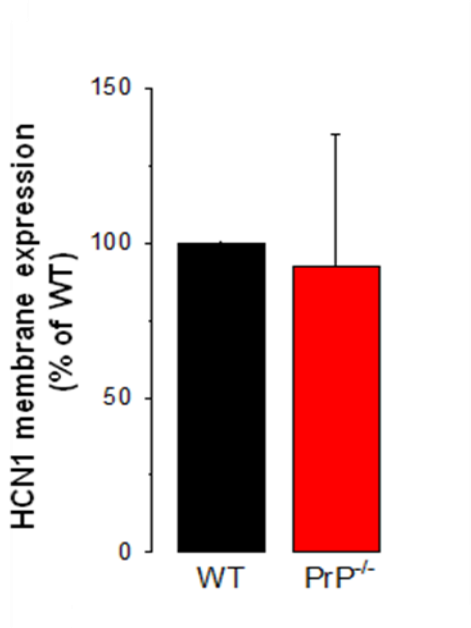
HCN1 membrane expression
(% of WT)
150
100
50
0
WT
PrP-/-

C

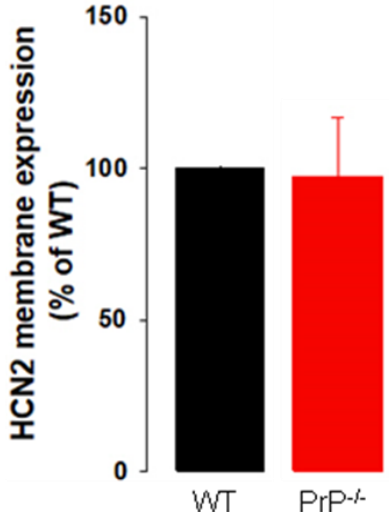
HCN2 membrane expression
(% of WT)
150
100
50
0
WT
PrP-/-

D

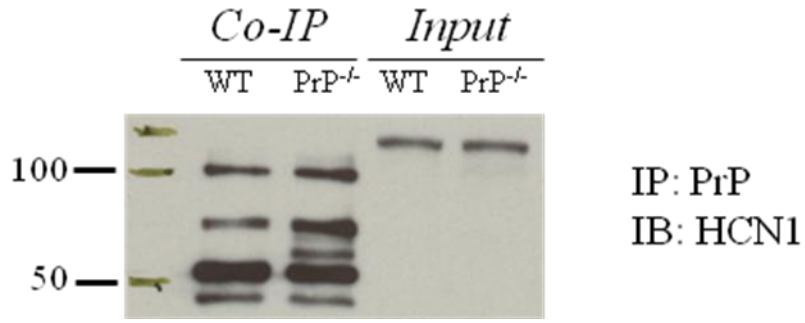
Co-IP
Input
WT
PrP-/-
WT
PrP-/-
100
50
IP: PrP
IB: HCN1

E

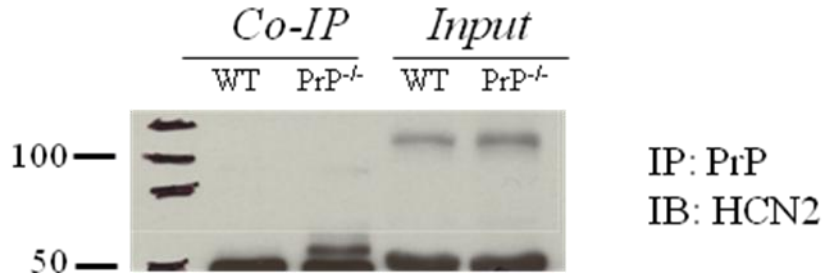
Co-IP
Input
WT
PrP-/-
WT
PrP-/-
100
50
IP: PrP
IB: HCN2

Supplementary Figure 4: Unpublished preliminary data related to my thesis work showing the expression of GFP-tagged Cav3.2 intracellular linkers, GFP-tagged Cav3.2 N-terminus and GFP-tagged Cav3.2 C-terminus with or without HCN coexpression in tsA-201 cells. An mKate-tagged membrane marker was cotransfected in all the conditions for a membrane surface localization. The red line corresponds to the position of the line scan shown under each image where peaks for GFP fluorescence (green) and cell surface signal (red) are clearly displayed.

GFP-C1 Linker I-II Linker II-III

+ pcDNA

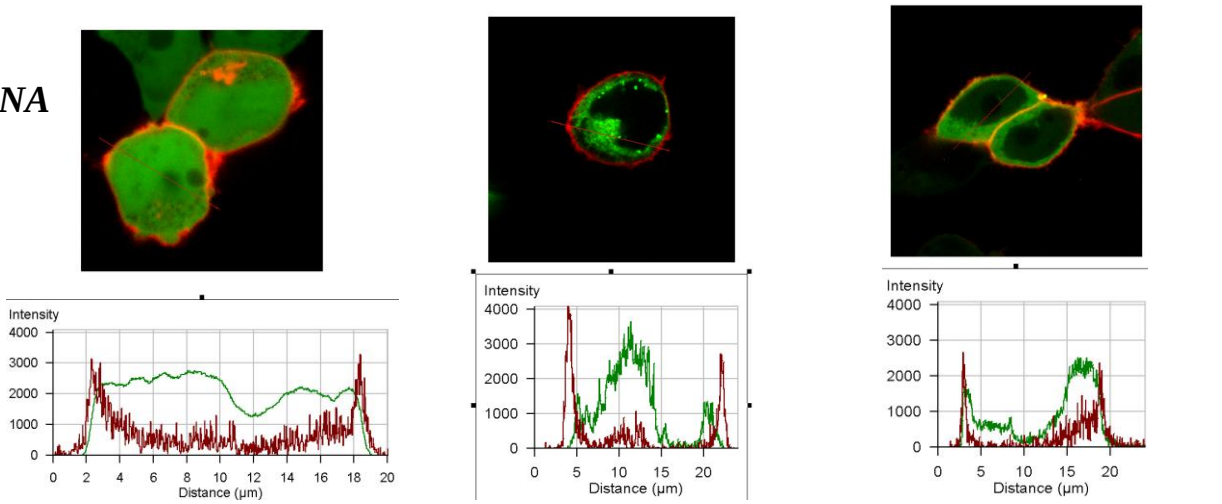

+ HCN1

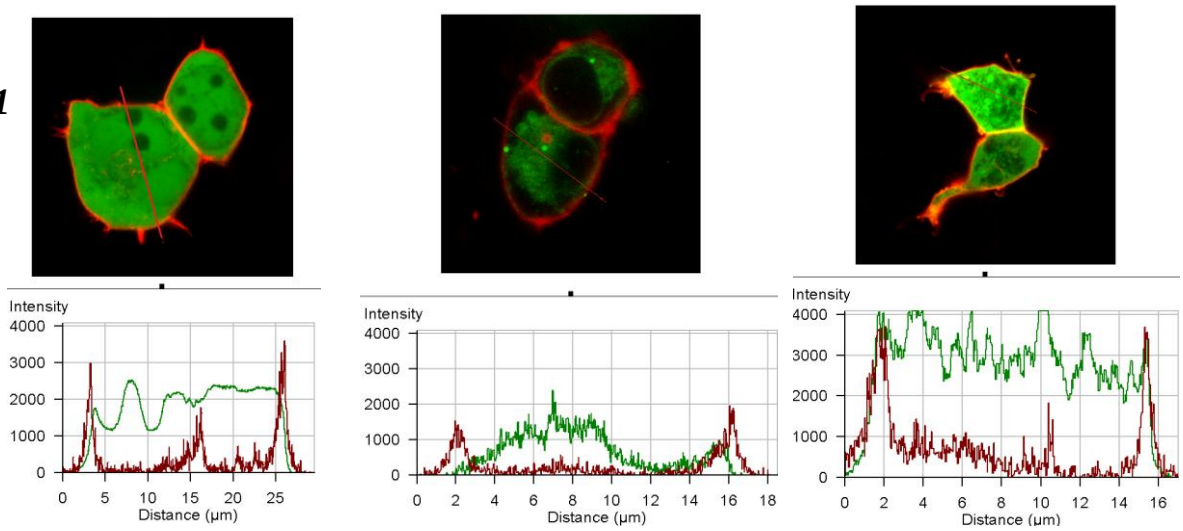

Linker III-IV N terminus C terminus

+ pcDNA

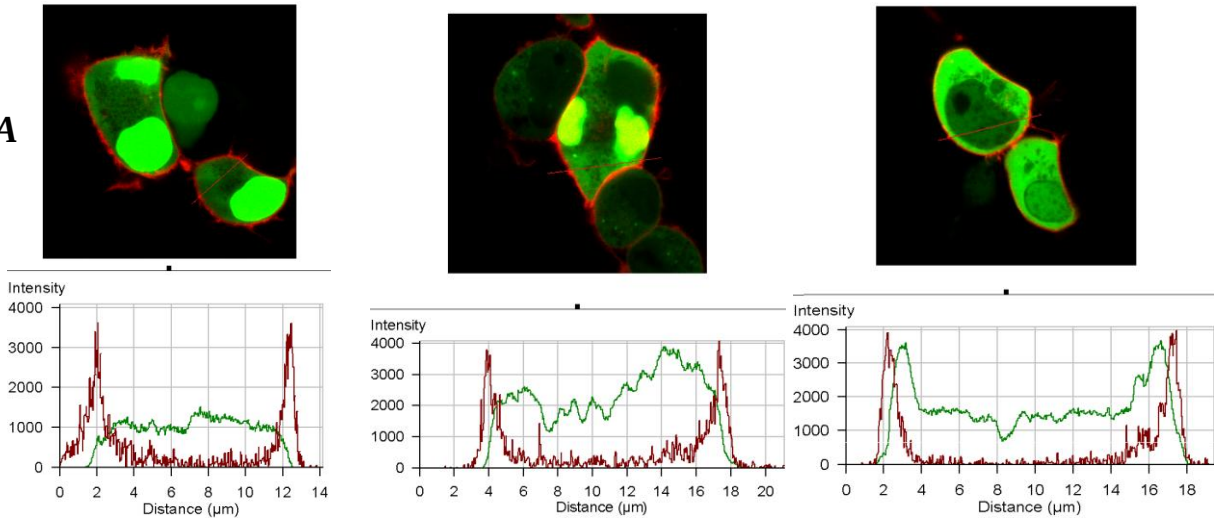

+ HCN1

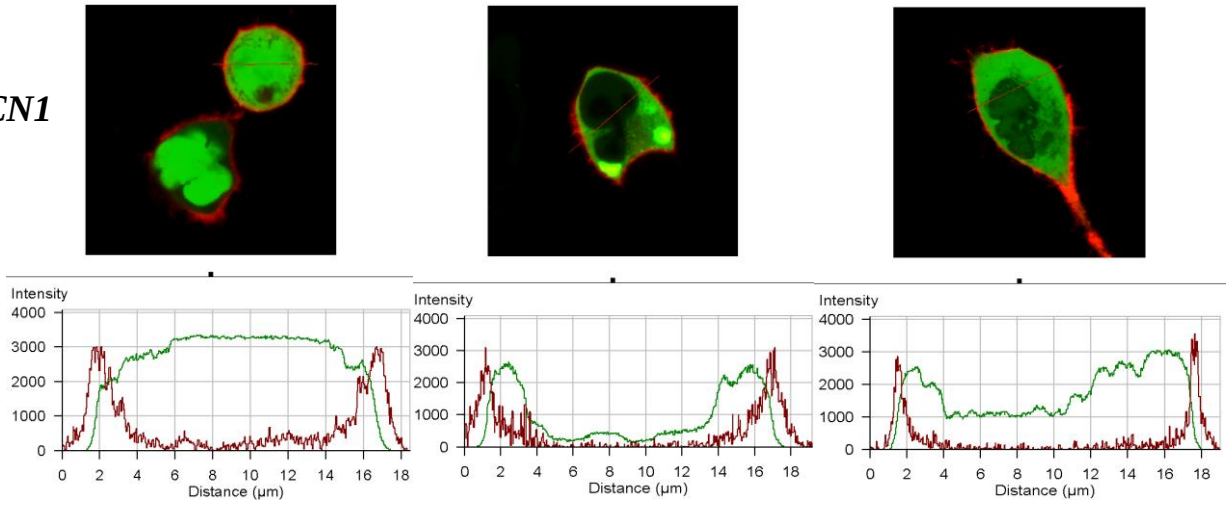

Appendix II: Collaborative work not related to my project

Maria A Gandini, Ivana A Souza, Jing Fan, Katherine Li, Gerald W Zamponi. Regulation of Ca_v2 channels by rabconnectin3. Abstract has been recently accepted by the 6th International Ion Channel Conference, 2017. J.F contributed to perform electrophysiology experiments.

Supplementary Figure 5: The functional role Rabconnectin3 (RB3) protein encoded by WDR7, has been implicated in Ca^{2+}-dependent exocytosis (Nagano et al., 2002). Here, in this study, we investigated the relationship of RB3 with N-type calcium channels which are primarily expressed at presynaptic terminals and are involved in neurotransmitter release (Zamponi et al., 2015).

From whole-cell voltage clamp recordings in tSA-201 cells, we found that RB3 significantly altered voltage-dependent properties of N-type channels as indicated by a reduced current density (A), a decreased maximal conductance (B), no change in half activation voltage (C), but an enhanced slope factor (D), a faster inactivation time constant (E) and a hyperpolarizing shift of the inactivation curve (F).

A

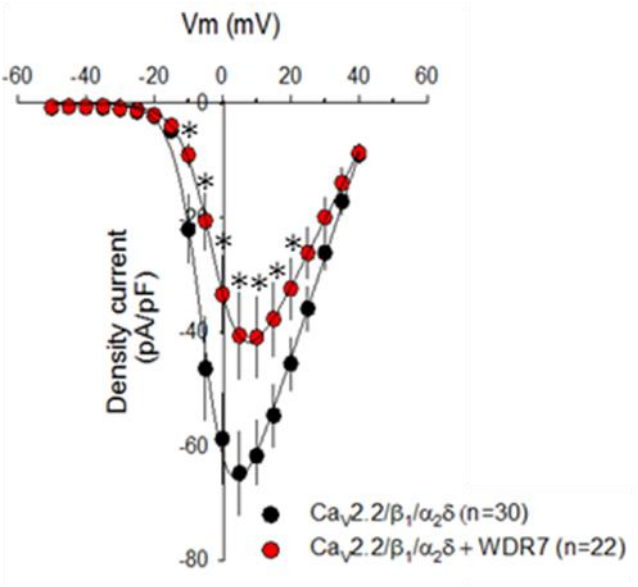
Vm (mV)
-60
-40
-20
0
20
40
60
Density current (pA/pF)
-40
-60
-80
$Ca_V2.2/\beta_1/\alpha_2\delta$ (n=30)
$Ca_V2.2/\beta_1/\alpha_2\delta$ + WDR7 (n=22)

B

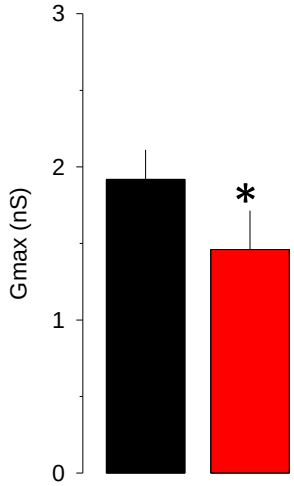
Gmax (nS)
3
2
1
0
*

C

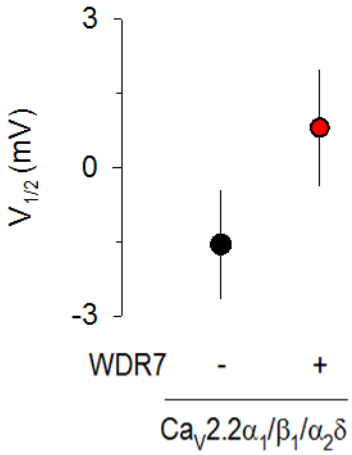
$V_{1/2}$ (mV)
3
0
-3
WDR7
-
+
$Ca_V2.2\alpha_1/\beta_1/\alpha_2\delta$

D

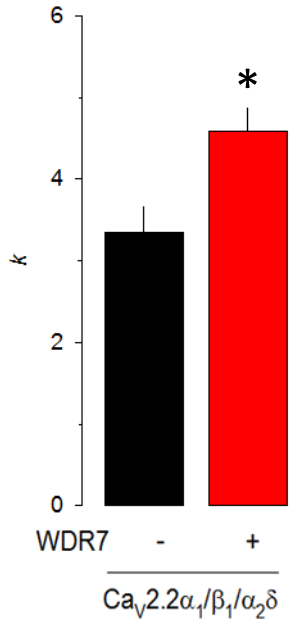
k
6
4
2
0
*
WDR7
-
+
$Ca_V2.2\alpha_1/\beta_1/\alpha_2\delta$

E

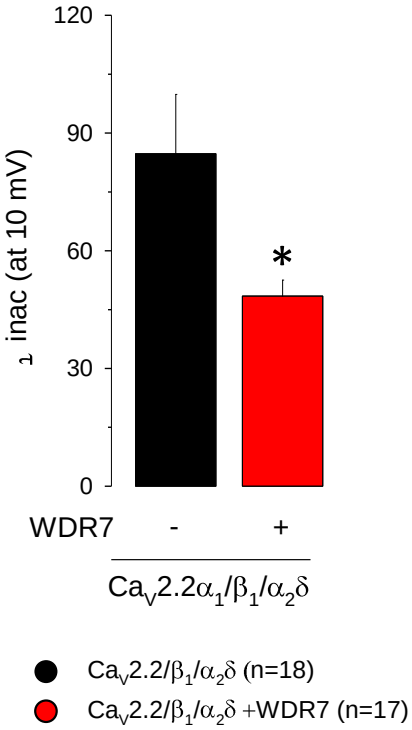
120
90
60
30
0
1 inac (at 10 mV)
*
WDR7
-
+
$Ca_V2.2\alpha_1/\beta_1/\alpha_2\delta$

$Ca_V2.2/\beta_1/\alpha_2\delta$ (n=18)
$Ca_V2.2/\beta_1/\alpha_2\delta$ +WDR7 (n=17)

F

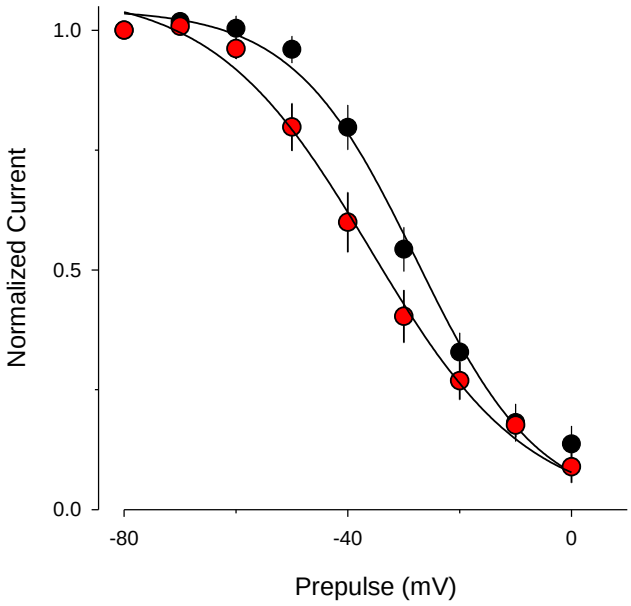
1.0
0.5
0.0
Normalized Current
-80
-40
0
Prepulse (mV)

Appendix III: Copyright permission

Open Access Statement

Specialty Chief Editors
Scope & Mission
Facts & Report
Submission
Open Access Statement
Copyright Statement
Quality
Contact

Frontiers' philosophy is that all research is for the benefit of humankind. Research is the product of an investment by society and therefore its fruits should be returned to all people without borders or discrimination, serving society universally and in a transparent fashion.

That is why Frontiers provides online free and open access to all of its research publications. For more information on open access click here **(https://www.frontiersin.org/about/open-access)**.

Open Access funder and institutional mandates: Frontiers is fully compliant with open access mandates, by publishing its articles under the Creative Commons Attribution licence (CC-BY). Funder mandates such as those by the Wellcome Trust (UK), National Institutes of Health (USA) and the Australian Research Council (Australia) are fully compatible with publishing in Frontiers. Authors retain copyright of their work and can deposit their publication in any repository. The work can be freely shared and adapted provided that appropriate credit is given and any changes specified.

Copyright Statement

I'm delighted to announce that ***Channels*** is now a **fully open access journal**. This means all the research the journal publishes will be available for anyone to read anywhere, at any time, with an internet connection.

We have taken this decision because of the continuing changes in scholarly communication and a growing demand for open access publishing. We are also aligning with the views of many funders and policymakers, who want the results of the work they fund to be available to as many people as possible, as quickly as possible. This is to ensure the widest potential impact for the work they have funded. Many are showing a preference for fully open access journals as the route for communicating the results of research funded by them, and are providing the funds for article publishing charges (APCs) to make open access a sustainable model.

As well as meeting their funders' requirements, our authors will also benefit from *Channels* being fully open access in several ways, including:

- Their work will gain greater visibility and an increased audience

Open access means that there is no barrier to readers. The published article will be universally free to access the moment it publishes online. Articles published open access with Taylor & Francis are used on average *eight times more* than articles published in subscription journals.

- They can promote their ideas freely and quickly

Rapid online publication ensures their work reaches its audience quickly. Authors can share their work immediately online via email or social media channels. Readers are also able to share the work easily.

- They will lay the foundation for future research

Authors will also be able to deposit their supplemental material (including research data) for public access into Figshare at no extra charge, as part of the publishing service provided by Taylor & Francis. This will allow others to reproduce, build on, and credit the research foundations they have created.

- They retain the choice of how people can reuse their article

We recommend the Attribution CC BY creative commons licence, which is mandated by several funders. However, if they prefer, and their funder agrees, there are options available for alternative Creative Commons licences.

Importantly, *the peer review for the journal will not change*. Our authors can be sure their papers have met the high standards expected of research in ion channels if their paper is published in the journal.

The APC for *Channels* has been set at £1,500, $1,950, €1,725. We believe this is in line with current funding and other journals in the field. Taylor & Francis, our publisher, has also negotiated APC discounts with many institutions who will cover their authors' APCs at a discounted rate. Information can be found at http://www.tandfonline.com/page/openaccess/members.

Channels publishes all aspects of ion channel research. The journal publishes high quality papers that shed new light on ion channel and ion transporter/exchanger function, structure, biophysics, pharmacology, and regulation in health and disease. *Channels* welcomes interdisciplinary approaches that address ion channel physiology in areas such as neuroscience, cardiovascular sciences, cancer research, endocrinology, and gastroenterology. Our aim is to foster communication among the ion channel and transporter communities and facilitate the advancement of the field.

I'm confident that moving *Channels* to a fully open access model will benefit:

- researchers submitting to the journal, who will have a greater potential audience
- ion channel research by making work widely available
- society more widely as the research will reach further diverse audiences.

Why not try us out by submitting your next paper to us? The online submission system is at https://www.editorialmanager.com/channels/default.aspx.

With best wishes,

Gerald W. Zamponi